UiT
THE ARCTIC
UNIVERSITY
OF NORWAY

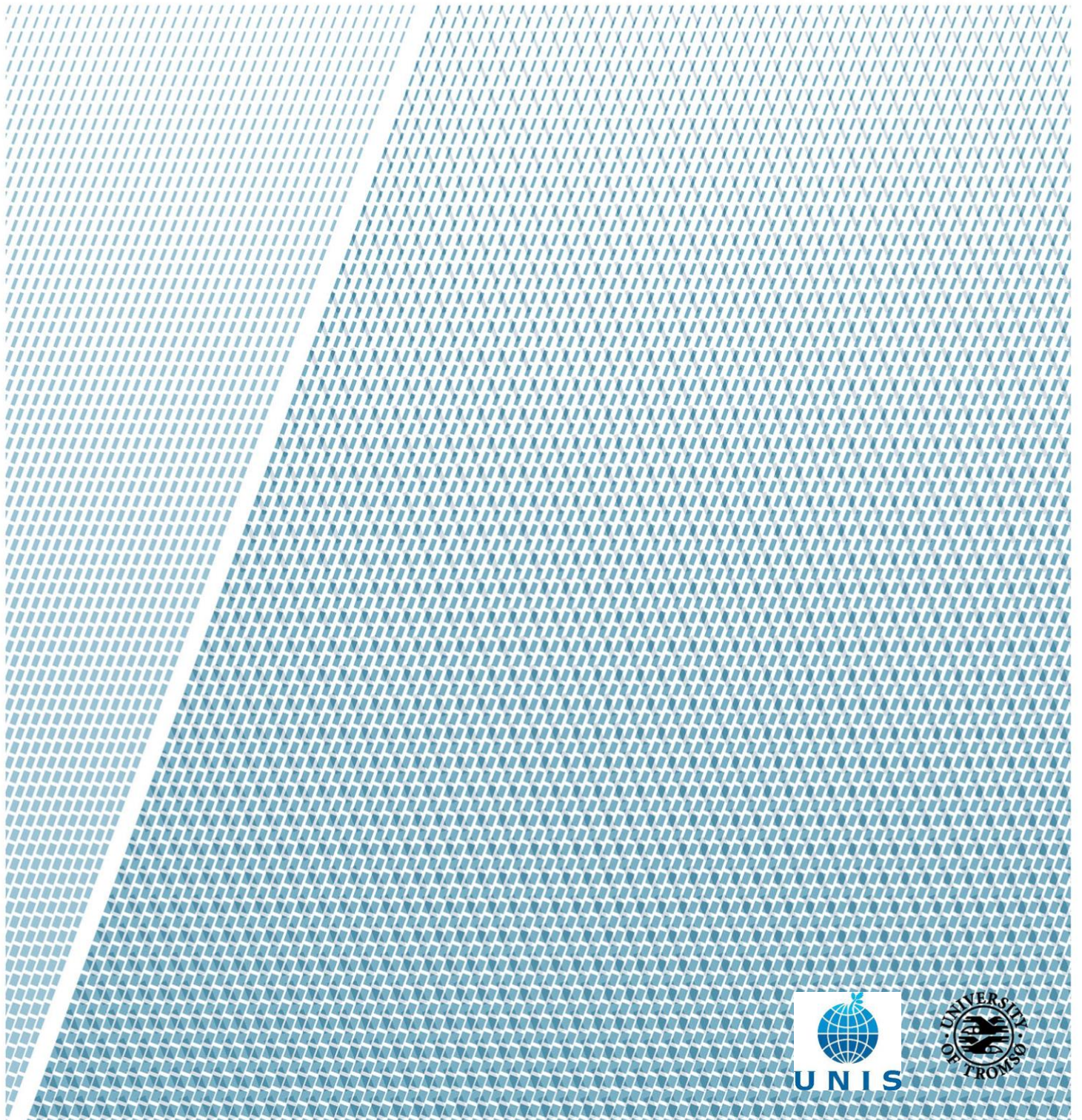Faculty of Science and Technology

Department of Geosciences

Holocene Glacial Dynamics of the Barentsøya ice cap, Svalbard

—

Juliane Leister
GEO-3900 Master's Thesis in Geology
May 2018

UNIS

UNIVERSITY OF TROMSØ

Abstract

This study investigates the glacial dynamics of Barentsjøkulen, a small ice cap located on Barentsøya, Svalbard. In order to reconstruct Barentsjøkulen's glacial history, three geomorphological maps of the glacier forefields of its main outlet glaciers, Besselsbreen, Duckwitzbreen and Freemanbreen, were created. The maps cover a total area of ca. 117 km^2 and were generated based on swath bathymetric datasets in combination with remotely sensed imagery. Ice front positions from ca. 1900 until present were reconstructed using historical data, oblique and vertical aerial imagery, satellite imagery and the GLIMS glacier database. The area of ice loss since the Little Ice Age was determined for Barentsjøkulen based on moraine positions under water and on land.

Barentsøya's landforms reveal a dynamic glacial history. The island was fully covered by the Svalbard-Barents Sea Ice Sheet during the Late Weichselian. After break-up of the ice sheet, a small ice cap remained on Barentsøya in the early Holocene - Barentsjøkulen. Barentsjøkulen has shown dynamic behaviour during the Holocene and has been in overall retreat since the Little Ice Age. An area of ice loss of ca. 147 km^2 since the Little Ice Age was calculated. Duckwitzbreen and Freemanbreen have surged after the Little Ice Age - but not Besselsbreen. Crevasse-squeeze ridges, landforms often considered to be uniquely formed by surge-type glaciers, were detected in front of Besselsbreen. The use of crevasse-squeeze ridges as characterising landforms for surge-type glaciers should therefore be reconsidered. Landform assemblages in the mapped glacier forefields show little to no correspondence to existing landsystem models. More sophisticated landsystem models are required to capture the complexity of glacier types on Svalbard. This study improves the overall understanding of ice cap dynamics in eastern Svalbard during the Holocene.

Keywords: Submarine landforms; Glacial geomorphology; Tidewater glaciers; Remote sensing; Eastern Svalbard; Holocene

Acknowledgements

Table of Contents

List of Figures

List of Tables

List of Abbreviations

CSR	Crevasse-Squeeze Ridges
DEM	Digital Elevation Model
GLIMS	Glacier Land Ice Measurements from Space
HTM	Holocene Thermal Maximum
IRD	Ice Rafted Debris
LGM	Last Glacial Maximum
LIA	Little Ice Age
m.a.s.l.	Meters above sea level
NHS	Norwegian Hydrographic Survey
NPI	Norwegian Polar Institute
PONAM	Polar North Atlantic Margins
SBSIS	Svalbard Barents Sea Ice Sheet
SEES	Scientific Expedition Edgeøya Svalbard
UNIS	University Center in Svalbard

1 Introduction

1.1 Motivation

Understanding past climate fluctuations is an important tool to predict the extent and impact of a warming climate on society in the future. Glaciers are sensitive to climate change and hence act as helpful tool in the understanding and reconstruction of climate variability (Oerlemans, 2005; Benn and Evans, 2010). Particularly landforms found in glacier forefields deliver opportunities to reconstruct recent glacier marginal activity. The activity can be linked to other measured and observed environmental parameters in order to unravel causes of changes in glacier extent and to predict future changes (Jakobsson et al., 2014). Marine environments often preserve glacial landforms better than terrestrial environments due to less erosion. Thus they contribute to a deeper understanding of past dynamics.

More than 42% of Barentsøya's area is covered by glacier ice (Figure 3.1B) (Lock et al., 1978). Information about Barentsøya and its ice cap, Barentsjøkulen, is sparse owning to its remote location and limited access due to sea ice. Most geological fieldwork carried out on Barentsøya originates from the PONAM expedition in 1991 focusing on Weichselian and Holocene landforms and sediments (Möller et al., 1992). Dowdeswell and Bamber (1995) describe the ice caps and glaciers of Barentsøya and Edgeøya as the least known of the entire Svalbard archipelago. Further research on Barentsøya's glacial history will not only shed light on the local ice cap evolution but will also contribute to the broader understanding of the structure and disintegration of the Svalbard-Barents Sea Ice Sheet (SBSIS) during the Late Weichselian.

Glaciers on Svalbard have been retreating and thinning during the last century (Dowdeswell et al., 1997; Liestøl, 1993; van der Meer, 2004; Błaszczyk et al., 2009; Nuth et al., 2010). Mass-balance measurements of most glaciers on Svalbard have been negative since the Little Ice Age (LIA) with retreat rates exceeding 200 m per year for some glacier margins (Hagen et al., 2003; Oerlemans, 2005; Nuth et al., 2013). Although overall retreating, many of Svalbard's glaciers experienced sudden rapid advances in form of surges including a significant number of marine-terminating glaciers (Liestøl, 1969; Schytt, 1969; Dowdeswell et al., 1991, 1995; Hagen et al., 1993; Hamilton and Dowdeswell, 1996; Sund et al., 2014; Farnsworth et al.,

2016). As surges and climate-driven glacier dynamics generate partially similar landforms, surge behaviour adds to the challenges of reconstructing glacier responses to temperature fluctuations.

Submarine glacial geomorphological mapping is a common tool in the reconstruction of ice sheet configurations and dynamics where ice masses were in contact with the seafloor including fjords to entire continental shelfs (Ottesen et al., 2008; Ottesen and Dowdeswell, 2009; Robinson and Dowdeswell, 2011; Rüther et al., 2012). Methods have improved significantly over the years leading to very high resolution and more detailed results (Jakobsson et al., 2016; Dowdeswell et al., 2018).

A detailed study of the dynamics of Barentsøya's outlet glaciers based on high-resolution aerial and satellite imagery combined with existing bathymetric data will add to the understanding of the behaviour of Barentsjøkulen and small ice caps in general in Svalbard during the Late Weichselian and Holocene.

1.2 Aims and Approach

The aim of this study is to investigate the dynamics and retreat history of Barentsjøkulen by analysing the landform record of the forefields of its three main outlet glaciers: Besselsbreen, Duckwitzbreen and Freemanbreen. A variety of high-resolution data including multibeam bathymetric data, remote sensing data and aerial imagery, digital elevation models (DEMs) and historical data are used for attainment.

Detailed marine geomorphological maps were created and combined with terrestrial data to analyse glacier behaviour. Historical maps and aerial and satellite images were merged with geomorphological data for ice-marginal reconstructions to demonstrate glacier fluctuations during the Holocene. The analysis of glacier behaviour and surge history was put in context with the local geology and morphology. In order to better understand Barentsjøkulen's recent retreat history, ice loss since the LIA was calculated. Finally, the applicability of common land-system models was tested for Barentsøya's outlet glaciers.

1.3 Surging Glaciers

Surge-type glaciers are characterised by a semi-periodic alternation of slow and fast flow rates (Lefauconnier and Hagen, 1991). They occur in a variety of climatic, tectonic and geological environments (Meier and Post, 1969; Jiskoot et al., 2000). Surge cycles can be divided into three phases: an accelerating phase, a decelerating phase and a quiescent phase (Murray et al., 2012). During the active surge phase,

flow rates can increase up to 100 times and are often accompanied by rapid glacier-front advances (Lefauconnier and Hagen, 1991). Ice velocities may vary between 2-5 m and up to 100 m per day during active surge phases. Active surge phases typically last 1-3 years whereas intermediate quiescent phases persist for 30-100 years (Meier and Post, 1969).

Although surging glaciers remain rather unknown, it appears that long (10-75 km) glaciers at high altitudes yield a higher potential to surge (Clarke et al., 1986). Climate variations may not affect surges but nevertheless have an effect on surge periods. However, surging glaciers put a limiting factor on the connection of glacier variations to climate variabilities (Liestøl, 1993).

The surge in itself can be divided into three stages of development. Initially, surface lowering can be observed in the upper part of the glacier, followed by thickening in the lower part of the glacier which leads to well-developed surge dynamics (Sund et al., 2009). However, some surges cease after stage two and never fully develop an active surge phase. This behaviour might be misinterpreted as rapid response to climate change (Sund et al., 2009).

1.3.1 Surge-Type Glaciers on Svalbard

According to Lefauconnier and Hagen (1991), 90% of Svalbard's glaciers are or have been of surge-type. Exact numbers are still undetermined. Nevertheless, it is widely agreed on that the majority of glaciers are or used to be of surge-type (Liestøl, 1969; Sund et al., 2009; Farnsworth et al., 2016). Compared to other regions, Svalbard's glaciers move considerably slower with active phases lasting 3-10 years and quiescent phases between 50-500 years (Dowdeswell et al., 1991; Benn and Evans, 2010). While active phases appear to be independent of glacier size (Dowdeswell et al., 1991), a glacier orientation in a broad arc clockwise from northwest to southeast seems to favour surge-behaviour (Jiskoot et al., 2000). Furthermore, a polythermal regime and fine-grained, potentially deformable beds are auxiliary to the surge potential of glaciers in Svalbard (Hamilton and Dowdeswell, 1996; Jiskoot et al., 2000).

The surge of Bråsvellbreen between 1936 and 1938 is considered to be a major surge that occurred recently (Solheim et al., 1990). Due to the increase in annual air temperatures after the LIA, most of Svalbard's glaciers have negative mass balance at present leading to a reduced intensity of glacier-surge activity (Dowdeswell et al., 1995). Glaciers which surged after the LIA now fail to accumulate the mass required to reinitiate surges and/or have switched from a polythermal to a cold-based regime. Tunabreen in central Spitsbergen and Blomstrandbreen in northern Spitsbergen are exceptions to this behaviour (Flink et al., 2015; Burton et al., 2016).

1.3.2 Surge Mechanism

Currently, there is no consensus about the triggering mechanisms for glacier surges. Meier and Post (1969) and Sharp (1988*a*) first suggested oscillations in conditions at the glacier bed to be a factor and eliminated the influence of external forcing such as earthquakes. Two ideas have been discussed since then - a hydrologic or a thermal switch initiating glacier surges (Clarke, 1976; Murray et al., 2003).

The hydrologic switch suggests that glacier surges are initiated by fundamental and pervasive changes in the geometry and water-transport characteristics of the system causing a built-up of higher water pressure (Kamb et al., 1985). This is often due to the change from an efficient subglacial conduit system during the quiescent to an inefficiently linked cavity system during active phase resulting in higher water storage (Kamb et al., 1985; Raymond, 1987). The theory is also used to explain changes in basal hydrology frequently observed during surges.

The thermal-switch theory suggests a change in the glacier's thermal regime (Fowler et al., 2001). Cold based-glaciers may be susceptible to thermal and dynamic instabilities if ice thickening raises basal temperatures. Thus, driving stress may lead to an increase in ice deformation and frictional heating at the glacier bed. The positive feedback between strain heating and ice creep causes an increase in ice temperatures up to pressure melting point. Continuous heat generation will melt ice and produce water at the bed which then acts as gliding layer (Fowler et al., 2001; Benn and Evans, 2010; Sevestre et al., 2015). With reinitiated thinning, the glacier resumes its cold-based regime after the surge.

Sevestre et al. (2015) combined the two ideas in their theory of enthalpy cycling. Glaciers must even out enthalpy gain by glacier flux with heat conduction and/or meltwater discharge to maintain a steady-state. An imbalance between energy accumulation and dissipation will lead to an unsteady glacier behaviour. Surges are considered to be a result of dynamic instabilities but relate to environmental forcing (Sevestre et al., 2015; Sevestre and Benn, 2015).

As previously mentioned, glaciers may change from a surge to a non-surge-behaviour based on climatic influences affecting thermal regime and mass accumulation in the reservoir area (Dowdeswell et al., 1995; Sevestre and Benn, 2015).

1.3.3 Surge Landforms

Glacier surges may leave traces on glaciers and the surrounding landscape. Landforms prove to be helpful in the reconstruction and classification of glacier surges. Glaciers often retain highly crevassed surfaces even decades after the end of the surge phase. Folded medial moraines, frontal changes and folded frontal moraines are often indicative of surge behaviour (Lefauconnier and Hagen, 1991).

Crevasse-squeeze ridges (CSR) are assumed to be unique landforms for glacier surges and are considered to be a useful tool in the classification of previous surge-type glaciers (Farnsworth et al., 2016). They have been observed on land (Sharp, 1985*a*; Evans and Rea, 1999; Schomacker et al., 2014; Lovell et al., 2015) and under water where they are often referred to as rhombohedral ridges or geometrical ridge networks (Ottesen and Dowdeswell, 2006; Ottesen et al., 2008; Flink et al., 2015; Burton et al., 2016; Lovell and Boston, 2017).

Icebergs often occur in front of tidewater glaciers during the active phase of a surge (Dowdeswell, 1989). Iceberg keels leave submarine ploughmarks behind acting as helpful indicators for glacier surges (Lefauconnier and Hagen, 1991).

The climatic state before and after glacier surges poses an important factor on the preservation of landforms (Lønne, 2014).

1.4 Landsystem Model Approach

Glacial landforms commonly appear in assemblages. They reflect a range of processes in specific glacier environments which can be used to connect sediments, landforms and landsystems with depositional processes (Benn and Evans, 2010).

Landsystem models for glacier forefields have been developed for a range of settings: Land- and marine-terminating glaciers exhibiting surge- and non-surge behaviour (Evans and Rea, 1999; Glasser and Hambrey, 2001; Plassen et al., 2004; Ottesen and Dowdeswell, 2006; Ottesen et al., 2008; Ingólfsson, 2011). Several landforms occur within all landform assemblages. Therefore, individual landforms are often not diagnostic for single glacier types but assemblages of landforms have proven to be a distinct tool for identification. Evans and Rea (1999) point out the significance of identifying surging glaciers and ice streams in glaciated landscapes to understand and reconstruct ice-sheet dynamics and climate.

Although landsystem models are considered to be a helpful tool, one must not forget that they are still simplified models and that glaciers often occur in more complex systems (Evans and Rea, 2003). Thus, it is still possible that case studies may miss surge landforms while glaciers are of surge-type (Evans and Rea, 1999; Ingólfsson, 2011). Case studies may also differ from the proposed model (Brynjólfsson et al., 2014) and landform proportions may vary (Ottesen et al., 2008). Furthermore, as the climate changes it is more common that glaciers exhibit a mixed marine and terrestrial termination (Flink et al., 2015; Allaart, 2016); consequently, existing landsystem models do not apply. A more extended approach by merging marine and terrestrial datasets may present helpful in the future.

As this work focuses on marine-terminating glaciers, only tidewater-glacier landsystems are referred to. Nonetheless, proposed models show clear similarities with
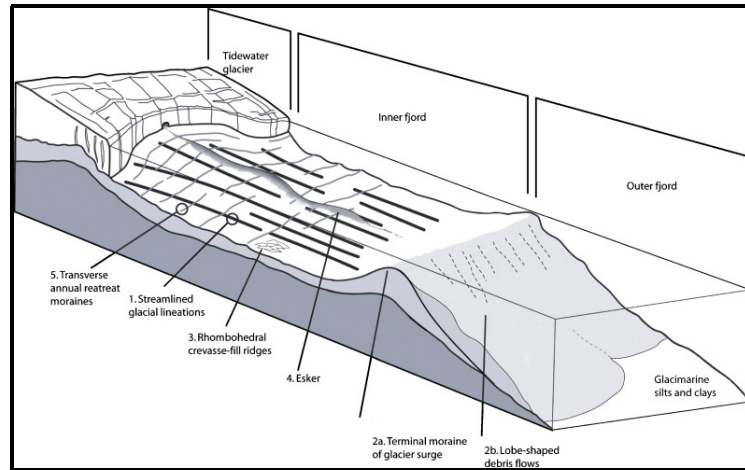
(A)
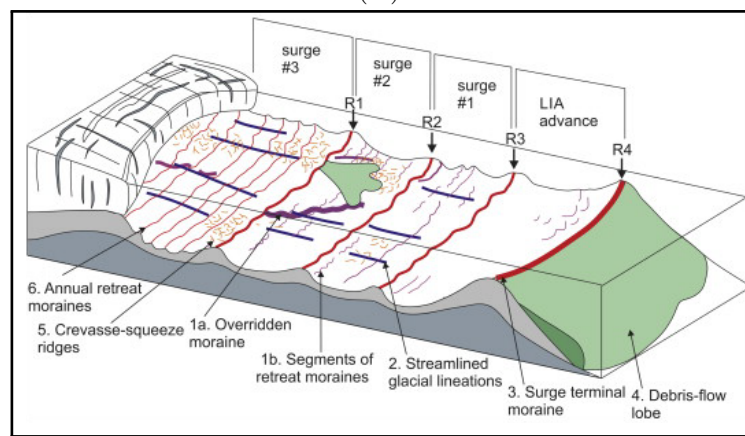
(B)
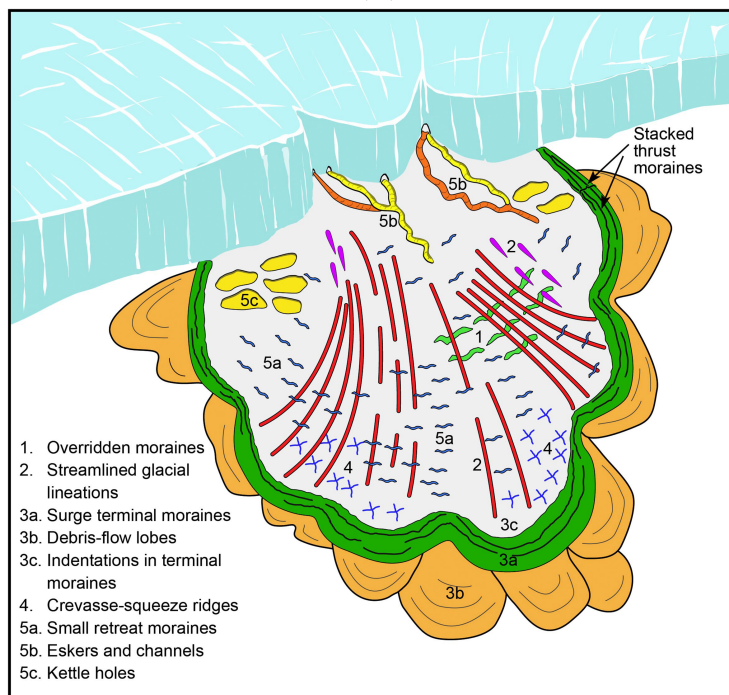
(C)

land-based landsystem models from Iceland and Svalbard (Sharp, 1985*b*; Evans and Rea, 2003).

1.4.1 Tidewater-Glacier Landsystems

A number of landsystem models for tidewater glaciers of surging and non-surging type have been developed based on marine geophysical evidence (Figure 1.1) (Plassen et al., 2004; Ottesen and Dowdeswell, 2006; Ottesen et al., 2008). Marine landsystem models are often considered as more complete since landforms are less exposed to post-depositional subaerial processes of erosion and periglacial activity (Ottesen and Dowdeswell, 2006; Ottesen et al., 2008).

Surging Behaviour

Ottesen and Dowdeswell (2006) and Ottesen et al. (2008) (Figure 1.1A) developed landsystem models for both known and suspected surge-type glaciers. Not only the presence of landforms but also their cross-cutting relationship is crucial to determine the order of formation processes. The models include a terminal moraine in the outer fjord with lobe-shaped debris flow on the distal side. The inner part exhibits streamlined glacial lineations, CSRs, eskers and annual retreat moraines.
Flink et al. (2015) (Figure 1.1B) refined the previously named model for frequently surging glaciers. Landforms become modified and overprinted by subsequent surges leading to a more complex assemblage. Multiple moraines based on individual surges were added to the model, and eskers were removed from the model.
While previous work focused on a restrictive fjord setting, Ottesen et al. (2017) (Figure 1.1C) developed a schematic model for submarine landforms linked to glacier surges into an open marine setting - a setting widely common in eastern Svalbard. The model presents an arcuate-shaped terminal moraine as landforms are not constraint by fjord walls. It also presents an often indented ice-proximal side of terminal

Figure 1.1 *(preceding page)*: Landsystem models for tidewater glaciers in Svalbard based on different scenarios. A) Landsystem model modified by Ottesen et al. (2008). The model is based on multiple tidewater glaciers in western Spitsbergen. B) Landsystem model modified by Flink et al. (2015) demonstrating assemblage affected by multiple surges. The model is based on Tunabreen in central Spitsbergen. C) Land-system model by Ottesen et al. (2017) for surging glaciers in an open-marine setting. The model is based on nine tidewater glaciers in eastern Svalbard including Besselsbreen on Barentsøya.

moraines. Streamlined lineations are distributed in fan-shaped patterns and kettle holes were added as a common feature.

Non-surging Behaviour

The first landsystem model for sedimentation of tidewater glaciers in the high Arctic was developed by Plassen et al. (2004) based on both surge-type and non-surging glaciers in Svalbard. The model exhibits glaciogenic deposits in proximal and distal basins. A terminal moraine marking the Neoglacial maximum extent separates the two basins. While the distal basins is filled with stratified sediments with a low amount of ice-rafted debris (IRD) and debris lobes, consists the proximal basin of morainal ridges, hummocky moraines and glaciomarine infill sediments. Nevertheless, the model lacks streamlined glacial lineations, CSRs and eskers in comparison to the surge-type setting.

2 Late Quaternary History of Eastern Svalbard

Ice sheets covered the Barents Sea multiple times during the Quaternary. Submarine landforms such as ice-marginal features (e.g. trough-mouth fans) and flutes provide evidence for the presence and extent of earlier ice sheets (Elverhøi and Solheim, 1983; Solheim et al., 1990; Elverhøi et al., 1993; Svendsen et al., 2004a; Ottesen and Dowdeswell, 2009; Dowdeswell et al., 2010a).

Grounded glaciers often erode and remove pre-existing deposits from fjord basins leading to depositional sequences in fjords typically being limited to the last glacial-interglacial cycle (Forwick et al., 2010). Therefore, sedimentological evidence is most complete from the Late Weichselian ice sheet (Svendsen et al., 2004a) due to its relative young age.

The SBSIS reached the shelf edge during the Last Glacial Maximum (LGM) around 24 ka BP (Landvik et al., 1998; Jessen et al., 2010). At that point, fast flowing ice streams drained the ice-sheet through fjords while less active ice covered the inter-fjord areas (Landvik et al., 2005; Ottesen et al., 2007; Landvik et al., 2014). Outer shelf areas started to become ice-free on the western margin of Svalbard around 20.5 ka BP (Jessen et al., 2010). Major parts of the Barents Sea were deglaciated by 12 ka BP while Svalbard was still fully covered by ice (Hormes et al., 2013; Ingólfsson and Landvik, 2013; Hughes et al., 2016). Around 10 ka BP, Svalbard's coasts and fjords became finally ice-free (Figure 2.1A) (Ingólfsson and Landvik, 2013).

Terrestrial and marine archives both present helpful in the reconstruction of extent and dynamics of the past glaciations and deglaciations (Ingólfsson, 2011). One unsolved question is the structure of the SBSIS. Depending on evidence, ice domes were proposed in multiple places such as north of Kong Karls Land (Mangerud et al., 1992b; Salvigsen et al., 1992a; Landvik et al., 2005; Svendsen et al., 2004b; Ingólfsson and Landvik, 2013), in the southern Hinlopen Strait area (Dowdeswell et al., 2010b; Hogan et al., 2010a) and centred on Nordaustlandet (Hormes et al., 2011; Flink et al., 2017b). The idea of multiple domes occurring through phases of the ice sheet is considered to be likely (Dowdeswell et al., 2010b; Hormes et al., 2013; Ingólfsson and Landvik, 2013).

The Lateglacial to early Holocene period is characterised by a rapid transition from a glacial to an interglacial environment on Svalbard (Ingólfsson, 2011; Hormes et al.,

2013; Landvik et al., 2014). Thus deglacial unloading began in eastern Svalbard by 10.5 ka BP (Forman et al., 2004) leading to a total uplift of 89 m until today at Kapp Ziehen (Figure 3.1B) (Bondevik et al., 1995).
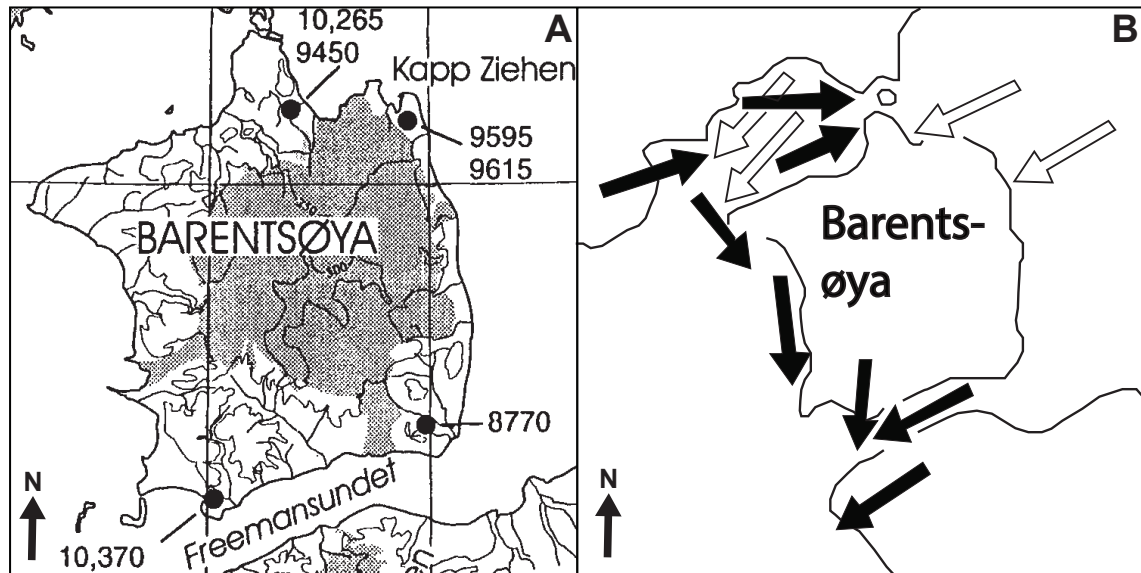
Figure 2.1: (A) Deglaciation dates in years before present on Barentsøya based on driftwood, shells and shell fragments, modified by Landvik et al. (1995). (B) Map of main ice movement around Barentsøya. Open arrows show direction of ice movement during the Svalbard Barents ice sheet. Black arrows show ice-movement direction during subsequent deglaciation. Directions are based on striated bedrock. Modified by Salvigsen et al. (1992a).

2.1 Holocene Glacial History

Svalbard's Holocene glacial history still exhibits a fair amount of blank areas as data is sparse and unevenly distributed. Landvik et al. (1992a) suggest that deglaciation of Barentsøya was mostly driven by ice calving into Olgastretet (Figure 3.1B) prior to 10.3 ka BP on the east coast and a few hundred years later on the west coast (Figure 2.1A). Abundant striae and erratics on Frankenhalvøya (Figure 3.1B) indicate last ice movement to have occurred from SW to NE across the peninsula. Thus, Kapp Ziehen was earlier deglaciated than Frankenhalvøya (Landvik et al., 1992a; Salvigsen et al., 1992a). Striated roche moutonnées on Kükenthalvøya (Figure 3.1B) imply ice movement from approx. SW towards 70° (Figure 2.1B) (Salvigsen et al., 1992a, 1995). The earliest bivalves (*Nuculana Pernula*) found on Barentsøya date back

to 10,265 ± 95 BP (Figure 2.1a) (Landvik et al., 1992a). Whereat other reported dates from Barentsøya and Edgeøya are likely to postdate the last deglaciation by at least 1000 years. Nevertheless, striae at Sundneset (Figure 3.1B) were presumably caused by a glacier in Freemansundet fed by high-lying areas on southern Barentsøya (Figure 3.1B) (Salvigsen et al., 1992a, 1995). The glacial striae found correspond with the idea of an ice dome located north of Kong Karls Land (Mangerud et al., 1992b; Landvik et al., 1998; Svendsen et al., 2004b; Ingólfsson and Landvik, 2013). Although evidence is sparse, moraines and glacial deposits indicate an early Holocene glacier readvance on Svalbard (Salvigsen et al., 1990; Lønne and Lyså, 2005; Forwick et al., 2010; van der Bilt et al., 2015; Farnsworth et al., 2017).

Subsequent to the readvance, the early Holocene is marked by a warm period - the Holocene thermal maximum (HTM). The HTM was initiated by increased Atlantic water inflow and the northward passing of the Polar front and therefore resulting feedback processes (Jessen et al., 2010; Rüther et al., 2012; Mangerud and Svendsen, 2017). Length and timing of the HTM are still discussed and vary between literature and location. It is assumed that the HTM lasted from 11.2 ka BP to 5.5 ka BP (Salvigsen et al., 1992a,b; Jessen et al., 2010). Van der Bilt et al. (2015) propose that the HTM reached its culmination around 9.5 ka BP while Mangerud and Svendsen (2017) found temperatures at least as warm as present but 6°C higher in August between 10.2 ka BP to 9.2 ka BP based on molluscs. Therefore, Svalbard's glacier cover was significantly reduced with small cirque glaciers disappearing completely (Svendsen and Mangerud, 1997; Snyder et al., 2000; Forwick et al., 2010; van der Bilt et al., 2015).

The HTM is displayed on Barentsøya by a change from glacier-proximal to marine deposits (Landvik et al., 1992a). Other indicators on Svalbard are the abundance of thermophilious molluscs and lower amounts of IRD suggesting a warmer climate than present.

Gradual decrease in temperatures lead to the onset of the Neoglacial cooling period around 5 ka BP (Gjerde et al., 2017; Mangerud and Svendsen, 2017). Svendsen and Mangerud (1997) suggest that present glaciers formed around 2500 years ago. After a Medieval warm period around the 12th century, the Neoglacial ended and climaxed with the largest and most significant glacial phase in the Holocene - the Little Ice Age (Humlum et al., 2005; Mangerud and Svendsen, 2017). Terrestrial and submarine moraines and lake sediments suggest that the LIA peaked between 1890 and 1920 on Svalbard with maximum glacier extent (Svendsen and Mangerud, 1997; Snyder et al., 2000; Grove, 2004; Humlum et al., 2005; Błaszczyk et al., 2009). Since then, annual air temperatures have risen by almost 5°C (Svendsen and Mangerud, 1997; Humlum et al., 2003, 2005; Nordli et al., 2014).

Martín-Moreno et al. (2017) suggest that Barentsjøkulen has lost 106.8 km^2 of ice resulting into 17.5% area loss since the LIA based on lateral-moraine positions.

Dowdeswell et al. (2018) go even further and propose a recent retreat of 130 km^2, 20% more than suggested by Martín-Moreno et al. (2017) based on the analysis of multibeam bathymetric data.

2.2 Research History of Barentsøya

Limited research was carried out on Barentsøya in the past owing to its remote location and limited access.

The first map showing Barentsøya was created in 1710 by Cornelis Giles and Outger Rep. However, at that time it was believed to be a part of Ny Friesland - the north-eastern part of Spitsbergen. Barentsøya was not recognised as a separate island until the 19th century (Lock et al., 1978). Multiple expeditions passed the island on their way but first accurate maps were not created until 1901.

In 1870, Heuglin visited Duckwitzbreen on his expedition to the Arctic Ocean. He describes the moraines as debris-ridge with beds striking parallel to the coast and dipping east. He considers the glacier to be in retreat (von Heuglin, 1872).

In 1901, Vasiliev created the first accurate map of Barentsøya's west coast including Duckwitzbreen (Figure 3.5) as part of the Russo-Swedish 'Arc of Meridian' expeditions between 1899 and 1901. The map shows the piled up moraine and Anderssonøyane. The latter were partly overrun by Duckwitzbreen as described by Tyrrell (1921) who was prospecting on behalf of the Scottish Spitsbergen Syndicate of Edinburgh in 1919 and 1920. He estimated a glacier advance of 5.4 km.

In 1927, the Hamburgische expedition visited Duckwitzbreen and first photographs of the moraine were captured (Figure 3.4) (Gripp, 1929). The photographs show that Duckwitzbreen did not overrun its frontal moraine but likely removed its remains sideways.

The Stauferland expedition visited Barentsøya in 1959 at Sundneset analysing the active layer and valley forming processes (Büdel, 1960). The expedition was followed by the Stockholm University Svalbard expedition in 1966 studying glacial uplift all around Svalbard (Schytt et al., 1968).

In May 1986, two radio-echo sounding profiles were obtained to determine ice thickness of Barentsjøkulen. The two profiles were arranged that ice thickness of all three major outlet glaciers was determined. Ice thickness was measured between 150 m and 200 m for the outlet glaciers and the ice cap has a maximum thickness just above Besselsbreen of 270 m (Dowdeswell and Bamber, 1995).

The PONAM expedition has been the most extensive fieldwork carried out on Barentsøya so far (Möller et al., 1992). Although the initial plan was to find sediments predating the Late Weichselian, most data obtained were of younger age. Glacial striae, beach ridges and sections were logged and dated to determine time of

deglaciation, isostatic uplift and ice-movement directions on Barentsøya (Landvik et al., 1992a; Mangerud et al., 1992b; Salvigsen et al., 1992a).

In 2015, the SEES expedition was able to retrieve sediment cores at Andersjøen, a lake located at Sundneset on Barentsøya. Time of isolation from marine waters was determined between 2500 and 3000 years ago (Hoek et al., 2016). Further, the ecological changes in the lake due to increase in annual air temperatures for the past ∼100 years were analysed (Woelders et al., 2018).

Obtained multibeam bathymetric data was used by Ottesen et al. (2017) to analyse geomorphic imprints of glacier surges into open-marine waters (Ottesen et al., 2017). The same data was used to determine ice loss by Dowdeswell et al. (2018). Satellite data was used by Martín-Moreno et al. (2017) using lateral moraines to determine ice loss.

3 Regional Setting

3.1 Barentsøya

Barentsøya is located between 78° 10' 10" N to 78° 30' 50" N and 20° 10' E to 22° 20' E (Figure 3.1). The island is separated from Spitsbergen by Ginervrabotnen and Heløysundet. Freemansundet separates the island from Edgeøya. The almost square-shaped island is with an area of 1288 km^2 the forth largest island of the Svalbard archipelago. The island consists mostly of plateau mountains with a maximum altitude of 654 m.a.s.l. (NPI, 2014). Barentsøya is covered by the Barentsjøkulen ice cap.

In older literature, Barentsøya is referred to as *Barents Land, Barents Øy, Barentsland, Barents-maa, Berensland, Bæren-I., Lorentsland, South East Land, Sydostland, Zuyd Ooster Land* (NPI, 2003).

3.2 Climate of Eastern Svalbard

Svalbard is located close to a confluence of ocean currents and air masses with differing thermal characteristics; warm waters of the northernmost margin of the North Atlantic Drift influence the weather on the west coast of the archipelago, while polar currents flow south along the eastern coast (Humlum et al., 2007). Particularly in winter, large weather variations are observed due to colliding mild air masses from the south and cold air masses form the north (Hanssen-Bauer et al., 1990; Humlum et al., 2007; Serreze and Barry, 2014).

The longest weather records for the high Arctic are recorded since 1911 at Svalbard airport (Førland et al., 1997, 2010; Nordli et al., 2014). Normal annual precipitation is measured at 190 mm at Svalbard airport which is located in an inner fjord setting (Figure 3.1A) and 525 mm at Isfjord Radio located at the mouth of Isfjorden on the west coast (Figure 3.1A) (Førland et al., 1997). The average annual air temperature is -7°C in Svalbard which is characteristic for a polar climate (Humlum et al., 2007). A general increase in temperature (Steffensen, 1982; Hanssen-Bauer et al., 1990) and precipitation of up to 25% (Førland et al., 1997) has been recorded since the beginning of weather recordings in 1911.

No extensive weather records exist from Barentsøya and very sparse data from the
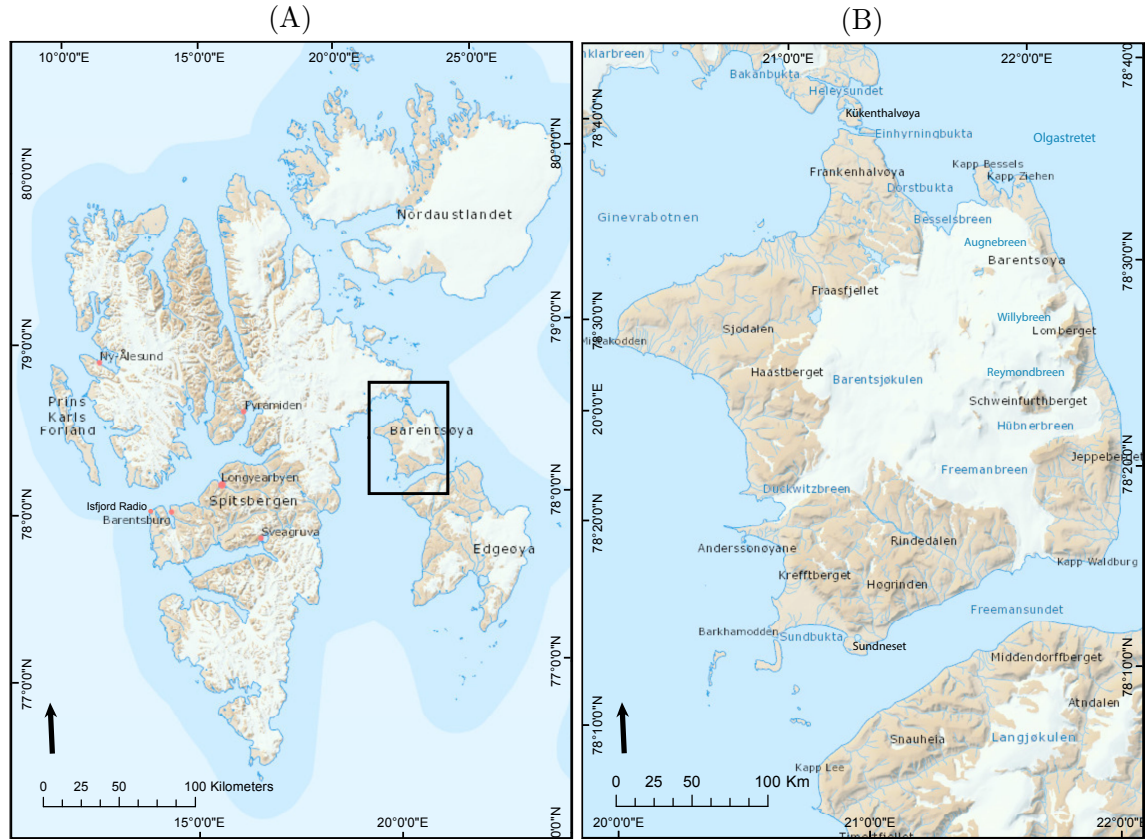
Figure 3.1: Topographic map of A) Svalbard and B) Barentsøya including position of all glaciers further mentioned NPI (2018).

eastern part of Svalbard in general. With polar currents affecting temperatures and sea-ice extent, eastern Svalbard experiences a colder climate than Longyearbyen (Summerhayes, 1928). Extensive amounts of sea ice have been covering the eastern part of Svalbard influencing the climate (Benestad et al., 2002) and leading to a later onset of spring in the south-east (Nordli et al., 2014). With temperatures rising, periods with sea ice become shorter and seasonal variabilities stronger (Dallmann, 2015). Where polar currents meet warm drift from south-east, fog often occurs, mostly during the summer months June and July (Summerhayes, 1928; Steffensen, 1982; Hanssen-Bauer et al., 1990). Thus, Pelt et al. (2016) suggests mean annual air temperatures to be 4-8°C lower in eastern Svalbard compared to central Spitsbergen.

Liestøl (1993) suggests that Barentsøya's glaciers profit from relatively moisture-laden southeasterly winds and that due to comparatively constant summer temperatures, a decrease of precipitation is a causing factor for glacier retreat. The asymmetry of Barentsøya's ice cap also suggests a decrease of precipitation from

east to west (Dowdeswell and Bamber, 1995).

3.3 Geology of Barentsøya

Barentsøya constitutes predominantly of Triassic sedimentary rocks (Figure 3.2) (NPI, 2016).

The oldest beds date back to the Upper Permian and are present in a small area in the northeastern part of the island. They constitute of alternating sandstone and silicious limestone (Harland et al., 1997). Brachiopods are abundant in the beds which are oriented in a gently southwestward-plunging syncline with a maximum thickness of 300 m (Hjelle, 1993).

The main part of the island comprises Triassic, almost undeformed, flat-lying beds of shales, siltstones and sandstones with a maximum thickness of 700 m (Flood et al., 1971; Dallmann, 2015). The sediments were most commonly deposited in near river estuaries and shallow marine shelf environments (Hjelle, 1993). A thin but widespread coal seam extends through the Upper Triassic part (Flood et al., 1971). The otherwise gently dipping Triassic beds show intensive folding on a NE-SW trending axis at Mistakodden (Figure 3.1B) in the far west of Barentsøya (Hjelle, 1993).

Dark dolerite sills or less common dykes occur at the transition from Jurassic to Cretaceous (Hjelle, 1993; Dallmann, 2015). The intrusions are most prominent in the north of Barentsøya around Frankenhalvøya (NPI, 2016).

While the Triassic sedimentary rock is poorly consolidated and easily weathered, the dolerite intrusions, sills and dykes yield helpful evidence in the reconstruction of past ice movement directions (Salvigsen et al., 1992a).

Quaternary sediments are primarily present in the coastal areas and in proximity of the glacier margins (Dallmann, 2015). They consist in greater parts of moraine deposits, raised shore deposits and glacio-fluvial deposits (Dallmann, 2015). Block fields cover greater parts of the island (Hjelle, 1993).
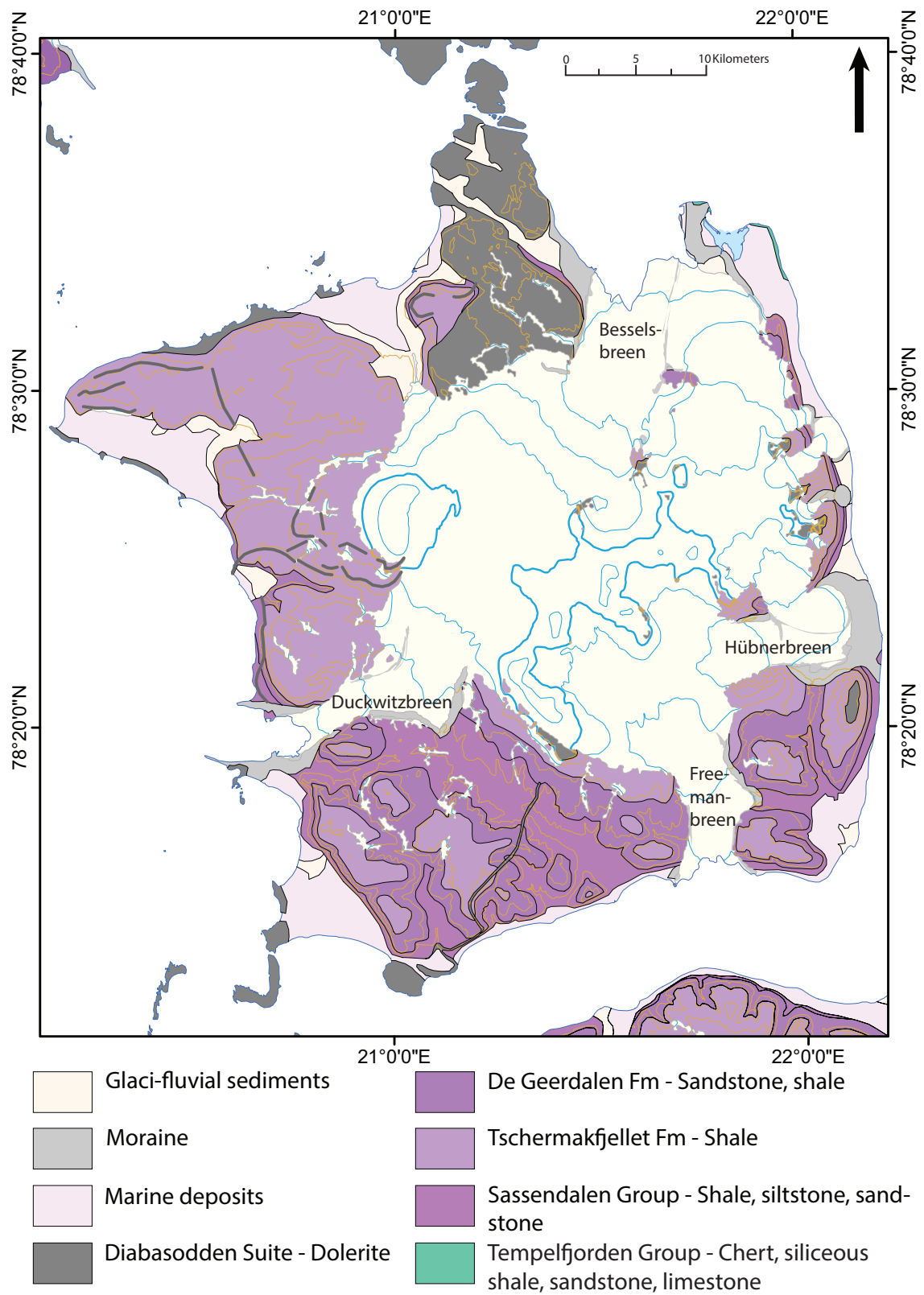
Figure 3.2: Detailed map covering the geological formations and structures on Barentsøya (NPI, 2016).

3.4 Glaciers of Barentsøya

The ice cap Barentsjøkulen covers 42% of Barentsøya with an area of 509 km^2 (GLIMS, 2018). Multiple outlet glaciers drain the ice cap (Table 3.1).Besselsbreen, Duckwitzbreen and Freemanbreen are considered to be the main outlet glaciers while smaller glaciers such as Augnebreen, Handbreen, Willybreen, Isormen, Reymond-breen and Hübnerbreen in the east of the island play a less important role in the drainage of the ice cap (Figure 3.1B) (Błaszczyk et al., 2009; Martín-Moreno et al., 2017).

The ice cap has a maximum ice thickness of 270 m with parts its bed at pressure melting point leading to a basal hydrological system in place (Dowdeswell and Bamber, 1995). Snow line elevation has been measured at 350 m a.s.l. on the eastern flank and at 400 m a.s.l. on the western flank of Barentsjøkulen (Dowdeswell et al., 1995). Glacier terminus observations have shown a negative mass balance for the outlet glaciers of Barentsjøkulen. Dowdeswell et al. (1995) suggest that changes in the mass balance are climatically-induced.

This thesis focuses on the above named larger outlet glaciers as all of them are or used to be marine-terminating in recent history. Comparatively high-resolution bathymetric data enable mapping of recent subglacial landforms and reconstructing the history of the Barentsjøkulen ice cap.

Table 3.1: List of main outlet glaciers on Barentsøya based on Lefauconnier and Hagen (1991), Hagen et al. (2003) and NPI (2003). Length and area are based on GLIMS (2018).

Glacier name	Coordinates	Area [km^2]	Length [km]	Type	Frontal Characteristics	Flow Direction
Augnebreen	78° 30' N 21° 41' E	69.1	16.1	outlet	calving	N
Besselsbreen	78° 32' N 21° 32' E	122.2	18.8	outlet	calving	N
Duckwitzbreen	78° 20' N 20° 30' E	86.5	14.7	outlet	calving	SW
Freemanbreen	78° 15' N 21° 30' E	89.7	18.4	outlet	calving	S
Hübnerbreen	78° 20' N 22° 00' E	48.1	14.9	outlet	land terminating	E
Reymondbreen	78° 20' N 22° 00' E	31.6	8.8	outlet	land terminating	SE
Willybreen	78° 30' N 22° 00' E	7.2	5.5	outlet	Piedmont	NE

3.4.1 Besselsbreen

Besselsbreen is located in the north-eastern part of Barentsjøkulen. The tidewater glacier covers an area of approx. 122 km^2 and has a maximum length of 18.8 km (GLIMS, 2018). Separated by a medial moraine, the glacier terminates into Dorstbukta west of Augnebreen. First evidence of the glacier's terminus position is an oblique photograph acquired by the Norwegian Polar Institute (NPI) in 1936 (Figure 3.3).

In 1936, the glacier extended over the eastern coast line but was constrained along its western shoreline. The lateral moraine to the west suggests that Besselsbreen reached its maximum before 1936 most likely during the LIA (Lefauconnier and Hagen, 1991). The glacier forms a low-gradient large lobe into the sea with a smooth, uncrevassed surface. The front edge appears to be situated only a few meters above the surface and the tongue is interpreted to be nearly floating (Lefauconnier and Hagen, 1991). The presence of tabular icebergs (Figure 3.3) supports the idea of a temporarily floating glacier terminus (Dowdeswell, 1989; Ottesen et al., 2017).

With most of its basin situated below equilibrium line altitude in 1936, Besselsbreen is prone to retreat (Lefauconnier and Hagen, 1991). Glacier retreat is also visible above sea level at the glacier boundary. Continuous retreat has been recorded since 1936 with the lateral moraine on the eastern side of the glacier front being washed away (Figure 3.3). Lefauconnier and Hagen (1991) estimate retreat rates of 100 $\frac{m}{a}$ between 1936 and 1970 and a stagnation of retreat rates to 30 $\frac{m}{a}$ after 1970 (Figure 5.9). Thus, the glacier front has retreated from a basin with 60 m depth to a shallow sea area (Lefauconnier and Hagen, 1991).

Ottesen et al. (2017) created a submarine geomorphological map of the submarine glacier forefield of Besselsbreen. The created map shows a ridge separating an eastern and a western basin and a large terminal ridge suggested to be either from LIA maximum position or an earlier surge. Although no surge has been recorded for Besselsbreen, Ottesen et al. (2017) assume the presence of rhombohedral ridges may be indicative for strong basal crevassing often associated with surge activity. Nonetheless, Lefauconnier and Hagen (1991) classify the glaciers Besselsbreen in combination with Augnebreen as glaciers which are able to surge in the near future but are less likely to do so.

The glacier can also be found under the name *Defantbreen* (Büdel, 1960) in combination with Augnebreen.

3.4.2 Duckwitzbreen

Duckwitzbreen is a glacier located on the western part of Barentsøya. With a length of 14.7 km, the glacier covers 86.5 km^2 (GLIMS, 2018). The former tidewater glacier
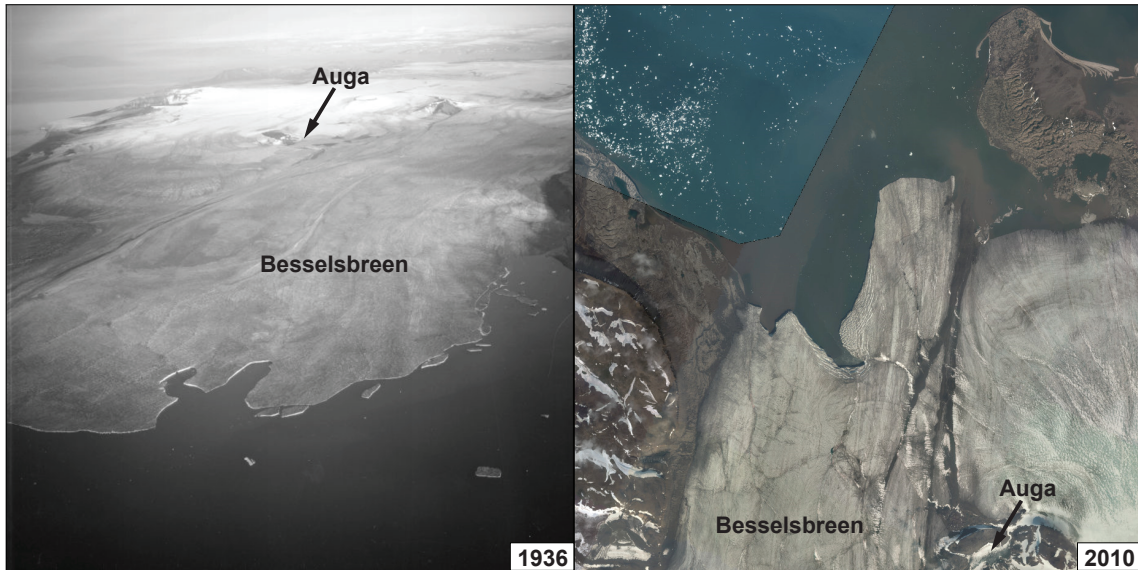
Figure 3.3: Aerial photographs of Besselsbreen demonstrating glacier terminus movement through time (NPI, 1936 and 2010).

used to terminate into Storfjorden.

Duckwitzbreen was first noted by von Heuglin (1872) who described the presence of a moraine along the entire front (van der Meer, 2004). Based on Heuglin's description, Gripp (1929) interprets the moraine as a push moraine. A map from the Russo-Swedish expedition in 1901 shows the glacier front in the same place (Figure 3.5). In 1919, Tyrrell (1921) discover that the glacier front had advanced 5.4 km partly overrunning Anderssonøyane (Figure 3.5). Previous moraine material was pushed sideways instead of overrun. The southern part of the glacier's terminus shows tremendous folding, crumpling and contortion of the stratigraphic planes of the ice (Figure 3.4) (Tyrrell, 1922). Gripp (1929) describes the ice lobe as only marginally extended leaving secondary push moraines at the sides. Lefauconnier and Hagen (1991) explain the advance by a surge that occurred either in the same or the previous two years. Liestøl (1993) determines 1918 as surge year.

Figure 3.4: Photograph of the SW end of Duckwitzbreen. The right side shows a considerably lowered glacier surface linked to a profound push moraine complex to the left side. Modified by Gripp (1929).

Aerial photographs show Duckwitzbreen relatively close to its maximum extension in 1936 (Figure 3.5). The surface was still interrupted by numerous crevasses and the marine part of the moraine showed waves characteristic for push moraines. A depression was visible in the upper basin with a step of geological origin 5-6 km away from the shore line. Small icebergs produced by calving were presumably stopped by the end moraine (Lefauconnier and Hagen, 1991). Lefauconnier and Hagen (1991) describe the retreat rates as very low and names ablation by melting a more important factor for ice-mass loss. On later observations and at present, it appears that most large parts of the frontal moraine have been washed away.

Duckwitzbreen likely reached its maximum extension during its surge in 1918 and has not been recorded surging since then (Lefauconnier and Hagen, 1991). Due to shallow sea, thick sediments and the frontal push moraine, no extensive calving occurred as usually typical for surging glaciers (Solheim, 1986).

Presently, Duckwitzbreen is no longer a tidewater-glacier as it retreated on land. It is now in the process of building a new land-based frontal moraine (Figure 3.5) (Lefauconnier and Hagen, 1991).

Duckwitzbreen has previously been mentioned as *Andersons-Gletscher*, *Duckwitz Gl.* (von Heuglin, 1872) and *Gregory Glacier* (Tyrrell, 1921) (NPI, 2003).
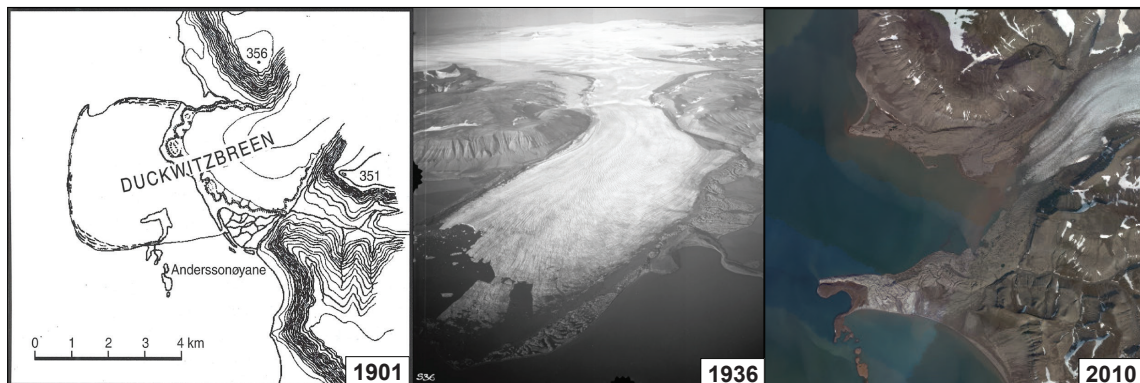
Figure 3.5: Historical map of Duckwitzbreen (left) demonstrating terminus position previous to and after surge in 1918, modified by van der Meer (2004). Aerial images showing Duckwitzbreen's terminus position in 1936 (centre) and 2010 (right) (NPI, 1936 and 2015).

3.4.3 Freemanbreen

Freemanbreen is a tidewater outlet glacier of Barentsjøkulen located in the south of Barentsøya which terminates into Freemansundet. The glacier is 18.4 km long and covers and area of 89.7 km^2 (GLIMS, 2018). First visual evidence of Freemanbreen can be found on aerial photographs by the NPI in 1936 (Figure 3.6).
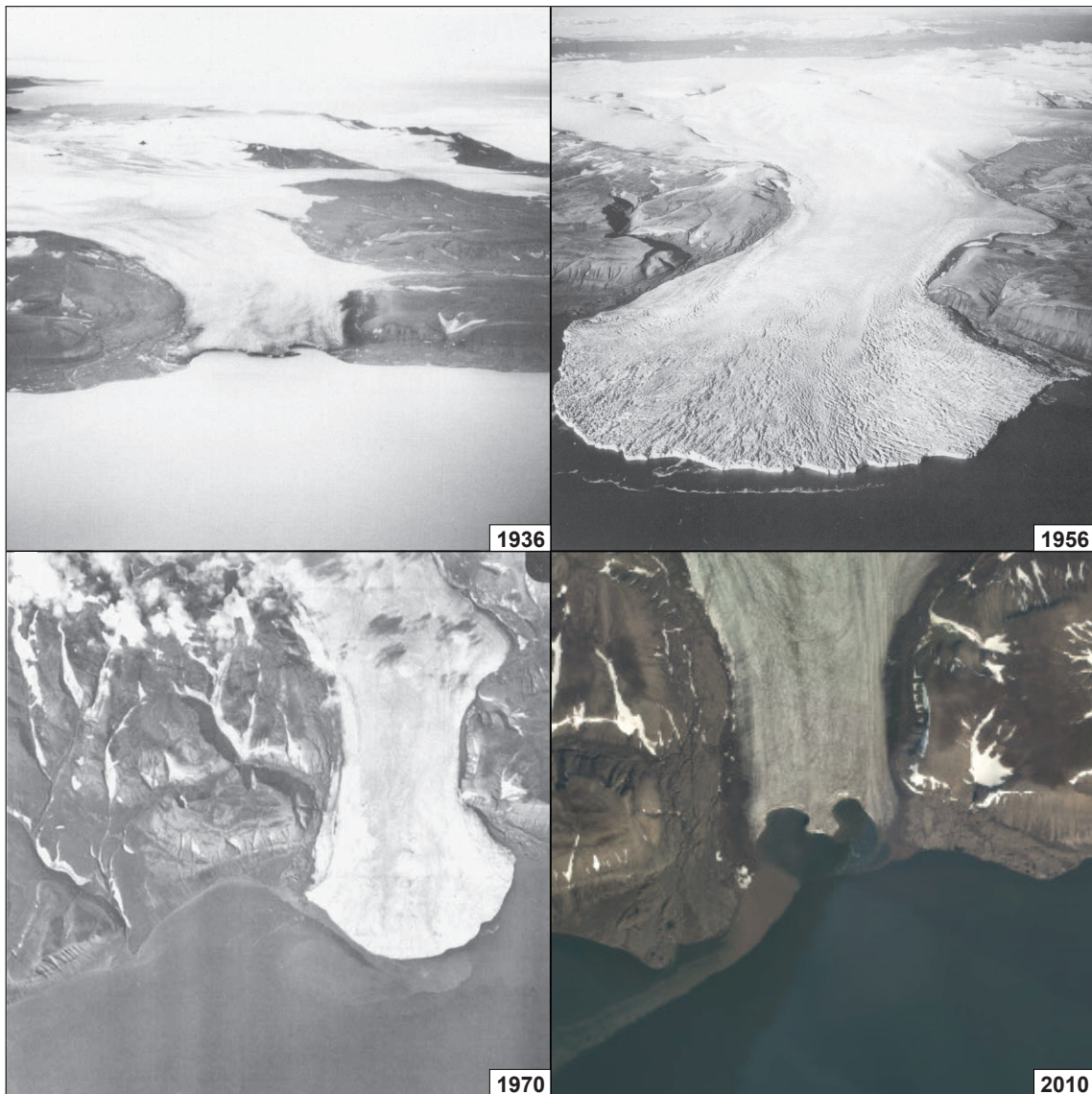
Figure 3.6: Aerial photographs of Freemanbreen. Rapid advance due to surging between 1955 and 1956 is clearly visible by comparing the images of 1936, 1956 and 1970. Today, the glacier is about to retreat on land and is unlikely to surge again (NPI, 1936, 1956, 1970 and 2015).

In 1936, Freemanbreen appears to be retreating from an important maximum extension which it has reached many years before (Lefauconnier and Hagen, 1991). Based on the morphology of lateral moraines on shore, the glacier developed a very large lobe into the sea. Marine maps published in 1987 support the idea by large arc-shaped ridges under water (Lefauconnier and Hagen, 1991).

Freemanbreen was recorded surging between 1955 and 1956 (Liestøl, 1993). The glacier did not reach its previous maximum position during the surge but produced

two submarine moraine ridges with a distance of 200 m (Lefauconnier and Hagen, 1991). A third ridge about 800 m to 1000 m downstream is classified to have been established by the LIA maximum by Lefauconnier and Hagen (1991). A comparison of aerial photographs shows differences in glacier terminus behaviour (Figure 3.6). The first rapid advance is associated with the active phase of a surge and the second is a more general retreat from moraine systems likely dating from a LIA maximum linked to changing environmental conditions (Figure 3.6) (Dowdeswell and Bamber, 1995).

Retreat rates were slow after the recorded surge with frontal position significantly close to surge position (Figure 5.9). Lefauconnier and Hagen (1991) estimates retreat rates to less than 10 $\frac{m}{a}$ accelerating to about 90 $\frac{m}{a}$ after 1970.

Freemanbreen has previously been named *Ascherson Gletscher* (von Heuglin, 1872) and *Freeman Strait Glacier* (NPI, 2003).

3.4.4 Other Glaciers

The following glaciers are part of the Barentsjøkulen ice cap and terminated into the sea at their maximum extension. However, due to lack of multibeam bathymetric data and their limited extent compared to previously mentioned glaciers, no geomorphological mapping was carried out in front of these glaciers. Nevertheless, their existence cannot be overseen and they do contribute to the dynamics of the ice cap. Furthermore, their glacier retreat has to be taken account of when calculating overall ice loss for Barentsjøkulen since the LIA.

Augnebreen

Augnebreen is a glacier located east of Besselsbreen in the northeastern corner of Barentsøya. The two glaciers are separated by a medial moraine ridge reaching all the way to the termini. Higher up, the two glaciers are disconnected by lake Auga (Figure 3.3). The tidewater glacier is 16.1 km long and covers an area of 69.1 km^2 (GLIMS, 2018).

Equally to Besselsbreen, first evidence of Augnebreen's terminus extent can be found on an oblique photograph from 1936 (Figure 3.3). At that time, the northern lobe of the glacier reached the shoreline but no calving was effective (Lefauconnier and Hagen, 1991). No surges are recorded for Augnebreen but Lefauconnier and Hagen (1991) classify the glacier in combination with Besselsbreen as able but less likely to surge in the near future.

Today Augnebreen's terminus shape (Figure 3.7) is very rounded making future surges unlikely. The glacier does terminate into Dorstbukta such as Besselsbreen. Nevertheless, Besselsbreen is the driving glacier in between the two and had major

impact on the seafloor, while little retreat can be observed from Augnebreen. Büdel (1960) names the glacier *Defantbreen* combining Augnebreen and Besselsbreen as one glacier.

Figure 3.7: Aerial photograph of Augnebreen in 2015 demonstrating the rounded, low-crevassed tongue (Anders Skoglund (NPI), 2015).

Hübnerbreen

Hübnerbreen is a land-terminating outlet glacier located in the eastern part of Barentsøya (Figure 3.1B). The glacier has a length of 14.9 km and covers an area of 48.1 km^2 (GLIMS, 2018). First information about the glacier can be found on aerial photographs taken in 1936.

Based on the analysis of the morphology of lateral moraines and grounded till, it is suggested that Hübnerbreen has reached the sea during its maximum extension (Lefauconnier and Hagen, 1991). The glacier has likely formed a large lobe into the sea and calving must have occurred. Taking into account that the glacier terminus was located 2 km from the shoreline in 1936, the maximum extension presumably was reached a long time before but cannot be pinned down to the LIA (Lefauconnier and Hagen, 1991).

Hübnerbreen was almost split into an upper and a lower part during its retreat. A boundary between those two parts appears as a depressed area on the surface and is caused by an important subglacial drainage system stretching over the entire width of the glacier (Lefauconnier and Hagen, 1991). Subglacial channels connected two lateral lakes.

In 1936, the two parts of the glacier were marked by an important step. While the upper part showed a significant number of crevasses and very convex lateral moraines, the subglacial drainage between the two parts was turned off (Lefauconnier and Hagen, 1991). As a result, only the upper part is assumed to have been affected by a surge which had already ended by 1936 (Lefauconnier and Hagen, 1991).

Hübnerbreen acted as a buffer for Reymondbreen's surge in 1956 with its lower part being severely affected by the surge. Large parts of the surge energy of Reymondbreen was dispersed into Hübnerbreen's front. Nonetheless, the two glaciers did not advance all the way to the sea as otherwise expected (Lefauconnier and Hagen, 1991).

The glacier has also been mentioned as *Hübner Gl.* (von Heuglin, 1872) and *Ritter-Eis* (Büdel, 1960).

Reymondbreen

Reymondbreen is a land-terminating outlet glacier in the eastern part of Barentsjøkulen (Figure 3.1B). The glacier expands over a length of 8.8 km and covers an area of 31.6 km^2 (GLIMS, 2018). It is first visible on aerial photographs in 1936. Like Hübnerbreen, Reymondbreen reached the sea well before its first recognition in 1936 (Lefauconnier and Hagen, 1991). Aerial images from 1956 show Reymonbreen surging. The neighbouring glacier's front was highly affected by the surge as pressure ran diagonally towards it (Lefauconnier and Hagen, 1991). This is also visible on aerial images in 1970 as the glacier front was continuously vertical.

As most energy of its surge was dispersed into Hübnerbreen, Reymondbreen did not reach the sea in 1956.

Willybreen

Willybreen is a small outlet glacier in the east of Barentsøya and north of Hübnerbreen and Reymondbreen. The glacier covers an area of 7.2 km^2 with a length of 5.5 km (GLIMS, 2018).

The glacier developed a lobe into the sea at its maximum extension. Nevertheless, calving hardly occurred (Lefauconnier and Hagen, 1991). Willybreen receded from being a tidewater to a land-terminating glacier between 1936 and 1970 (Lefauconnier and Hagen, 1991). Willybreen has also been named *Nansen Gl.* in the literature (NPI, 2003).

4 Methodology

4.1 Material

4.1.1 Bathymetry

High-resolution swath bathymetry datasets covering the submarine glacier forefields of Freemanbreen and Besselsbreen were collected by the Norwegian Hydrographic Service (NHS) in 2007 using the Kongsberg echosounder system EM3002D and EM 3000, respectively. The data were gridded to a 10 x 10 m isometric grid.

In 2013, a high-resolution swath bathymetric dataset at Duckwitzbreen's submarine glacier forefield was collected by UNIS using the Kongsberg EM2040 multibeam echosounder installed on UNIS' small research vessel 'Viking Explorer'. These data were gridded using a grid cell size of 2 x 2 meters.

The depth data collected by the NHS were reproduced according to the permission 13/G706.

4.1.2 Satellite Imagery and Aerial Imagery

Aerial images of the glacier fronts of Besselsbreen, Duckwitzbreen and Freemanbreen were collected in 1936, 1970, 2010, 2011 and 2015 (Table 4.1). The images were reproduced during flight campaigns carried out by the Norwegian Polar Institute. Images from 1936 and 2015 were taken at an oblique angle while the rest is vertically oriented. Aerial images taken in 2010 and 2011 were retrieved by taking screenshots of TopoSvalbard (NPI, 2018).

4.1.3 Historical Maps

A map covering the terminus position of Duckwitzbreen in 1901 drawn by Vasiliev and later modified by Tyrrell (1921) was copied from van der Meer (2004) (Figure 3.5).

4.1.4 GLIMS Glacier Database

The GLIMS Glacier Database is a project monitoring glaciers worldwide. Optical satellite instruments such as SPOT-5 and ASTER gather the data. Work on

Svalbard is implemented in collaboration with the NPI. Glacier margins and area measurements of Barentsøya's glaciers were captured in the years 2001, 2004 and 2008 (Table 4.1).

4.2 Methods

4.2.1 Geomorphological Mapping

Based on the analysis of bathymetric data, geomorphological maps of submarine landforms in front of three tidewater outlet glaciers were generated for Besselsbreen, Duckwitzbreen and Freemanbreen. Geomorphological mapping as a method has developed considerably over the years as the understanding of landform formation improved (Smith et al., 2011).

Multibeam swath bathymetric datasets were visualised in 3D, and cross-sections were drawn using the QPS Fledermaus software package. Geomorphological mapping was carried out in ArcMap 10.4.1. Bathymetric datasets were visualised and analysed both in colour and grayscale.

Landforms were distinguished by their shape and surface texture. Cross-sections were created using Fledermaus and were consulted to confirm landform interpretation. Geomorphological maps were compiled using ArcMap in a scale of 1:75,000 for Besselsbreen, 1:15,000 for Duckwitzbreen and 1:20,000 for Freemanbreen.

4.2.2 Georeferencing and Projection

All data imported to ArcMap was georeferenced using the UTM 33N coordinate system and projection, and WGS84 datum. While bathymetric datasets were already georeferenced, the aerial images required rectifying and georeferencing. Mountain tops, river bends and coast lines were identified on the satellite basemap as ground control points to georeference aerial image screenshots from the years 2010 and 2011 in ArcMap. Overlapping screenshots were then georeferenced to each other also using snow patches, whenever necessary.

4.2.3 Symbols and Legend

Surface covers and larger landforms are represented by polygons (Figure 5.1). Elongated landforms such as glacial lineations, eskers and channels are represented by polylines.

In order to maintain consistency, similar legends and symbols were applied to all maps for landforms both on land and under water.

Table 4.1: List of data types and sources utilised for geomorphological mapping.

Year	Source	Data Type	Resolution/ scale	Original numbers
1901	van der Meer (2004)	Historical Map	1 : 150,000	-
1936	NPI	Oblique aerial image	3000m altitude	S36_3638, 3680, 3841
1956	NPI	Oblique aerial image	-	S56_1393
1970	NPI	Vertical aerial image	-	S70_4568
1991	Lefauconnier and Hagen (1991)	Maps	1:100,000	Glacier front position reconstructed based on aerial imagery
2001	GLIMS	Glacier information, ESRI Shapefiles	-	104032 (Handbreen), 104033 (Augnebreen)
2004	GLIMS	Glacier information, ESRI Shapefiles	-	104027 (Hübnerbreen, 104028 (Reymondbreen), 104030 (Isormen), 104031 (Willybreen)
2007	NHS	Bathymetry	10 x 10 grid	Barentsøya
2008	GLIMS	Glacier information, ESRI Shapefiles	-	103897 (Besselsbreen), 103907 (Freemanbreen), 103908 (Duckwitzbreen), 103909 (Solveigdomen S), 103910 (Solveigdomen N)
2010	NPI	Vertical aerial image	40-50 cm	13920/616, 652, 654, 730, 737, 739, 741, 755, 757, 774, 776
2010	NPI	DTM	5 m	-
2011	NPI	Vertical aerial image	40-50 cm	25166/16
2013	UNIS	Bathymetry	2 x 2 grid	Duckwitzbukta
2015	NPI	Oblique aerial image	-	NP057864, NP061759, NP061986

4.2.4 Ice Front Position Reconstruction

Barentsjøkulen has been in overall retreat since the LIA (Dowdeswell and Bamber, 1995). An overview map of Barentsøya showing glacier terminus position in the past was created in a scale of 1:115,000. Ice front positions were reconstructed using available historical maps, Esri shape files provided by the GLIMS glacier database, aerial imagery and ice front position maps previously published by Lefauconnier and Hagen (1991) (Figure 5.9, Table 4.1).

Two glacier front positions of Duckwitzbreen were reconstructed using historical maps. Aerial images were used to reconstruct ice front position in 1936, 1970, 2010 and 2011. Five ice front positions were reconstructed by georeferencing maps provided by Lefauconnier and Hagen (1991). The ice front positions in 2008 are based on the Esri shape files provided by the GLIMS glacier database. Ice front positions from 2012 are based on the satellite basemap provided by the Norwegian Polar Institute. LIA ice front position of Besselsbreen are based on the position of their submarine terminal moraine ridges interpreted to have been formed during LIA maximum extent.

4.2.5 Ice Loss Calculation

The area of ice loss since the LIA was calculated using swath bathymetric data, the historical map of Duckwitzbreen and aerial imagery. LIA maximum extension were interpreted based on terminal moraine positions on land and under water. ESRI shape files provided by the GLIMS glacier database were used for current glacier extension (GLIMS, 2018). Areas between maximum extension and the shape files were mapped and calculated in ArcMap 10.4.1. The calculated area was then compared to Dowdeswell et al. (2018) (Figure 5.10).

5 Results

Three geomorphological maps were created covering the marine glacier forefields of Besselsbreen (Figure 5.2), Duckwitzbreen (Figure 5.3) and Freemanbreen (Figure 5.4). The maps cover a seafloor area of 98.4 km^2 at Besselsbreen, 8.78 km^2 at Duckwitzbreen and 9.70 km^2 at Freemanbreen. Additionally, prominent geomorphological features were mapped in the subaerial forefields of the glaciers. Furthermore, aerial images of the entire island were studied to detect glacial landforms helpful for the reconstruction of Barentsjøkulen's dynamics.

The subaerial data were acquired in 2010 and 2011 while multibeam bathymetric data was obtained during two campaigns in 2007 at Besselsbreen and Freemanbreen and in 2013 in Duckwitzbukta.

Small gaps between submarine and subaerial datasets occur in coastal areas where ships were unable to navigate due to shallow water depth.

As this work focuses mostly on submarine data, terrestrial mapping covers larger and more prominent landforms such as moraine ridges, smaller ridges and eskers.

Glacial Lineations
Esker
Outline
Channels
Lobate Ridges
Rhombohedral Ridges
Crescentic Ridges

Retreat Moraines
Bedrock
Kettle Holes
Debris-Flow Lobes
Medial Moraine
Terminal Moraine
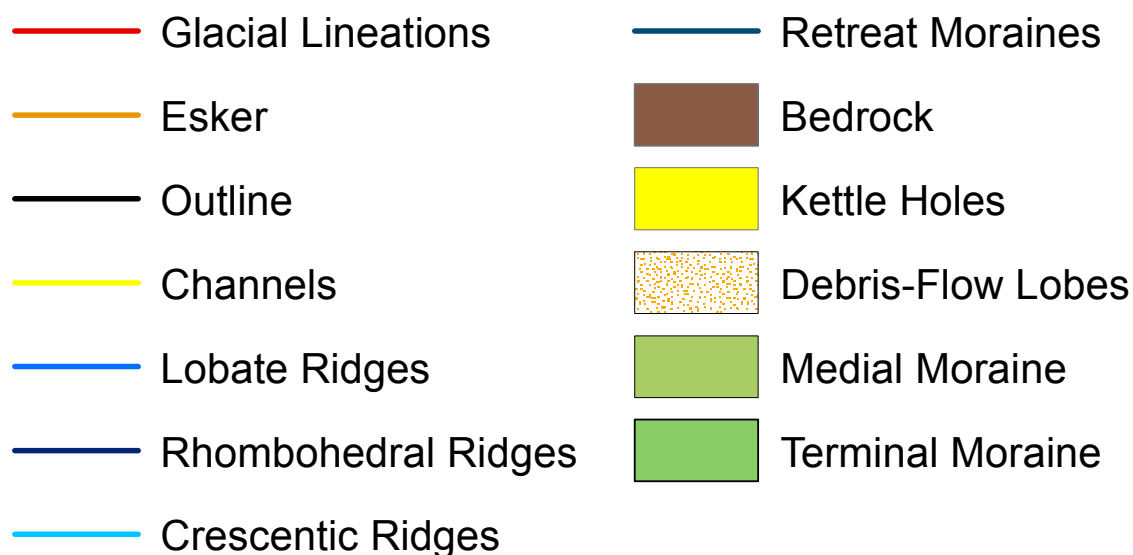
Figure 5.1: Legend for geomorphological maps. Similar symbology has been used for all glacier forefields.
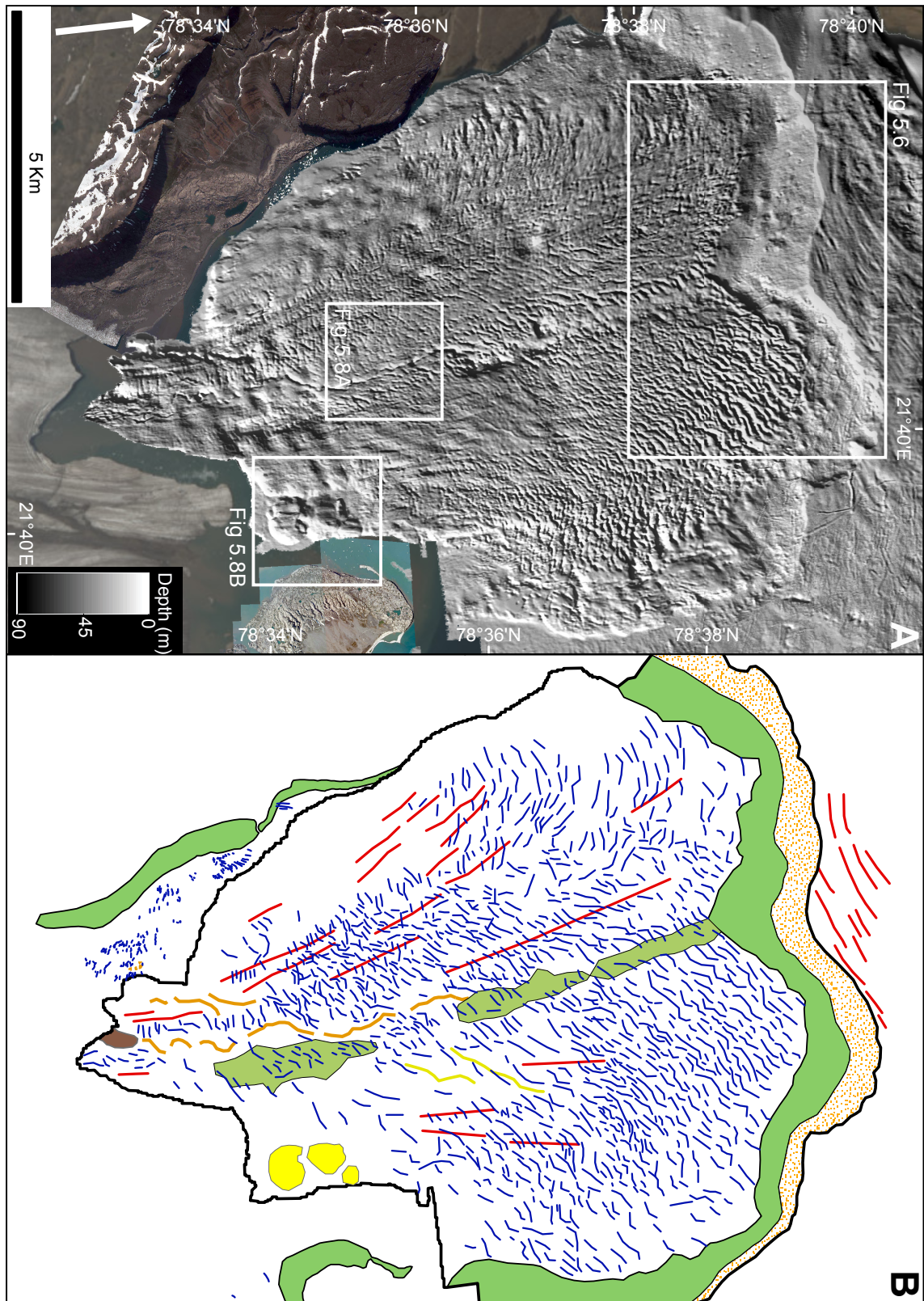
Figure 5.2: A) Bathymetric map of Dorstbukta in front of Besselsbreen and B) its geomorphological interpretation. Squares indicate zoomed-in areas in Figures 5.6 and 5.8.
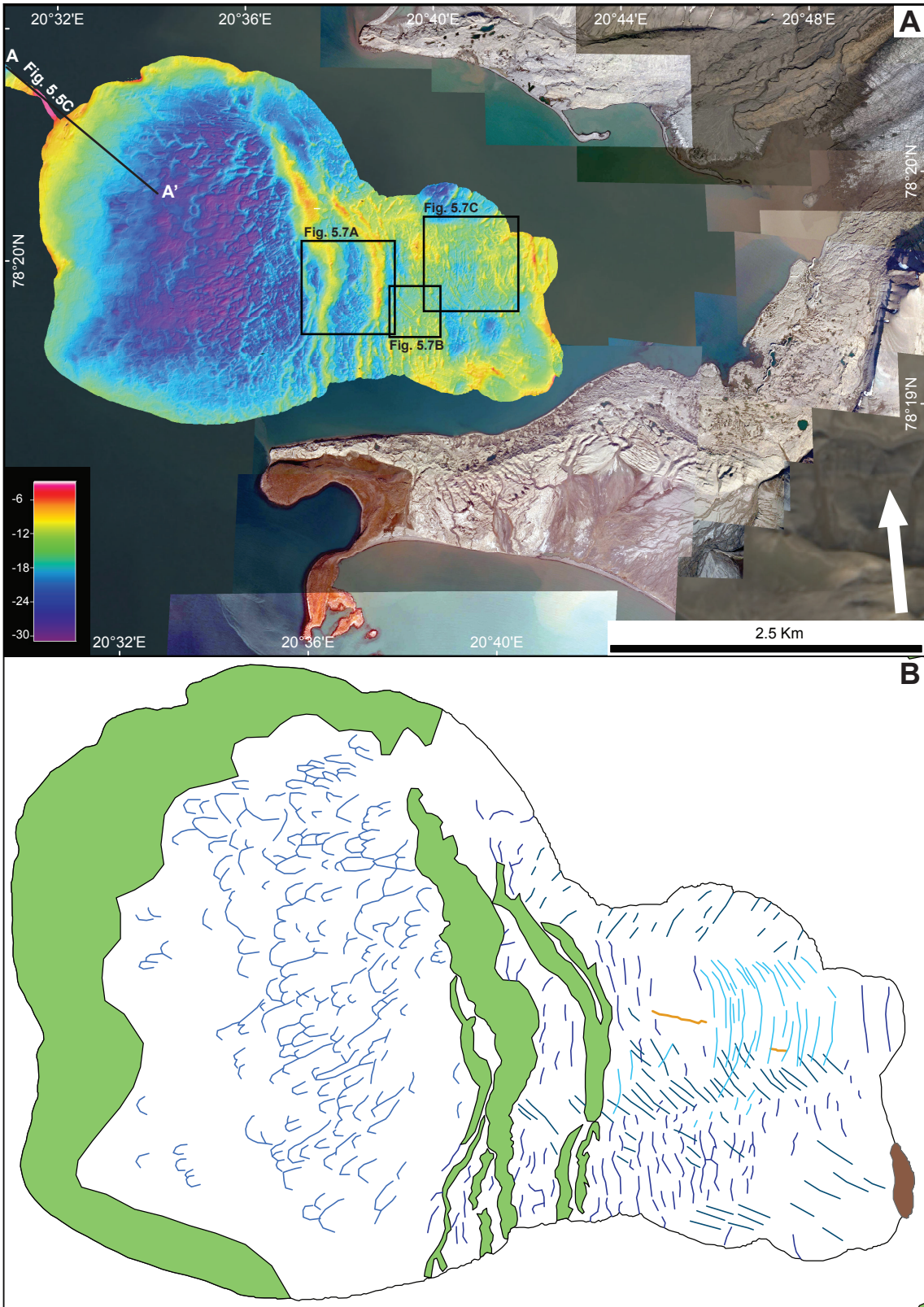
Figure 5.3: A) Bathymetric map of Duckwitzbukta and B) its geomorphological interpretation. The squares indicate zoomed-in areas in Figure 5.7. Corresponding cross-section to indicated line is visible in Figure 5.5.
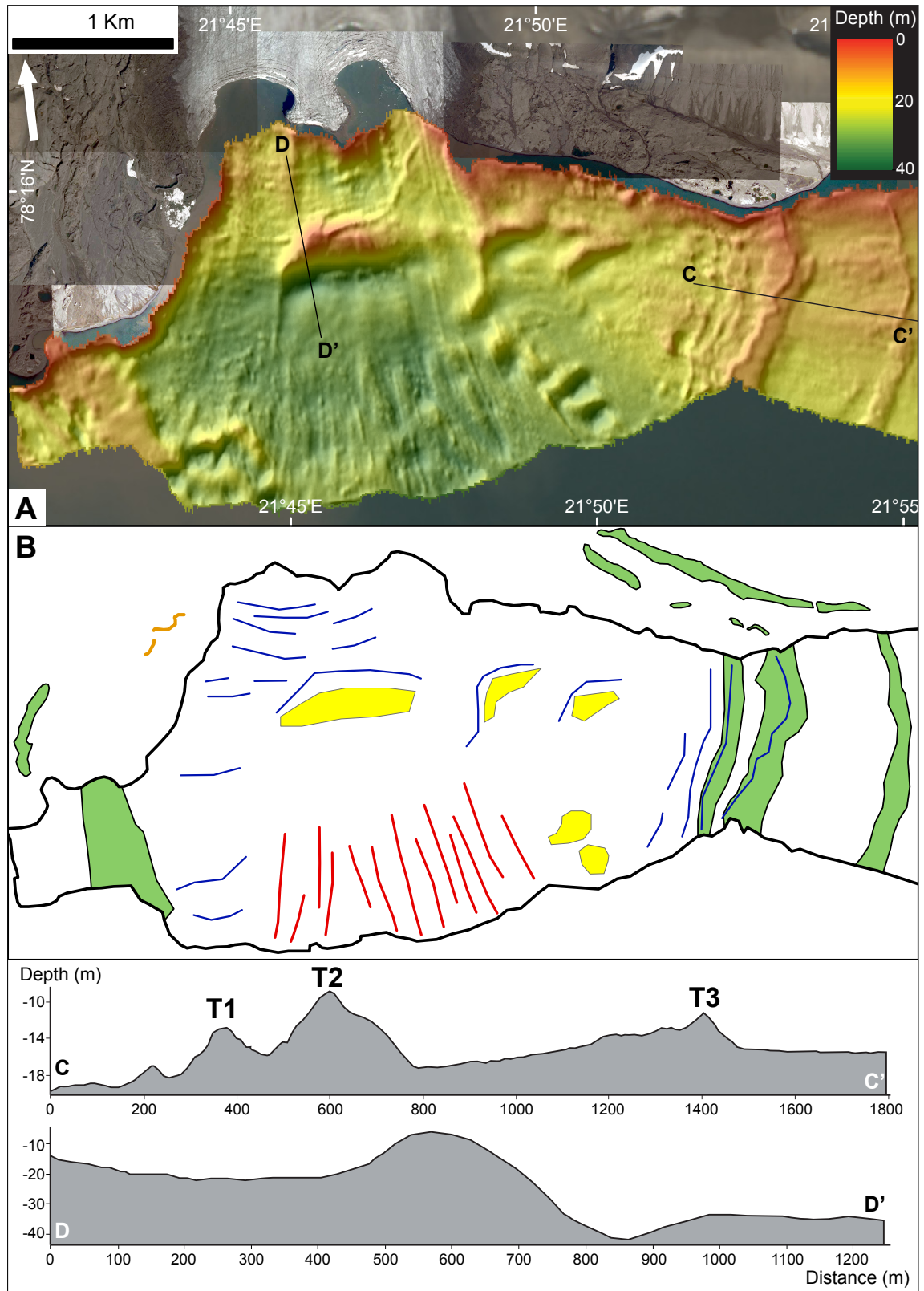
Figure 5.4: A) Bathymetric map of Freemansundet and B) its geomorphological interpretation. C) cross-section of terminal moraine ridges, extent indicated in A). D) cross-section of small retreat moraine and corresponding depression, extent indicated in A).

5.1 Submarine Landforms

5.1.1 Streamlined Bedforms - Glacial Lineations

Description

Elongated, fjord-parallel, streamlined bedforms were observed within the areas of the terminal moraine ridges of Besselsbreen (Figure 5.2) and Freemanbreen (Figure 5.4). Their lengths vary from 500 m up to 5 km. Heights of up to 2.7 m were measured and widths range from $\sim$10 to $\sim$20 m. This yields maximum elongation ratios ($E = \frac{l}{w}$) of 1:25. For Besselsbreen, the streamlined bedforms are in general unevenly spaced, and they are orientated in a fan shape with azimuth angles between 315° and 20°. A number of streamlined bedforms are partially overprinted by small transverse ridges. At Freemanbreen, the subparallel set of bedforms occur around 3 km south of the glacier front (Figure 5.4).

A third set of elongated streamlined bedforms was identified north of the terminal moraine ridge of Besselsbreen (Figures 5.6A and C). Their lengths range between 500 m and 2000 m with an orientation subparallel to the terminal moraine ridge. One of the linear features appears to be overridden by the lobate features originating from the terminal moraine ridge (Figure 5.6A).

Interpretation

The streamlined characteristics and elongation ratios of the bedforms lead to the interpretation as glacial lineations produced by soft-sediment deformation at the glacier-bed interface (Stokes and Clark, 2002; King et al., 2009; Robinson and Dowdeswell, 2011). Glacial lineations are common features in Svalbard fjords and submarine troughs (Ottesen et al., 2008; Hogan et al., 2010a; Flink et al., 2017b; Flink and Noormets, 2017c). The determined elongation ratios are within the characteristic ratio of 10:1 for mega-scale glacial lineations. Mega-scale glacial lineations are interpreted to typically form under fast-flowing ice. Usually, they have a length of 100-200 km and widths of several km (Stokes and Clark, 2002; Ottesen et al., 2008). The glacial lineations found in front of Besselsbreen and Freemanbreen do not fit into the criteria to be of mega sale. Nevertheless, their elongation ratio is an indicator of fast flowing ice in soft deformation tills (Stokes and Clark, 2002; King et al., 2009). The fan-shaped orientation of lineations is likely due to the lack of constraining fjord sides in Dorstbukta (Ottesen et al., 2017) and Freemansundet. Glacial lineations are often used as indicators for fast-flowing ice in connection with glacier surges (Stokes and Clark, 2002; Ottesen and Dowdeswell, 2006; King et al., 2009). The lineations at Besselsbreen most likely formed during a major advance of Besselsbreen that also formed the terminal moraine. The glacial lineations at

Freemansundet are interpreted to be the results of Freemanbreen's surge in 1955 and 1956.

Based on their orientation vertical to ice flow direction and their location outside of the major transverse ridge, the glacial lineations situated north of Besselsbreen's terminal moraine are interpreted to have formed by a separate ice flow. The suggested ice flow at the time of formation is from SW to NE. Ice flow direction is in accordance with Landvik et al. (1992a) suggesting similar ice flow during disintegration of the SBSIS during Late Weichselian.

5.1.2 Large Transverse Ridges - Terminal Moraines

Description

Large transverse ridges are present in all studied submarine and subaerial glacier forefields. The outer margin of Besselsbreen's submarine glacier forefield is marked by a prominent, continuous ridge stretching from the western to the eastern shore (Figure 5.2). The ridge is divided into two arcuate components, and is located ~12 km from the present glacier front. Its crest ranges in height between 20 m to 30 m compared to the surrounding terrain with its width varying between 500 m and 1.8 km (Figures 5.6A and B). At its glacier-distal end, an often uniform slope with a slope angle of 3° is observed dropping down and marking the end of the basin. The glacier proximal slope declines a an angle around 1°.

On land, the western part of Besselsbreen's glacier forefield is marked by a north-south trending discontinuous ridge which starts approx. 6 km from the glacier front and merges with Besselsbreen's lateral moraine (Figure 5.2A). The ridge is split in several parts by fluvial systems with sections ranging in width between 200 m and 500 m. The outer ridge flank exhibits a steeper gradient than the inner/glacier proximal part. The eastern part of he subaerial glacier forefield exhibits a folded ridge which appears to be a continuation of the subaqueous ridge which merges with the ice front in the south. The ridge ranges in width between 100 m and 600 m with a steeper slope gradient on the glacier distal side. The surface is affected by erosion and several fluvial systems cutting it.

In front of Duckwitzbreen, a large submarine transverse ridge stretches along the western extent of the bathymetric dataset Figure (5.3). The dataset does not cover the full extent of the ridge likely caused by the landform reaching above 10 m below sea level making ship navigation unsafe. However, a small track (Figure 5.3A) collected while the boat went inside the glacier forefield indicates the presence of a large transverse ridge. The dataset demonstrates the eastern part of a large arc-shaped ridge which stretches over ca. 3.5 km. The displayed slope ranges between

10 m and 23 m below sea level over a width of up to 500 m. The crest of the ridge reaches up to 4 meters below sea level giving the ridge a total height of 19 m. The submarine ridge is asymmetrical with a steeper glacier distal slope of 3.5°-4° and a shallower slope of 1.5° on the glacier proximal side (Figure 5.5). Due to limited mapping, little can be said about the glacier distal part of the ridge.

A set of two N-S aligned, medium cross-fjord ridges occur in the centre of the basin in front of Duckwitzbreen, separating the dataset in an eastern and a western basin (Figure 5.7A). The most prominent ridge lies to the west. The multi-crested ridge is 250 m wide at its widest point and reaches a height of 13 m. The ridges are asymmetrical with a steeper slope of 10°-15° on the glacier proximal side and a more gradual slope of 8°-10°on the glacier distal part (Figure 5.7D). More narrow ridges surround the bigger ridges and range between 100 m and 160 m in width with heights between 7 m and 9 m. The ridges have a slight crescentic shape which is convex to the ice front.

On land, two E-W aligned ridges can be found in the northern and southern glacier forefields of Duckwitzbreen. They both start around the position of the medium transverse ridges and stretch for more than 3 km until they join with the lateral moraines of the present glacier. Their width varies between 100 m and 800 m. Occasionally, the ridges are interrupted by fluvial systems.

Three major transverse ridges (T1, T2, T3) were identified in the bathymetric dataset in front of Freemanbreen (Figure 5.4). The first two ridges, T1 and T2, are located approximately 3 km away from the ice front with only 200 m distance in between (Figure 5.4C). Due to data limitations, not the entire extent of the ridges could be mapped. However, visible parts of the ridges suggest that all three ridges are arc-shaped. The most prominent parts of the ridges are visible in the east but similar ridge features also appear on the western side with corresponding heights and extent. Ridge T1 measures a height of 6 m while ridge T2 reaches up to 10 m in height (Figure 5.4C). Both ridges have an asymmetrical shape with steep glacier proximal slopes (3.5° and 2.5°) and shallower glacier distal slopes (2.3° and 2°), respectively.

Ridge T3 is located 800 m to 1000 m further east of ridge T1 and T2. The ridge is only 4 m high and exhibits an opposite asymmetrical shape with a steep glacier distal slope of 1.5° and a gradually ascending slope of 0.7° from ridge T2 to ridge T3 (Figure 5.4C).

On land, several large ridges were identified using aerial imagery (Figure 5.4B). On the eastern side of Freemanbreen, two discontinuous major ridges were located with around 250 m distance in between (Figure 5.4B). The ridges are oriented from NW to SE parallel to the ice margin. The ridges seem to connect with the submarine ridges. To the west, a similar set of major ridges was identified on land. They are also located parallel to the ice margin which is oriented almost N-S striking. The

ridges are discontinuous but meet up with the western part of the submarine ridges.

Interpretation

The large transverse ridges are interpreted as terminal moraines that stretch along the submarine and subaerial datasets. Shape and dimension concur with previously described terminal moraines on Svalbard (Ottesen and Dowdeswell, 2006, 2009; Kristensen et al., 2009; Ottesen et al., 2017). Terminal moraine ridges form by advancing glacier fronts pushing up sub- and proglacial sediments in front of their termini (Boulton et al., 1996; Kristensen et al., 2009). While terminal moraine ridges on the western part of Svalbard are often associated with LIA maximum extent (Lefauconnier and Hagen, 1991; Plassen et al., 2004; Ottesen et al., 2008), new evidence in eastern Svalbard suggests that terminal moraines may have formed through surges prior to the LIA (Flink et al., 2017a; Flink and Noormets, 2017c).
The presence of only one large terminal moraine in front of Besselsbreen indicates that it was formed by one major glacier advance, possibly the LIA (Lefauconnier and Hagen, 1991). The large ridges on land are a subaerial continuation of the terminal ridge. At Duckwitzbreen, the presence of two terminal moraines in front suggest at least one glacier surge. Based on a historical map (Figure 3.5) it is suggested that the outer moraine ridge was formed during the surge in 1918. Thus, the inner moraine ridges are interpreted to be the overwritten remains of the terminal moraine existing before the surge. At Freemansundet, three terminal moraine ridges suggest three major glacier advances. One surge was observed between 1955 and 1956 forming the innermost terminal moraine. Ridge T2 is interpreted to have formed during Neoglacial maximum extent, while the outermost terminal moraine is interpreted have formed at an earlier stage during the Holocene.
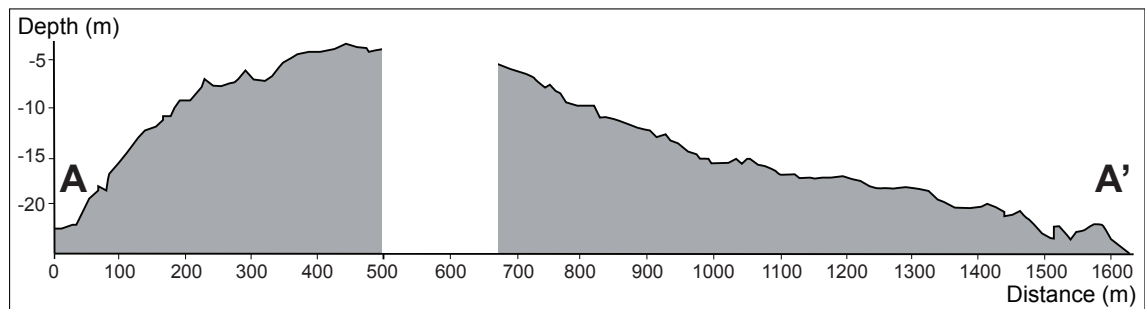
Figure 5.5: Cross-section of terminal moraine in Duckwitzbukta. For reference points, see Figure 5.3. The central gap is a result of missing data.
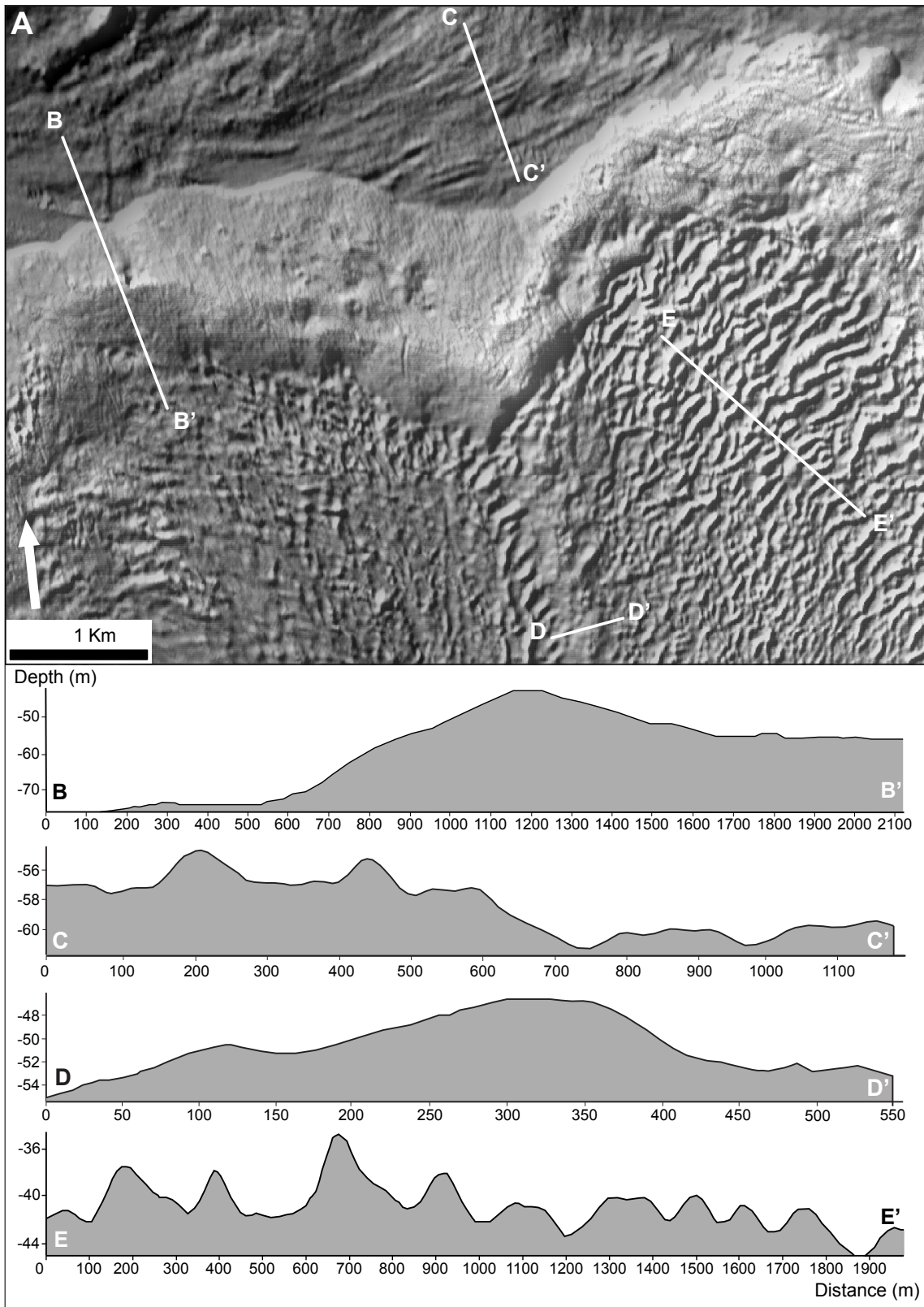
Figure 5.6: A) Landforms and their corresponding cross-sections occurring in front of Besselsbreen, see Figure 5.2A for reference. B) cross-section of terminal moraine, C) cross-section of glacial lineations outside of the glacier forefield, D) cross-section of medial moraine, E) cross-section of evenly spaced retreat moraines.

5.1.3 Sediment Lobes - Debris-Flow Lobes

Large, lobate accumulations of sediment cover the glacier distal flank of Bessels-breen's submarine terminal moraine ridge (Figure 5.2). The coalescing lobes cover an area of 6.2 km^2. The sediment lobes have a maximum width of 1.2 km. As they mark the transition between terminal moraine slope and lobate features, they stretch between water depths of 40 m to 50 m and 55 m to 70 m at the sea bottom.

Interpretation

Based on their shape, surface and position, the sediment lobes are interpreted as debris-flow lobes (Dowdeswell et al., 2016b; Ottesen et al., 2017). Debris flows are often caused by slope failure of sediments delivered by deforming subglacial layers (Dowdeswell et al., 2016b). Ottesen and Dowdeswell (2006) often associate debris-flow lobes with debris extruded from glacier termini during surge events. However, no surge has been recorded for Besselsbreen since the LIA. The timing when the debris flow occurred is difficult to assess but likely it happened shortly after the formation of moraine ridge.

5.1.4 Large Parallel Ridge - Medial Moraine

Description

At Besselsbreen, a major submarine ridge separates the submarine basin into an eastern and a western part (Figure 5.2). It stretches from the terminal moraine almost to the current glacier front. Some discontinuations occur with almost 2 km missing in the central part. The ridge shows a fairly symmetrical shape with a width between 500 m and 1000 m and a height of ∼18 m. Slope angles range from 6° on the western side and 8° on the eastern side (Figure 5.6D).

Interpretation

Based on its parallel orientation to ice-flow direction, the ridge can be interpreted as medial moraine (Benn and Evans, 2010). Medial moraines often form by the redistribution of supra-, en-, and subglacial debris in shear zones between converging glaciers (Sharp, 1988b; Noormets et al., 2016). Nonetheless, the ridge is not connected to the subaerial moraine located between Besselsbreen and Augnebreen (Ottesen et al., 2017). Medial moraines may mark former ice-flow paths.

5.1.5 Small Transverse Ridges - Retreat Moraines

Description

A significant number of small ridges was identified in the two submarine basins in front of Besselsbreen (Figure 5.2). The ridges are oriented subparallel to the terminal moraine ridge with lengths at 300-1000 m (Figure 5.6A). Heights range between 2 m and 6 m. In the eastern basin of Dorstbukta, a set of parallel small transverse ridges was observed with a regular spacing of ∼100 m (Figure 5.6E). The ridges are slightly asymmetrical with a steeper glacier distal slope of 4.5° and a more gradual glacier proximal slope of 3.5°.

Small transverse ridges were mapped in the eastern part of the basin in front of Duckwitzbreen (Figure 5.3). A series of evenly spaced NE-SW aligned ridges occurs with an angle of a 45° to ice-front position (Figures 5.7B and E). The ridges are between 200 m and 350 m long, up to 30 m wide and 2.5 m high. They exhibit an asymmetrical shape with a glacier distal slope of 10° and a glacier proximal slope of up to 20°. A major sequence appears in the central part of the eastern basin stretching from the ice front to the overrun terminal moraine ridge. There is a second set visible but oriented SW-NE striking. The ridges in the northern part are symmetrical.

At Freemansundet, small transverse ridges are observed ranging between 300 m and 2 km. The ridges are 2-4 m high and and up to 30 meters wide. Three ridges in ice-front proximity are more prominent with heights of up to 10 m and width between 100 m and 200 m (Figure 5.4D). The three ridges have a concave glacier-proximal side. Rounded depressions occur on the glacier distal side of the ridges.

Interpretation

The ridges are interpreted as retreat moraines which form during minor glacier advances and winter stillstands (Solheim, 1991; Boulton et al., 1996; Ottesen and Dowdeswell, 2006). The regular spacing between ridges indicates a formation during uniform retreat or time windows. They often override glacial lineations (Solheim, 1991; Ottesen et al., 2008) as they are formed during glacier retreat. This is also the case in the glacier forefield of Besselsbreen. This and and the even spacing suggest that the retreat moraines formed during slow retreat after Besselsbreen had formed its terminal moraine ridge. The ridges cannot be retraced to specific years due to missing observational data.

At Duckwitzbreen, despite their orientation of 45° to the ice front, the even spacing and the asymmetric shape of the ridges suggest formation by ice push (Boulton et al., 1996) and thus are interpreted as retreat moraines.

The three larger transverse ridges may have formed during major stillstands of
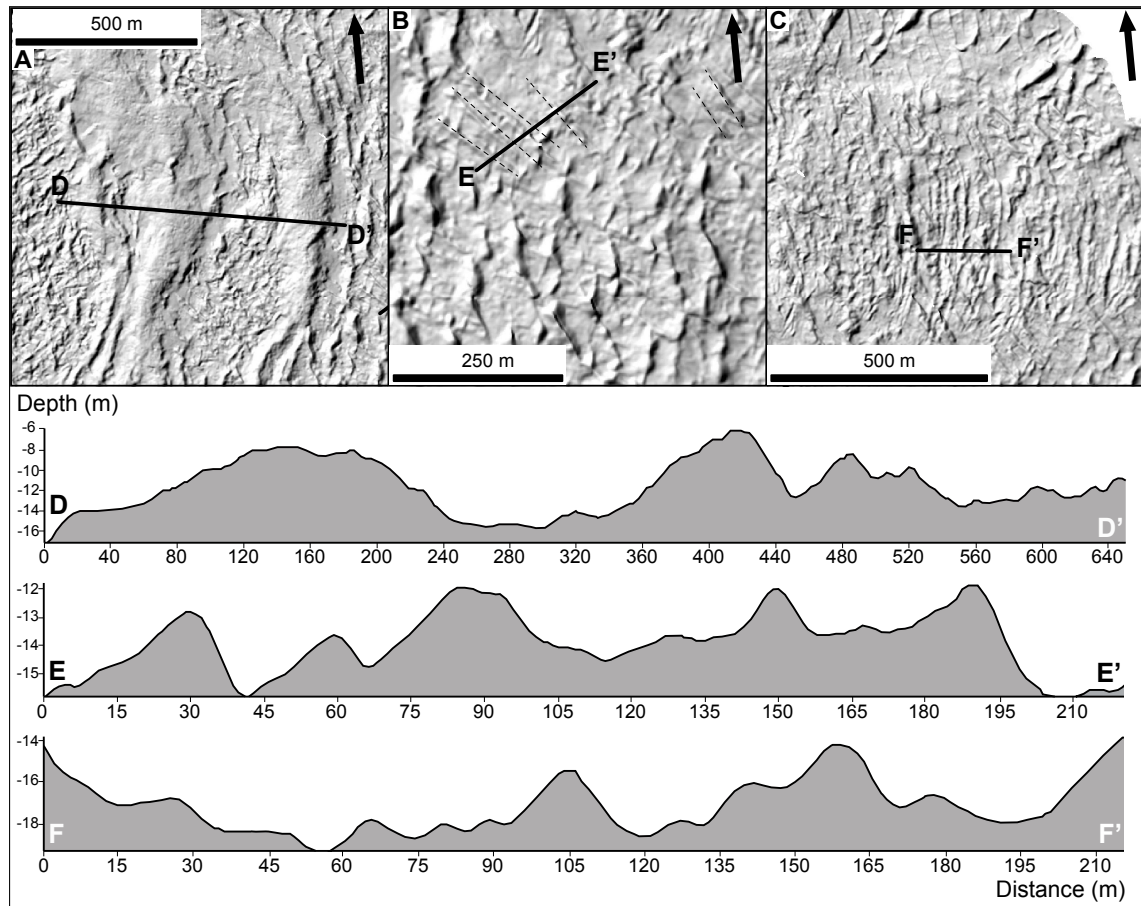
Figure 5.7: Landforms in front of Duckwitzbreen and their corresponding cross-sections, see Figure 5.3 for reference. A) and D) Overwritten terminal moraine ridges, B) Crevasse-squeeze ridges indicated by dashed lines plus rhombohedral ridges in the lower part of the image and E) cross-section through evenly spaced small transverse ridges, C) and F) Crescentic ridges.

Freemanbreen during retreat. In combination with underlying bedrock, the ridges may have acted as pinning points and affecting retreat behaviour.

5.1.6 Sinuous Ridges - Eskers

Description

Sinuous ridges are observed in the submarine glacier forefields of Besselsbreen and Duckwitzbreen. Two sinuous ridges are present in the western submarine basin of Besselsbreen (Figure 5.2) and two ridges are present in an area proximal to the glacier front of Duckwitzbreen (Figure 5.3). The ridges in front of Besselsbreen are 1.8 and 6.5 km long with widths of 100 m. The eastern sinuous ridge connects the

mapped scoured bedrock area with the large medial moraine located in the centre of the basin (Figure 5.8A). The submarine ridges in front of Duckwitzbreen are 100 m and 400 m long, and up to 30 m wide. All ridges show symmetric cross-sections and they are 5-14 m high (Figure 5.8C). A small, 500 m long sinuous ridge was observed in the western subaerial glacier forefield of Freemanbreen (Figure 5.4B).

Interpretation

The sinuous shape and the direction of the ridges lead to the interpretation as eskers that formed by sediment infill in subglacial conduits (Benn and Evans, 2010; Kristensen et al., 2009; Dowdeswell and Ottesen, 2016; Ottesen et al., 2017). Subglacial meltwater conduits are often located under medial moraines and eskers also reveal the location of conduits at the glacier bed (Benn et al., 2009; Benn and Evans, 2010). The eastern esker at Besselsbreen connecting with the medial moraine is a good example for that (Figure 5.8A). The presence of eskers indicates efficient subglacial drainage (Shreve, 1985; Kamb et al., 1985) which leads to the conclusion that they formed after surge stagnation. During the active phase of a surge, subglacial drainage is assumed to be inefficient (Section 1.3). Thus, the eskers in front of Duckwitzbreen likely formed after its surge in 1918. At Freemanbreen, the esker is interpreted to have formed after Freemanbreen's active surge phase in the 1950's.

5.1.7 Sinuous Depressions - Channels

Description

Two SSW-NNE oriented sinuous depressions occur east of the medial moraine of Besselsbreen (Figure 5.2). The depressions are 2 km and 2.5 km long, ca. 2 m deep and less than 50 m wide.

Interpretation

The sinuous depressions are interpreted as subglacial meltwater channels that were formed by subglacial meltwater erosion (Hogan et al., 2016). Subglacial meltwater channels indicate prolonged pressurised water flow (Hogan et al., 2010b). Their presence in combination with eskers indicate efficient subglacial drainage (Ottesen and Dowdeswell, 2006).
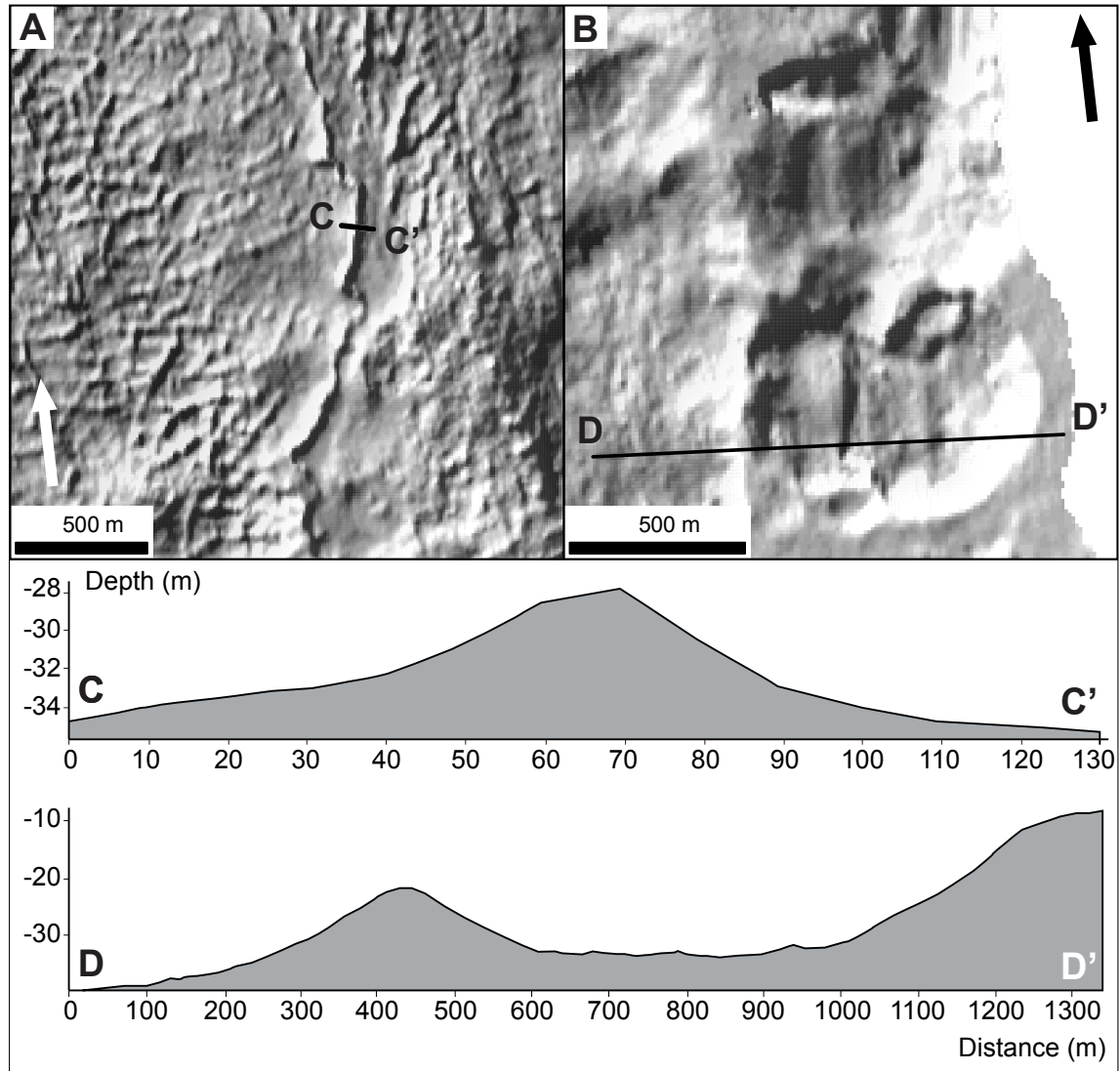
Figure 5.8: A) Esker in front of Besselsbreen stretching between bedrock and medial moraine with corresponding cross-section in C). B) Kettle holes in front of Besselsbreen and corresponding cross-section in D).

5.1.8 Geometric Ridge Networks - Crevasse Squeeze Ridges

Description

Small ridges oriented in various directions occur in the submarine glacier forefields of Besselsbreen (Figure 5.2) and Duckwitzbreen (Figure 5.3). The ridges often cross-cut each other, forming geometric networks, and they overprint glacial lineations. The ridges are found close to the terminal moraine of Besselsbreen and in proximity of the glacier front at Duckwitzbreen (Figure 5.7B). Individual ridges are 50-150 m long, 3-7 m high and 10-15 m wide. The ridges have a symmetrical cross-section. The majority of the ridges in oriented subparallel to the terminal moraine ridge. Due to poor data resolution, it is difficult to determine the transition between geometric ridge networks and small transverse ridges in front of Besselsbreen. Therefore, they are not differentiated in the map (Figure 5.2B). However, a detailed description and interpretation of small transverse ridges as retreat moraines can be found in Section 5.1.5.

Interpretation

Similar dimension and geometrical patterns of the ridges lead to the interpretation as crevasse-squeeze ridges (CSR) (Ottesen and Dowdeswell, 2006; Ottesen et al., 2008; Flink et al., 2015; Lovell et al., 2015). As CSRs intersect with retreat moraines, in front of Besselsbreen, distinction could not be made in the map. However, CSRs are of smaller size and have a more symmetrical cross-profile. The ridge networks form through debris injection into basal crevasses due to high subglacial water pressures with following melt-out (Rea and Evans, 2011). Due to their size, the ridges erode easily and/or are prone to burial caused by high sedimentation rates (Flink et al., 2015). CSRs have been identified as important component of surging glacier land systems (Evans and Rea, 1999, 2003; Brynjolfsson et al., 2012; Schomacker et al., 2014). Although CSRs were identified in the glacier forefield of Besselsbreen, the glacier has not surged since 1936. The CSRs in front of Duckwitzbreen were likely formed by its crevassed glacier terminus in connection with its surge in 1918.

5.1.9 Crescentic Ridges - Retreat moraines

Description

Crescentic ridges occur in a small, shallow part of the north-eastern part of Duckwitzbreen's submarine glacier forefield (Figure 5.7C). The roughly evenly spaced crescentic-shaped ridges occur convex in relation to the glacier front. The length of

the ridges varies between 200 m and 750 m. The ridges are up to 25 m wide and around 3 m high (Figure 5.7F).

Interpretation

Although of quite differing shape, the ridges are interpreted as crevasse-squeeze ridges. Curved crevasses form on the side of ice-streams (Vornberger and Whillans, 1990). They are often of relatively consistent length and curve concave down glacier. Based on their location in the centre of the glacier and their convex shape, the mapped ridges are more likely to be retreat moraines formed by a convex-shaped part of the glacier front in combination with crevasse-squeeze ridges formed by crevasses formed parallel to the glacier front.

5.1.10 Lobate Ridges

Description

Small, U-shaped ridges cover major areas of the slope on the western side of the overwritten terminal moraine of Duckwitzbreen (Figure 5.3). The lobe-shaped ridges have an opening towards east and are often arranged in connected systems. They have lengths between 100 m and 300 m. Their widths range between 50 m and 100 m with a maximal height of 5 meters. The ridges have openings of up to 250 m. They lie between 18 m and 25 m below sea level.

Interpretation

No exact process can be pinpointed to form the landforms. However, their opening to the east might indicate that formation was influenced by ice-flow direction.
The ridges could also be caused by icebergs ploughing the seabed - so called iceberg plough ridges. Yet, iceberg plough ridges usually occur in combination with iceberg ploughmarks (Dowdeswell et al., 2016c) which were not observed in the bathymetric dataset of Duckwitzbreen. Iceberg ploughmarks often cover long distances (Ottesen and Dowdeswell, 2006; Ottesen et al., 2008). Another factor is the depth at which the ridges occur; they do not appear above 18 m below sea level which again, is an argument against the formation by iceberg keels. Iceberg grounding pits - rounded pits caused by icebergs ploughing through sediments were also investigated as possible source (Hodgson et al., 2014). However, as previously mentioned, no other iceberg plough marks were observed in the area and the aerial photograph from 1936 (Figure 3.5) indicates very little iceberg activity.
Ribbed moraines (Dunlop and Clark, 2006) were also taken into account as possible interpretation but appearance, size and the lack of cross-cutting argue against this

interpretation.

Further research in form of sediment sampling or seismic profiling is required in order to give a final interpretation.

5.1.11 Depressions - Kettle Holes

Description

Three fairly large depressions covering an area of 0.7 km^2 were found in proximity to Besselsbreen (Figures 5.2 and 5.8B). The depressions are almost circular in shape with ranging diameters of 300 m, 600 m and 800 m. The depressions vary between 12 m and 15 m with raised rims, steep sides and flat floors (Figure 5.8D). At Freemanbreen, five large depressions were identified (Figure 5.4). The depressions are up to 15 m deep and are between 200 m and 1 km wide. Three of the depressions occur in combination with transverse ridges on the glacier-proximal side (Figure 5.4D).

Interpretation

The depressions are interpreted as kettle holes caused by dead-ice melting after retreat (Benn and Evans, 2010; Eilertsen et al., 2016; Ottesen et al., 2017). Commonly, icebergs get trapped in seabed sediments, buried and finally melt out. Irregular shapes occur where multiple ice blocks get deposited and melt out (Benn and Evans, 2010). For Freemanbreen, the three ridges may have acted as pinning points causing larger portions of ice to melt out.

5.1.12 Bedrock - Scoured Bedrock

Description

A total area of 0.14 km^2 was mapped as bedrock in the submarine glacier forefield of Besselsbreen (Figure 5.2B). The area occurs very proximal to the glacier front and less than 15 meters below the surface. The area shows a prominent step towards lower lying areas located around it. The surface is characterised by a rugged, irregular surface.

An area of 0.03 km^2 in proximity to the front of Duckwitzbreen was mapped as bedrock (Figure 5.3). The surface is less than 7 meters below the surface.

Interpretation

The areas are interpreted as glacially scoured bedrock due to their surface structure visible in the bathymetric datasets. Based on their proximity to the ice front, exposure of bedrock probably occurred fairly recently. Elevations under water such as

bedrock exposures often act as pinning points for retreating ice masses (Sund et al., 2009).

5.2 Unmapped Landforms

The following landforms were not mapped in this study. However, their presence is still considered important in order to reconstruct glacial dynamics.

5.2.1 Furrows - Iceberg Plough Marks

Description

Linear and curved furrows occur in the north-eastern part of the Besselsbreen dataset (Figure 5.2A). The furrows reach lengths between 500 m and 2 km, are up to 2 m deep and 20 m wide. They show U- and V-shaped profiles in cross-sections and appear in random patterns on top of the north-eastern terminal moraine ridge up to 60 m depth.

Interpretation

Based on their curvilinear shape and characteristic U- and V-shaped profile, the furrows are interpreted as iceberg plough marks formed by iceberg keels ploughing the seabed (Ottesen and Dowdeswell, 2006). Iceberg plough marks are indicative of oceanic current patterns. However, due to their limited appearance in the dataset, the landforms are only noted and not mapped in this study.

5.2.2 Hummocky Moraines

Areas of hummocky moraine were identified in all three terrestrial glacier forefields using aerial imagery. Hummocky moraine is indicative of dead-ice developement in terrestrial forefields (Benn and Evans, 2010). However, ground verification is necessary in order to identify and map the areas accurately (Benn and Evans, 2010). Therefore, the feature hummocky moraine was not mapped in this work.

5.2.3 Glaciofluvial Landforms

Glaciofluvial landforms such as outwash fans and active and relict meltwater channels are present in the terrestrial glacier forefields of all three glaciers. The landforms play an important part in the preservation of glacial landforms (Lønne and Lyså, 2005). However, as this work focuses on marine data, they were not mapped out.

Furthermore, ground verification is important in order to identify active and relict meltwater channels.

5.2.4 Coastal Landforms

Raised beach ridges are present in multiple areas around Barentsøya. The most prominent ones can be found at Kapp Ziehen, east of Mistakodden and north of Sundneset. According to Bondevik et al. (1995), they were formed due to isostatic uplift after the last deglaciation. Raised beach ridges can act as helpful tool to determine uplift rates in combination with dateable samples collected in the field.

5.3 Ice Front Position Reconstruction

Twenty-six ice front positions were reconstructed based on multiple data sources (Figure 5.9, Table 4.1). The sources include historical maps, old and modern aerial images, bathymetric data, previous ice position reconstructions and satellite images.

Ice front position reconstructions are an important tool for piecing together the glacier retreat history (Lefauconnier and Hagen, 1991; Oerlemans, 2005). Tidewater glaciers are more suitable for the reconstruction of ice front positions as their snouts are not covered by debris compared to terrestrial glaciers. However, glacier sides are often land-based making reconstruction in those areas more difficult. However, only Freemanbreen seems to be affected by it.

Seven ice front positions were determined for Besselsbreen. The glacier has retreated 12.5 km since the LIA. Since the maximum extent is based on the outline of the bathymetric ridge, the ice front position cannot be assigned to a specific year. However, maximum position was likely reached in the early 20th century. Based on the ice front position in 1936, glacier retreat rates are estimated around 154 $\frac{m}{a}$ after the LIA. Rates then stagnated to 100 $\frac{m}{a}$ from 1936 to1970 and stagnated even further to 30 $\frac{m}{a}$ since then (Lefauconnier and Hagen, 1991).

Ten ice front positions were marked for Duckwitzbreen. The glacier retreated 6.6 km since its surge in 1918. The oldest ice positions are based on a historic map by Vasiliev in 1901 (Figure 3.5). The ice front position in 1901 is also considered as LIA maximum extent. Ice front positions between 1936 and 1938 show rapid retreat between the years.

Nine ice front positions mark Freemanbreen's retreat. The oldest position is marked unknown and is based on the ridge T3 in the eastern part of the glacier forefield (Figure 5.4). As the terminal moraine ridge has not been dated, no age can be given but it likely formed before the LIA. Ridge T2 was interpreted as LIA terminal moraine which likely formed early in the 20th century. The ice front position from
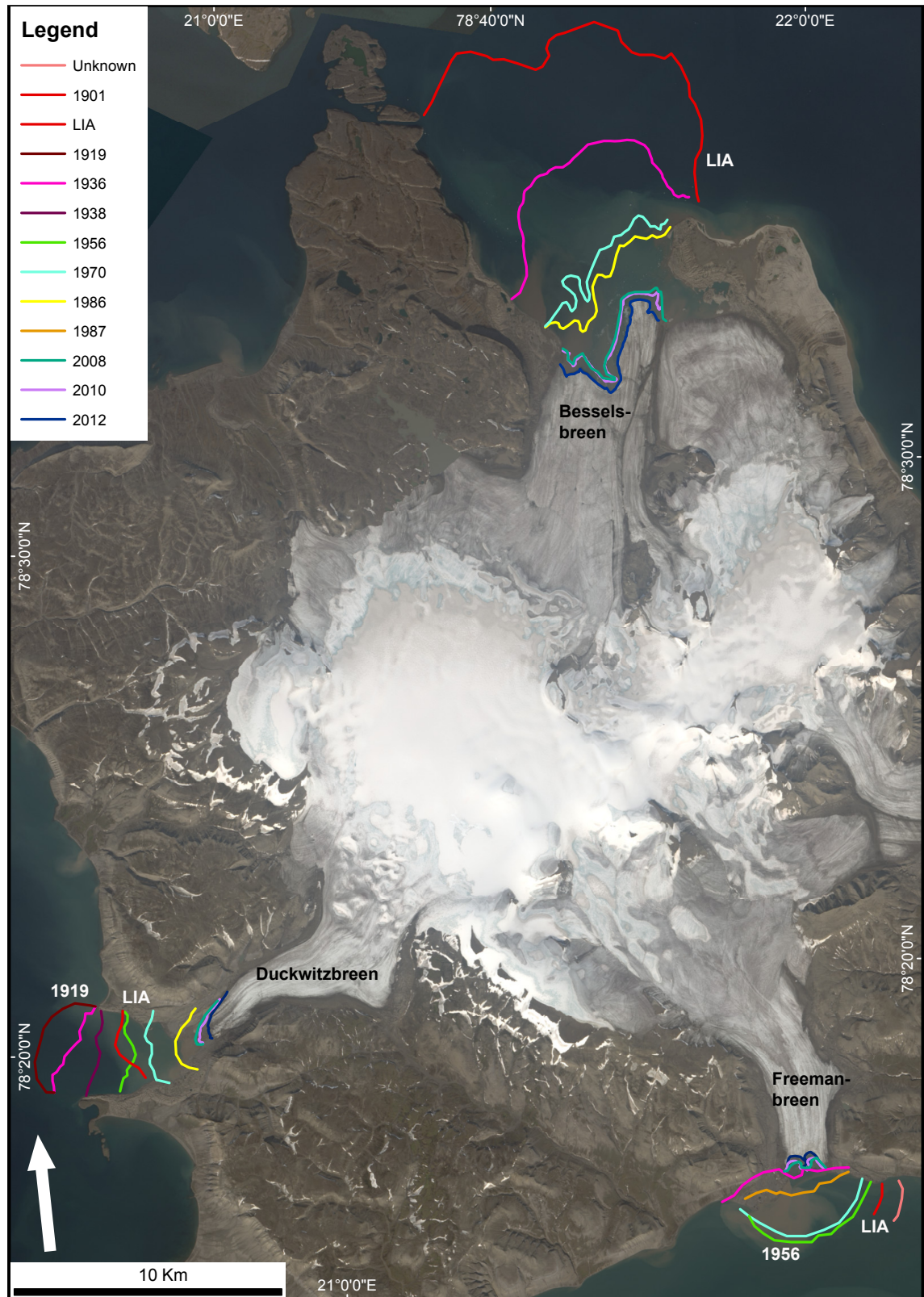
Figure 5.9: Reconstruction of glacier front positions with time. Each colour marks a specific year or LIA maximum position. The year of surge is also marked on the graphic. Front position based on Lefauconnier and Hagen (1991), van der Meer (2004), GLIMS (2018), aerial images and satellite images (NPI, 2018).

1936 (Figures 3.6 and 5.9) shows that Freemanbreen retreated almost to its present position by 1936. Glacier retreat rates stagnated significantly after Freemanbreen's surge between 1955 and 1956. Until 1970, the glacier has only retreated 230 m. After that, retreat rates increased to 70 $\frac{m}{a}$. Since the early 2000s, a small island in the centre of the ice front has been acting as a resting spot for parts of the ice front. Thus, Freemanbreen's terminus has developed from a fan-shape, to a straight line and then to the shape of a double horse shoe through time (Figure 5.9).

5.4 Ice Loss Calculation

The area of ice loss was calculated using a historic map, swath bathymetric datasets and aerial imagery.

The total area of ice loss was calculated to 146.5 km^2 (Figure 5.10). Most retreat has taken place at Besselsbreen, Duckwitzbreen and Freemanbreen. Besselsbreen is responsible for most parts of the area loss with 102.4 km^2. Freemanbreen lost 11.7 km^2 and Duckwitzbreen lost 10.2 km^2 from their LIA maximum extent. Although the land-terminating glaciers to the east play only a minor role in the retreat of the ice cap, they cannot be disregarded. A total of 20.2 km^2 was lost on the eastern side of Barentsøya since the LIA.

Compared to a total glacier area of 509.0 km^2 today, an area loss of 28.8% is calculated.
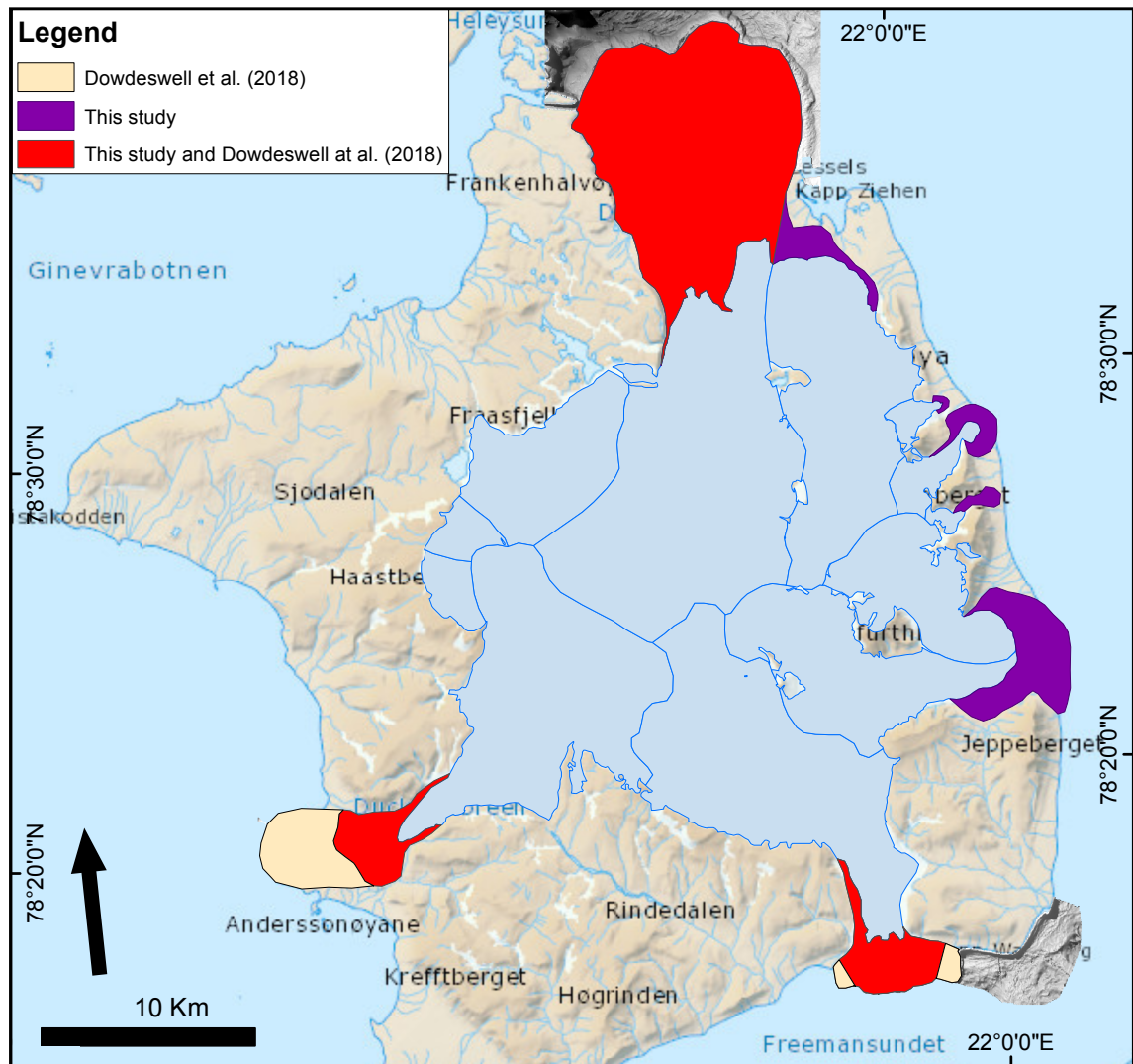
Figure 5.10: Map indicating the areas of ice loss of Barentsjøkulen since the LIA.
Light blue polygons represent present glacier extent provided by GLIMS
(2018). Areas are compared to Dowdeswell et al. (2018): Red polygons
represent overlapping areas between this study and Dowdeswell et al.
(2018), purple polygons represent areas only interpreted in this study
and beige polygons represent areas only interpreted by Dowdeswell
et al. (2018).

6 Discussion

Both terrestrial and marine archives demonstrate that most prominent landforms on Barentsøya are from the latest glacier advance in the region. There are regional discrepancies on Svalbard in terms of timing of the latest glacial advance. While glacier forefields of western Svalbard are often constrained by terminal moraines which were formed during the LIA maximum (Landvik et al., 2014), differing behaviour has been observed for eastern Svalbard. The few firmly dated terminal moraines in eastern Svalbard pre-date the LIA by far (e.g. > 2.6 ka BP at Hinlopenbreen (Flink and Noormets, 2017c) and 7.7 ka BP at Mohnbukta (Flink et al., 2017a)). Thus, the following discussion of Barentsjøkulen's glacial dynamics is purely based on interpretation of the three geomorphological maps created for the main outlet glaciers in combination with historical data, aerial imagery and previous studies. Dating of the terminal moraines is required in order to provide a final Holocene glacial history of Barentsøya's ice cap.

Nevertheless, two of the three main outlet glaciers have surged after the LIA. The mapped landform assemblages are then compared with existing landsystem models.

6.1 Glacial History of Barentsjøkulen

6.1.1 Late Weichselian/Early Holocene

During its most extensive state of the Late Weichselian glaciation, Barentsøya was covered by the SBSIS (Figure 6.1A). The ice sheet is believed to have had its centre close to Kong Karls Land (e.g. Mangerud et al., 1992b; Landvik et al., 2005; Svendsen et al., 2004b; Ingólfsson and Landvik, 2013). Glacial striae found by Salvigsen et al. (1992a) in high-lying areas of Barentsøya support the idea as they indicate ice movement from east to west.

Salvigsen et al. (1995) suggest an alteration of flow direction with disintegration of the SBSIS: ice flow changed towards east fed by glaciers on eastern Spitsbergen and northern Storfjorden (Figure 6.1B). Glacial striae on Frankenhalvøya (Salvigsen et al., 1992a) and glacial lineations mapped outside of Besselsbreen's terminal moraine (Figures 5.2 and 5.6) are indicative of an SW-NE-trending ice stream extending over the northernmost part of Barentsøya. The southwestern part of Barentsøya is marked by southward-trending glacier flow through Storfjorden as indicated in local
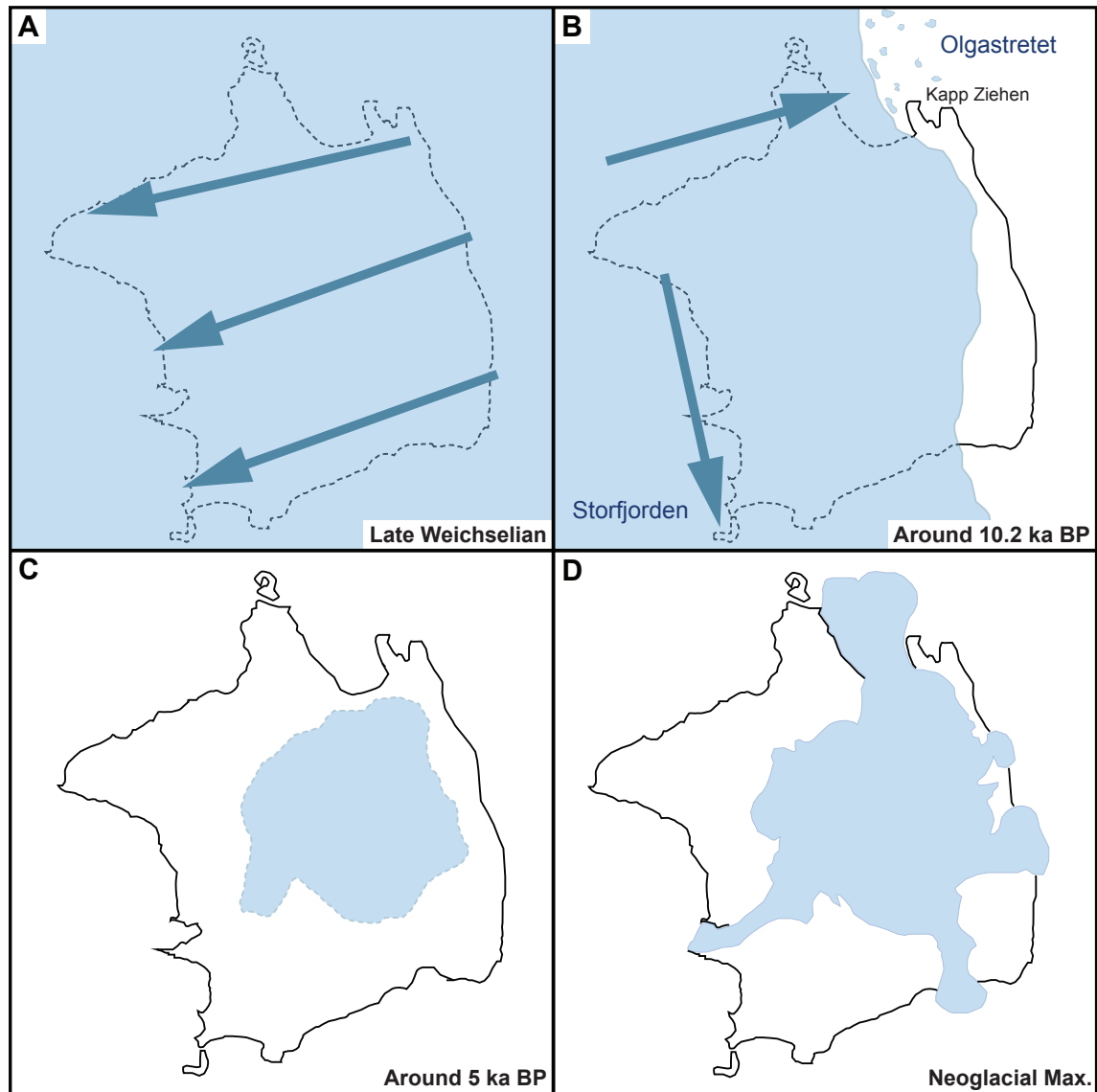
Figure 6.1: A summary of Barentsjøkulen's glacial history from the Late Weichselian to the LIA. Arrows indicate ice-flow direction of the covering ice sheet at the time. A) Barentsøya is still fully covered by the SBSIS with ice moving from east to west originating from the ice sheet centre north of Kong Karls Land. B) Barentsøya during the break-up of the SBSIS, ice flow originates from eastern Spitsbergen into Olgastretet and Storfjorden. Small dots represent calving icebergs. C) Barentsjøkulen receding to an unknown position due to climate warming during mid-Holocene. No exact positions available due to lacking data. D) Barentsjøkulen's extension during the LIA based on terminal moraine positions on land and under water.

dolerite outcrops (Figure 6.1B) (Salvigsen et al., 1992a, 1995).

Landvik et al. (1992a) suggested that the timing of deglaciation of Barentsøya's east coast occurred at 10.3 ka BP and at the west coast a few hundred years later (Figure 6.1B). At that time, a large percentage of the marine based part of the SBSIS vanished rapidly (Landvik et al., 1995). Barentsøya deglaciated late in comparison with Spitsbergen's outer coasts where deglaciation began around 13 ka BP (Mangerud et al., 1992a; Forman et al., 2004). However, Barentsøya occupied a more central part within the ice sheet which also applied to the more central fjords of Spitsbergen which did not become ice free before 10 ka BP (Mangerud et al., 1992a). Fjords such as Wahlenbergfjorden located between the outer outer shelf areas of Svalbard and Barentsøya, deglaciated around 11.5 ka BP (Flink et al., 2017b). The idea that deglaciation was primarily driven by ice calving into Olgastretet is supported by the fact that Kapp Ziehen was earlier deglaciated than Frankenhalvøya (Figure 6.1B). Younger striae at Sundneset also indicate the presence of a glacier in Freemansundet fed by higher-lying areas of southern Barentsøya and northern Edgeøya (Salvigsen et al., 1995). The beginning of the deglaciation also marks the transition of an ice sheet into an ice cap covering Barentsøya.

Well-developed raised beach ridges are prominent features in aerial imagery of Barentsøya. They occur most dominantly around Kapp Ziehen, east of Mistakodden and north of Sundneset. Previous studies measured the upper marine limit at 89 m.a.s.l. at Kapp Ziehen (Mangerud et al., 1992b; Bondevik et al., 1995). Dating methods may have improved since the study was undertaken in the 90s, resulting in higher resolution for sea-level curves and emersion rates. Hoek et al. (2016) dated lake isolation from marine waters between 2500 and 3000 years ago based on a lake core extracted at 15 m.s.l. at Sundneset.

With ongoing retreat of the SBSIS, the Barentsjøkulen ice cap was born. As temperatures increased in the beginning of the Holocene, it is likely that previously marine-terminating glaciers partly retreated well beyond present limits (Svendsen and Mangerud, 1997) similarly to what has been suggested for Albrechtbreen on Edgeøya (Ronnert and Landvik, 1993; Landvik et al., 1995). Due to its proximity analogical behaviour may be assumed for Barentsøya's outlet glaciers. Furthermore, in order to form previously mentioned marine terraces, an ice-free coast is required. Due to following glacier advances, it is likely that evidence which could determine the scope of retreat was overwritten.

Albrechtbreen advanced around 8.6 ka BP (Ronnert and Landvik, 1993). The advance corresponds to a colder period starting around 8.2 ka BP (Rasmussen and Thomsen, 2015) and comparable behaviour may be assumed for Barentsjøkulen. However, changes in temperature presumably affected only the outlet glacier termini as no terminal moraines were observed beyond present moraine position on Barentsøya's plateaus.

After its advance, Albrechtbreen receded to an unknown position until it advanced once more during the LIA (Ronnert and Landvik, 1992). According to Ronnert and Landvik (1993) differing lithology in moraine ridges indicate varying states of permafrost which was more extensive during LIA than during the earlier advance. Corresponding to that, Stäblein (1970) described the state and occurrence of ice-wedges at higher altitudes of 170 to 410 m.a.s.l. on Barentsøya. Humlum et al. (2003) estimates ice wedges near sea level in central Spitsbergen to have been initiated around 2.9 ka BP. Thus areas accommodating ice-wedges on Barentsøya must have been ice-free for at least the same amount of time. Again, no lithological evidence is available on Barentsøya but due to proximity, glacier retreat may also be assumed for Barentsjøkulen (Figure 6.1C). Furthermore, another glacier nearby, Hayesbreen in Mohnbukta on the east coast of Spitsbergen, also shows significant fluctuations prior to the LIA (Flink et al., 2017a).

6.1.2 Neoglacial Extent

Based on the shape of the medial moraine between Besselsbreen and Augnebreen and the seafloor morphology such as the fan-shaped glacial lineations (Figure 5.2), Besselsbreen may have been the dominating glacier of the two during Neoglacial advance (Ottesen et al., 2017). Due to a lack of sedimentological evidence and visual proof predating 1936, timing of formation of the terminal moraine cannot be defined. Previous studies (Lefauconnier and Hagen, 1991; Dowdeswell et al., 2018) interpret the terminal moraine to have formed during LIA maximum extent. This concurs with studies mostly based on western Svalbard which place timing of maximum extension ∼1900 (Snyder et al., 2000; Humlum et al., 2005; Evans and Rea, 2003; Evans, 2014). On the other hand, terminal moraines pre-dating the LIA in eastern Svalbard (Flink et al., 2017a; Flink and Noormets, 2017c) may suggest that the terminal moraine was formed at an earlier stage during the Holocene. The presence of glacial lineations, debris-flow lobes and rhombohedral ridges may lead to the interpretation that Besselsbreen's terminal moraine was formed during a surge (Figure 5.2). Duckwitzbreen's limited extent before its surge in 1918 (Figure 5.9) may also support the idea that Besselsbreen's terminus was of less extent during the Neoglacial. However, the presence of only one terminal moraine in the dataset indicates that one major advance occurred during the Holocene which may have overprinted previous advances. The idea of a floating glacier tongue due to thinning (Dowdeswell, 1989) during Neoglacial maximum extent may be overruled as sedimentation at a grounding line would be observed (Powell and Alley, 1997; Ottesen et al., 2008; Rüther et al., 2017). Dating of the terminal moraine is required in order to draw a final conclusion. However, this study complies with previous studies

from western Svalbard and implies formation of the terminal moraine during the LIA maximum.

Gripp (1929) presents the extent of Duckwitzbreen marked during Vasiliev's visit in 1901 (Figures 3.5 and 5.9). Based on these records, it may be concluded that Duckwitzbreen reached a far smaller extent during the LIA than during its surge in 1918. As glacier surges are a product of internal processes (Meier and Post, 1969) and not climate-induced, the advance occurred independent of the Neoglacial maximum extent. The mapped overwritten terminal moraines are interpreted to mark the Neoglacial maximum extent (Figures 5.3 and 5.7) as they align with the position marked by Vasiliev in 1901 (Figure 5.9).

Freemanbreen also lacks sedimentological and visual records before and from the Neoglacial period. Freemanbreen surged in 1955 and 1956 (Section 6.2) and the position of the innermost moraine ridge T1 aligns with the glacier front position based on an aerial photograph acquired in 1956 (Figures 3.6 and 5.9). Lefauconnier and Hagen (1991) interpret the outermost terminal moraine ridge T3 to mark the Neoglacial maximum extent (Figure 5.4). However, an aerial photograph from 1936 shows the glacier terminus at a position proximal to its present position (Figure 3.6). Based on the assumption that retreat rates increased in the second half of the 20th century due to increase in annual air temperatures, it is unlikely that the glacier retreated from the position of ridge T3 all the way to its position in 1936 in ca. 40 years. Therefore, ridge T2 is interpreted to mark the Neoglacial maximum extent and ridge T3 was formed by a surge earlier in the Holocene. This would also concur with glacier behaviour of other glaciers in eastern Svalbard (Flink et al., 2017a; Flink and Noormets, 2017c). Nevertheless, dating of the moraine ridges is required in order to draw a final conclusion.

In recent years, two studies attempted to mark the LIA extent of Barentjøkulen to estimate its subsequent retreat. Martín-Moreno et al. (2017) based their results on aerial images and positions of lateral moraines while Dowdeswell et al. (2018) combines aerial images with multibeam bathymetric data. The difference in results points out that the Neoglacial maximum extent cannot be determined on visual evidence alone but dating of landforms is required in order to achieve realistic results. This study concurs with the Neoglacial maximum extent chosen for Besselsbreen by Dowdeswell et al. (2018). However, the maximum positions chosen for Duckwitzbreen and Freemanbreen are considered to be overestimated.

This study is purely based on the interpretation of landform positions, a final conclusion can only be drawn by dating the moraine ridges.

6.1.3 Twentieth Century Retreat

All three observed glaciers have retreated in the 20th century (Dowdeswell and Bamber, 1995). However, Duckwitzbreen's and Freemanbreen's retreat rates in connection with increase in annual air temperatures cannot be determined due to interrupting surges. The surge events are further discussed in Section 6.2. Not only surge events challenge climate reconstruction, also the lack of high resolution data leads to smaller readvances and longer stillstands being overseen. However, marine data is crucial to a better understanding as glacier movements are often recorded on the seafloor by annual retreat moraines in form of small transverse ridges. Exact dating of the ridges remains a challenge.

Terrestrial geomorphological records may be helpful to determine bedrock features on land which might continue into the sea as elevated bedrock features often act as pinning points during glacier retreat (Sund et al., 2011). Freemanbreen's ice front has been shaped by a small island of bedrock since 2008 (Figure 5.9). As glacier ice rests longer on the island, the ice front transformed to two concave arcs left and right of the island. By 2015, Freemanbreen has overcome the obstacle and its front reestablished a straight shape. Similar behaviour was observed at Nordenskiöldbreen in central Spitsbergen (Allaart, 2016). The kettle holes in front of Freemanbreen might indicate that similar behaviour during earlier retreat (Figure 5.4). The corresponding ridges on the glacier proximal side may have acted as pinning points resulting in ice blocks becoming separated from the ice front and melting out after getting buried on the seafloor.

North of Duckwitzbreen's glacier forefield a dolerite dike is present (Figure 3.2) (NPI, 2016). Even though it appears to not continue further south, it may influence the morphology of the northern glacier forefield. Also, Frankenhalvøya west of Besselsbreen mostly consists of dolerite. As dolerite is of higher resistance to erosion as the surrounding Triassic sedimentary rocks, it has an effect on the formation and shape of glacial landforms (Figure 3.2) (Harbor, 1995). Seismic lines may be valuable in the identification of bedrock types.

Martín-Moreno et al. (2017) and Dowdeswell et al. (2018) both attempted to determine the total ice loss for Barentsjøkulen since its Neoglacial maximum extent. Martín-Moreno et al. (2017) estimated a glacier area loss of 106.8 km^2 (17.5%) since the LIA - the highest rate in eastern Svalbard. However, the numbers are based on lateral moraine positions which are difficult to use on Barentsøya as all three main outlet glaciers terminate in an open-marine setting. Therefore, Dowdeswell et al. (2018) included multibeam bathymetric data in order to map subaqueous terminal moraine ridges. They conclude that Barentsjøkulen has lost 130 km^2 of ice since the LIA - a number that is 20% greater than estimated by Martín-Moreno et al. (2017). However, based on the figures, both numbers may be questioned for the following

reasons:

First, Martín-Moreno et al. (2017) provides a number but on the complementary figure only Freemanbreen is marked with an area of ice loss. Additionally, Duckwitzbreen is not mentioned in the text but instead Hübnerbreen is referred to. Hübnerbreen did reach the sea during its maximum extent but converted relatively quick into a land-terminating glacier (Section 3.4.4) (Lefauconnier and Hagen, 1991). Therefore, it is uncertain what glaciers were used to determine ice loss.

Second, Dowdeswell et al. (2018) marked Duckwitzbreen's surge extent as the LIA extent. By using the surge moraine as LIA maximum extent, the effect of the LIA on Duckwitzbreen's advance is overestimated (Figure 5.10).

Third, Martín-Moreno et al. (2017) mark Freemanbreen's maximum extent based on lateral moraine ridges and interpret a fan-shaped ice extent. The interpreted area is greater than the area estimated by Dowdeswell et al. (2018). However, Dowdeswell et al. (2018) base their estimate on the same data as used in this work and interpret ridge T3 as LIA maximum extent (Figures 5.4 and 5.10). The dataset does not cover the entire area within the terminal moraine ridges based on the fact that ridge T3 was used as LIA extent, it may be concluded that both Martín-Moreno et al. (2017) and Dowdeswell et al. (2018) overestimated area loss for Freemanbreen.

Finally, in order to determine more accurate numbers of ice loss, the area was calculated incorporating the LIA maximum extension determined in this study (Figure 5.10). Furthermore, retreat of the land-based glaciers to the east was included. Whilst previously assumed by Martín-Moreno et al. (2017) and Dowdeswell et al. (2018), ice loss of the now land-based glaciers on the east coast of Barentsøya cannot be disregarded. The calculated area of 146.5 km^2 is significantly higher than previous estimates. Figure 5.10 clearly points out that the increased number is caused by the glaciers to the east of Barentsøya. It may be concluded that although land-terminating glaciers often retreat more slowly than marine-terminating glaciers (Benn and Evans, 2010), their ice loss cannot be neglected.

6.2 Glacier Surges of Barentsøya

Both Duckwitzbreen and Freemanbreen surged during the 20th century (Gripp, 1929; Lefauconnier and Hagen, 1991; Hagen et al., 1993).

Duckwitzbreen exhibits rhombohedral ridges (Figures 5.3 and 5.7B) which are often used as an indicator for glacier surges and play an important role in landsystem models of surge-type tidewater glaciers (Solheim and Pfirman, 1985; Ottesen and Dowdeswell, 2006; Ottesen et al., 2008). A glacier advance of 5.4 km within 17 years not connected to a surge is highly unlikely as these clearly exceed regular glacier advance rates (Gripp, 1929). The timing of surge cannot be extracted from the

geomorphological data provided but must be based on Tyrrell (1921) visiting Duck-witzbreen in 1919 proposing the surge to have occurred in 1918. Duckwitzbreen experienced steady retreat until now changing from a marine-terminating to a land-terminating glacier. Thus and with mass balances being negative (Hagen and Liestøl, 1990; Dowdeswell and Bamber, 1995), future surges are unlikely to occur.

Although Freemanbreen surged between 1955 and 1956, no rhombohedral ridges were found in the multibeam bathymetric dataset. Although rhombohedral ridges are a common feature in glacier forefields, they do not form necessarily during a surge (Farnsworth et al., 2016). However, glacial lineations clearly indicate fast ice flow (Figure 5.4B) and the presence of three terminal moraines (Figure 5.4D) suggests multiple glacier advances in the past. Aerial imagery displaying an advanced, highly crevassed glacier snout in 1956 (Figure 3.6) provides final evidence for a surge.

Noteworthy is also the lack of iceberg keel marks around the submarine glacier forefields of the two recorded surge-type glaciers. Surges are often associated with large amounts of small icebergs during active phases (Dowdeswell, 1989). However, little iceberg calving in front of Duckwitzbreen might have been caused by its termi-nal moraine ridge reaching above water acting as constraining barrier (Figure 3.5) (Lefauconnier and Hagen, 1991). Additionally, the bathymetric dataset is limited to the inner part of the glacier forefield, iceberg plough marks might occur outside of the dataset.

Again, little to no iceberg activity was observed in front of Freemanbreen in aerial images (Figure 3.6), and iceberg keel marks might have remained unnoticed due to data resolution.

Besselsbreen has not been recorded surging. However, Farnsworth et al. (2016) marks it as potential surge-type glacier based on the presence of CSRs in the sub-aerial glacier forefields. Rhombohedral ridges were also found under water (Figure 5.2) and Lefauconnier and Hagen (1991) marks the glacier as potentially but not likely to surge in the future. Additionally, further landforms indicative for but not unique to surge-type glaciers such as glacial lineation, debris-flow lobes and iceberg plough marks were mapped in front of Besselsbreen (Figure 5.2).

The presence of CSRs in combination with absent surge behaviour challenges previous literature that assumes that the landform is only formed by surging glaciers on land (e.g. Sharp, 1985*a*; Evans and Rea, 1999, 2003; Rea and Evans, 2011; Schomacker et al., 2014) and as rhombohedral ridges under water (e.g. Ottesen et al., 2008; Dowdeswell et al., 2016a). As a result, the idea of using CSRs as so called smoking-gun indicators (Allaart, 2016; Farnsworth et al., 2016) for surge-type glaciers might have to be reconsidered. Glaciers can show highly crevassed termini without a surge (Harper et al., 1998). Evans et al. (2012) suggest that debris ridges arranged in a geometric network may be created due to elevated meltwater pressure and ice hydrofracturing causing densely spaced crevasses which are then filled. Little

is known about Besselsbreen's thermal properties so this might be a possible explanation for the presence of rhombohedral ridges without a recorded surge. Although aerial images are quite sparse during the 20th century, it is unlikely that the glacier surged unnoticed as the surface would have been visibly crevassed (Clarke et al., 1986; Benn and Evans, 2010). However, the possibility remains that Besselsbreen's terminal moraine and subglacial landforms were formed by a surge well predating the LIA.

Most tidewater glaciers on the east coast of Spitsbergen and on Edgeøya surged at least once since the LIA (Farnsworth et al., 2016).

6.3 Potential of Geomorphological Mapping

Geomorphological maps provide a short but detailed overview over the morphology of the glacier forefield at the time data was obtained. However, several factors need to be considered:

Glacier forefields are quickly changing environments. Dead-ice melting, nivation and postglacial erosion trigger relief adjustments and changes in sedimentological characteristics in particular in terrestrial glacier forefields (Christiansen, 1998; Ballantyne, 2002).

Geomorphological mapping will always be subject to the author's interpretation.

The resolution of mapping depends on the input data.

Therefore, this thesis works mostly with multibeam bathymetric data as not only major parts of the glacier forefields are located under water but also preservation potential of marine landforms are significantly higher. This is mostly due to lack of fluvial erosion and permafrost reworking (Evans and Rea, 1999, 2003; Ottesen et al., 2008; Flink et al., 2015). However, submarine postglacial sedimentation may restrict surface expression of landforms; hence landforms of low height such as CSRs may be draped and eventually buried by glaciomarine sediments with time (Flink et al., 2015).

This thesis and in particular the geomorphological maps of Duckwitzbreen and Freemanbreen (Figures 5.3A and 5.4A) provide a good example how data resolution affects results. When comparing the resolution of Figure 5.3B to Figure 5.4B, the amount of landforms mapped may be noticed. As the dataset of Duckwitzbreen is available in a 2 x 2 m grid, more landforms can be observed also in more detail than in the 10 m x 10 m grid of Freemanbreen. Finer features such as iceberg plough marks or crevasse-squeeze ridges may get overseen in datasets with low resolution.

By comparing the outlines of Martín-Moreno et al. (2017) and Dowdeswell et al. (2018), the importance of marine geomorphological maps for tidewater glaciers is highlighted. Major parts of glacier forefields remain disregarded and important in-

formation might get lost if only the terrestrial parts of the glacier forefields are studied. On the other hand, multibeam bathymetric data retrieval requires a significant amount of time and resources compared to aerial imagery which is often easily accessible for Svalbard. Consequently, a combination of marine and terrestrial geomorphological maps will give best results as glacier behaviour also varies between land and water.

Finally, it is important to notice that even the most detailed geomorphological maps will not provide any chronology. Therfore, dating of landforms is essential to comprehensively reconstruct glacier dynamics.

6.4 Application of Landsystem Models

The understanding and description of landform assemblages characteristic for glacier surges (Sharp, 1985*a,b*; Evans and Rea, 2003; Ottesen and Dowdeswell, 2006; Ottesen et al., 2008) are of importance to distinguish between glacier advances driven by internal glaciological processes (Kamb et al., 1985; Raymond, 1987; Fowler et al., 2001; Murray et al., 2003; Sevestre and Benn, 2015) and glacier advances driven by climatically induced glacier fluctuations. In order to better understand geological records, surge-type and non-surge-type glaciers must be distinguished. Landsystem models may offer a relatively easy way to identify glacier type based on a suite of landforms when lacking observational data (Ottesen and Dowdeswell, 2006; Brynjolfsson et al., 2012).

Surging glaciers are often used as analogue to terrestrial paleo-ice streams and surging ice-sheet lobes in regard to assemblage but at much higher scale (Evans and Rea, 1999, 2003; Ottesen et al., 2008; Schomacker et al., 2014). Nevertheless, further evidence is required to determine if landsystem models can be scaled (Ingólfsson et al., 2016).

Meanwhile, one must keep in mind that landsystem models are often based on a limited number of glaciers in a restricted area. Glacier behaviour and dynamics depend clearly on bed conditions, resistant forces, glacier location, precipitation and termination type - an amount that cannot be compressed into a single, simple model. Furthermore, substratum plays a crucial role and has so far not been incorporated in models. Ottesen et al. (2017) added to the number of existing landsystem models by creating a model for glacier surges into an open-marine setting (Figure 1.1C). Bathymetric datasets in front of nine tidewater glaciers were used. However, the glaciers used are limited to eastern Svalbard. In addition, the model includes glaciers that are known to not have surged (e.g. Besselsbreen, Lefauconnier and Hagen, 1991).

Besselsbreen's landform assemblage fits well into the landsystem model for surging

glaciers in an open-marine setting by Ottesen et al. (2017) (Figure 1.1C). Equal to the model, the glacier forefield exhibits fan-shaped glacial lineations, kettle holes, an arc-shaped terminal moraine with debris-flow lobes, eskers and small retreat moraines (Figure 5.2B). The match may be obvious as Besselsbreen was part of the dataset the landsystem model was based on. However, as previously explained, although Besselsbreen exhibits rhombohedral ridges, it has no recorded-surge history. Freemanbreen exhibits similar arc-shaped terminal moraines and fan-shaped glacial lineations (Figure 5.4) as the model suggested by Ottesen et al. (2017). On the other hand, the occurrence of several moraine ridges (Figure 5.4C) may suggest that the fjord has more in common with the multiple-surge glacial landsystem by Flink et al. (2015) (Figure 1.1B). The absence of eskers in the submarine dataset comply with the model by Flink et al. (2015).

Duckwitzbreen lacks any glacial lineations which are omnipresent in landsystem models for surge-type glaciers (Ottesen and Dowdeswell, 2006; Ottesen et al., 2008; Flink et al., 2015; Ottesen et al., 2017). However, a variety of small ridges are present in the basin (Figures 5.3B and 5.7B). Existing landsystem models often recognise the presence of small ridges. Nevertheless, their varying shapes and properties are not regarded in detail. The shape of the terminal moraine, although not fully displayed in the dataset, suggests an open-marine setting similar to Ottesen et al. (2017). On the other hand, remaining landforms and their orientation do not match the model of an open-marine setting. Furthermore, the central large transverse ridges interpreted as overridden terminal moraines are absent from the model.

Lefauconnier and Hagen (1991) referred to shallow water surging glaciers as 'Duckwitzbreen type'. One may conclude that there might be a pattern and a need for a new model capturing landform assemblages of shallow-water surge-type glaciers. Glaciers with similar properties need to be determined before a sufficient landsystem model can be created. Based on Duckwitzbreen's landform assemblage, a wider range of small ridge types need to be included. However, by basing a landsystem model on the properties of a single glacier forefield, false assumptions may be made.

6.5 Further Studies

This study aimed at combining seafloor morphology with historical data and previous studies to gain a better understanding of Barentsøya's ice cap, Barentsjøkulen. However, projects are often limited by time, resources and data. In the following, suggestions are made to eliminate outstanding uncertainties.

Great efforts were made by the PONAM expedition (Landvik et al., 1992b) in order to gain a better understanding of Barentsøya's deglaciation. Dating techniques have improved significantly since 1991. Therefore, it might be helpful to conduct

more fieldwork and collect new and varying samples (e.g. lake cores, Hoek et al., 2016). In particular sediment cores from proglacial lakes have become a helpful tool to provide a better age constraint of the timing of Neoglacial advances and climate variabilities for eastern Svalbard such as Lovévatnet provides for western Svalbard (van der Bilt et al., 2015). There are multiple lakes in Barentsøya's north which might have potential to act as coring site and would add to other efforts in eastern Svalbard (Schomacker et al., 2017). Lake cores could provide insight on the advance and retreat dynamics of Barentsjøkulen prior to the LIA.

Bathymetric data with higher resolution for Freemanbreen and Besselsbreen will deliver a broader picture of the genesis of subglacial landforms. Marine cores and sub-bottom profiles contribute to a deeper understanding of internal composition, formation and timing of terminal moraines. By dating the terminal moraines, a final explanation may be given if the ridges in front of Besselsbreen and Freemanbreen were formed by surge events earlier during the Holocene or during Neoglacial maximum extension. Sub-bottom profiles may provide thickness of glaciogenic sediment and reveal potentially buried landforms (Flink et al., 2015).

As this study is purely based on remote sensing data for its terrestrial part, detailed sedimentological investigations are required. Field investigations are essential for ground verification in order to create detailed and comprehensive geomorphological maps. By excavating large sections and collecting sediment samples, more can be learned about internal structures of landforms in relation to glacier dynamics and paleoglaciology (Schomacker and Kjær, 2008). Visits to all terrestrial glacier forefields are recommended to provide sedimentological data and ground verification.

As a geomorphological map only provides an overview at the time it was generated, continuous studies over time will lead to a better understanding of landform preservation and evolution in glacier forefields. Furthermore, continuous retreat leads to revelation of new landforms which then need to be analysed and mapped further. Field observations are optimal but constant documentation using aerial imagery will already generate helpful results given a sufficient periodicity.

Further studies on Edgeøya could provide supportive information where data on Barentsøya is absent. Due to their proximity, the two islands are often regarded collectively (Landvik et al., 1992b; Dowdeswell and Bamber, 1995). Further data points are required in eastern Svalbard and data needs to be connected to fully understand the dynamics of the region during and after the LGM.

Since Duckwitzbreen has now retreated on land and mass balance decreases continuously, future surges are unlikely. Additionally, surges of Besselsbreen and Freemanbreen become more and more improbable. Nevertheless, if the glaciers happen to surge, satellite imagery will play an important role for continuous observations.

7 Conclusion

- The submarine glacier forefields of Besselsbreen, Duckwitzbreen and Freeman-breen were recorded in geomorphological maps. The geomorphological maps present subglacial imprints of the glaciers during the Holocene caused by surges and climatically-induced glacier advances.

- Barentsjøkulen's Holocene glacial dynamics were discussed based on geomor-phological maps, historical maps, literature and aerial imagery. Dating of the terminal moraines is essential in order to provide a complete glacial history.

- Barentsjøkulen has continuously lost ice area since the LIA. The area of ice loss was estimated to 146.5 km^2 - an area 12% greater compared to previous studies.

- Duckwitzbreen and Freemanbreen surged after the LIA.

- Existing landsystem models only apply in limited form to Barentsøya's glaciers. Duckwitzbreen's glacier forefield reveals the need for a new landsystem model for shallow-water surge-type glaciers.

- The assumption that crevasse-squeeze ridges are landforms unique to surge-type glaciers may be obsolete.

- The study improves an overall understanding of post LGM glacier dynamics in eastern Svalbard.

8 References

Allaart, L. (2016), Combining terrestrial and marine glacial archives: A geomorphological map of the Nordenskiöldbreen forefield, Svalbard, Master's thesis, NTNU.

Ballantyne, C. K. (2002), 'Paraglacial geomorphology', *Quaternary Science Reviews* **21**(18-19), 1935–2017.

Benestad, R., Hanssen-Bauer, I., Skaugen, T. and Førland, E. (2002), 'Associations between sea-ice and the local climate on Svalbard', *Oslo: Norwegian Meteorological Institute Report* **7**(02).

Benn, D. and Evans, D. (2010), *Glaciers and Glaciation*, 2nd edn, Arnold Publishers, London.

Benn, D. I., Kristensen, L. and Gulley, J. D. (2009), 'Surge propagation constrained by a persistent subglacial conduit, Bakaninbreen–Paulabreen, Svalbard', *Annals of Glaciology* **50**(52), 81–86.

Błaszczyk, M., Jania, J. A. and Hagen, J. O. (2009), 'Tidewater glaciers of Svalbard: Recent changes and estimates of calving fluxes', *Pol. Polar Res* **30**(2), 85–142.

Bondevik, S., Mangerud, J., Ronnert, L. and Salvigsen, O. (1995), 'Postglacial sea-level history of Edgeøya and Barentsøya, eastern Svalbard', *Polar Research* **14**(2), 153–180.

Boulton, G., Van der Meer, J., Hart, J., Beets, D., Ruegg, G., Van der Wateren, F. and Jarvis, J. (1996), 'Till and moraine emplacement in a deforming bed surge - an example from a marine environment', *Quaternary Science Reviews* **15**(10), 961–987.

Brynjolfsson, S., Ingólfsson, Ó. and Schomacker, A. (2012), 'Surge fingerprinting of cirque glaciers at the Tröllaskagi peninsula, North Iceland', *Jökull* **62**, 151–166.

Brynjólfsson, S., Schomacker, A. and Ingólfsson, Ó. (2014), 'Geomorphology and the Little Ice Age extent of the Drangajökull ice cap, NW Iceland, with focus on its three surge-type outlets', *Geomorphology* **213**, 292–304.

Büdel, J. (1960), 'Die Frostschutt-Zone Südost-Spitzbergens', *Colloquium Geographicum* **6**.

Burton, D. J., Dowdeswell, J. A., Hogan, K. A. and Noormets, R. (2016), 'Marginal fluctuations of a Svalbard surge-type tidewater glacier, Blomstrandbreen, since the Little Ice Age: a record of three surges', *Arctic, Antarctic, and Alpine Research* **48**(2), 411–426.

Christiansen, H. H. (1998), 'Nivation forms and processes in unconsolidated sediments, NE Greenland', *Earth Surface Processes and Landforms* **23**(8), 751–760.

Clarke, G. K. (1976), 'Thermal regulation of glacier surging', *Journal of Glaciology* **16**(74), 231–250.

Clarke, G. K., Schmok, J. P., Ommanney, C. S. L. and Collins, S. G. (1986), 'Characteristics of surge-type glaciers', *Journal of Geophysical Research: Solid Earth* **91**(B7), 7165–7180.

Dallmann, W. K., ed. (2015), *Geoscience Atlas of Svalbard*, Rapportserie 148, Norsk Polarinstitutt.

Dowdeswell, J. A. (1989), 'On the nature of Svalbard icebergs', *Journal of Glaciology* **35**(120), 224–234.

Dowdeswell, J. A. and Bamber, J. L. (1995), 'On the glaciology of Edgeøya and Barentsøya, Svalbard', *Polar Research* **14**(2), 105–122.

Dowdeswell, J. A., Canals, M., Jakobsson, M., Todd, B., Dowdeswell, E. K. and Hogan, K. (2016c), 'The variety and distribution of submarine glacial landforms and implications for ice-sheet reconstruction', *Geological Society, London, Memoirs* **46**(1), 519–552.

Dowdeswell, J. A., Hagen, J. O., Björnsson, H., Glazovsky, A. F., Harrison, W. D., Holmlund, P., Jania, J., Koerner, R. M., Lefauconnier, B., Ommanney, C. S. L. et al. (1997), 'The mass balance of circum-Arctic glaciers and recent climate change', *Quaternary research* **48**(1), 1–14.

Dowdeswell, J. A., Hamilton, G. S. and Hagen, J. O. (1991), 'The duration of the active phase on surge-type glaciers: contrasts between Svalbard and other regions', *Journal of Glaciology* **37**(127), 388–400.

Dowdeswell, J. A., Hodgkins, R., Nuttall, A.-M., Hagen, J. and Hamilton, G. (1995), 'Mass balance change as a control on the frequency and occurrence of glacier surges in Svalbard, Norwegian High Arctic', *Geophysical Research Letters* **22**(21), 2909–2912.

Dowdeswell, J. A., Hogan, K., Evans, J., Noormets, R., Cofaigh, C. Ó. and Ottesen, D. (2010b), 'Past ice-sheet flow east of Svalbard inferred from streamlined subglacial landforms', *Geology* **38**(2), 163–166.

Dowdeswell, J. A., Jakobsson, M., Hogan, K., O'Regan, M., Backman, J., Evans, J., Hell, B., Löwemark, L., Marcussen, C., Noormets, R. et al. (2010a), 'High-resolution geophysical observations of the Yermak Plateau and northern Svalbard margin: implications for ice-sheet grounding and deep-keeled icebergs', *Quaternary Science Reviews* **29**(25), 3518–3531.

Dowdeswell, J. A. and Ottesen, D. (2016), 'Eskers formed at the beds of modern surge-type tidewater glaciers in Spitsbergen', *Geological Society, London, Memoirs* **46**(1), 83–84.

Dowdeswell, J. A., Ottesen, D. and Bellec, V. (2018), The changing recent extent of marine-terminating glaciers and ice caps in northeastern Svalbard from marine-geophysical records. Under review.

Dowdeswell, J. A., Ottesen, D. and Plassen, L. (2016b), 'Debris-flow lobes on the distal flanks of terminal moraines in Spitsbergen fjords', *Geological Society, London, Memoirs* **46**(1), 77–78.

Dowdeswell, J. A., Solheim, A. and Ottesen, D. (2016a), 'Rhombohedral crevasse-

fill ridges at the marine margin of a surging Svalbard ice cap', *Geological Society, London, Memoirs* **46**(1), 73–74.

Dunlop, P. and Clark, C. D. (2006), 'The morphological characteristics of ribbed moraine', *Quaternary Science Reviews* **25**(13-14), 1668–1691.

Eilertsen, R., Bøe, R., Hermanns, R., Longva, O. and Dahlgren, S. (2016), 'Kettle holes,'dead-ice'topography and eskers on a lake floor in Telemark, southern Norway', *Geological Society, London, Memoirs* **46**(1), 113–114.

Elverhøi, A., Fjeldskaar, W., Solheim, A., Nyland-Berg, M. and Russwurm, L. (1993), 'The Barents Sea Ice Sheet - a model of its growth and decay during the last ice maximum', *Quaternary Science Reviews* **12**(10), 863–873.

Elverhøi, A. and Solheim, A. (1983), 'The Barents Sea ice sheet - a sedimentological discussion', *Polar Research* **1**(1), 23–42.

Evans, D. (2014), *Glacial Landsystems*, Routledge.

Evans, D. J. and Rea, B. R. (1999), 'Geomorphology and sedimentology of surging glaciers: a land-systems approach', *Annals of Glaciology* **28**, 75–82.

Evans, D. J. and Rea, B. R. (2003), Surging glacier landsystem, *in* 'Glacial landsystems', Taylor and Francis.

Evans, D. J., Strzelecki, M., Milledge, D. G. and Orton, C. (2012), 'Hørbyebreen polythermal glacial landsystem, Svalbard', *Journal of Maps* **8**(2), 146–156.

Farnsworth, W. R., Ingólfsson, Ó., Noormets, R., Allaart, L., Alexanderson, H., Henriksen, M. and Schomacker, A. (2017), 'Dynamic Holocene glacial history of St. Jonsfjorden, Svalbard', *Boreas* **46**(3), 585–603.

Farnsworth, W. R., Ingólfsson, Ó., Retelle, M. and Schomacker, A. (2016), 'Over 400 previously undocumented Svalbard surge-type glaciers identified', *Geomorphology* **264**, 52–60.

Flink, A. E., Hill, P., Noormets, R. and Kirchner, N. (2017a), 'Holocene glacial evolution of Mohnbukta in eastern Spitsbergen', *Boreas* .

Flink, A. E. and Noormets, R. (2017c), 'Submarine glacial landforms and sedimentary environments in Vaigattbogen, northeastern Spitsbergen', *Marine Geology* .

Flink, A. E., Noormets, R., Fransner, O., Hogan, K. A., ÓRegan, M. and Jakobsson, M. (2017b), 'Past ice flow in Wahlenbergfjorden and its implications for late Quaternary ice sheet dynamics in northeastern Svalbard', *Quaternary Science Reviews* **163**, 162–179.

Flink, A. E., Noormets, R., Kirchner, N., Benn, D. I., Luckman, A. and Lovell, H. (2015), 'The evolution of a submarine landform record following recent and multiple surges of Tunabreen glacier, Svalbard', *Quaternary Science Reviews* **108**, 37–50.

Flood, B., Nagy, J. and Winsnes, T. S. (1971), *The Triassic succession of Barentsøya, Edgeøya, and Hopen (Svalbard)*, number 100 *in* 'Meddelelser', Norsk Polarinstitutt.

8 References

Førland, E., Hanssen-Bauer, I. and Nordli, P. (1997), 'Climate statistics and longterm series of temperature and precipitation at Svalbard and Jan Mayen', *DNMI report* **21**(97), 43.

Førland, E. J., Benestad, R. E., Flatøy, F., Hanssen-Bauer, I., Haugen, J. E., Isaksen, K., Sorteberg, A. and Ådlandsvik, B. (2010), *Klimautvikling i Nord-Norge og på Svalbard i perioden 1900–2100: klimaendringer i norsk Arktis: NorACIA delutredning 1*, number 135 *in* 'Rapportserie', Norsk Polarinstitutt.

Forman, S., Lubinski, D., Ingólfsson, Ó., Zeeberg, J., Snyder, J., Siegert, M. and Matishov, G. (2004), 'A review of postglacial emergence on Svalbard, Franz Josef Land and Novaya Zemlya, northern Eurasia', *Quaternary Science Reviews* **23**(11), 1391–1434.

Forwick, M., Vorren, T. O., Hald, M., Korsun, S., Roh, Y., Vogt, C. and Yoo, K.-C. (2010), 'Spatial and temporal influence of glaciers and rivers on the sedimentary environment in Sassenfjorden and Tempelfjorden, Spitsbergen', *Geological Society, London, Special Publications* **344**(1), 163–193.

Fowler, A., Murray, T. and Ng, F. (2001), 'Thermally controlled glacier surging', *Journal of Glaciology* **47**(159), 527–538.

Gjerde, M., Bakke, J., D'Andrea, W. J., Balascio, N. L., Bradley, R. S., Vasskog, K., Olafsdottir, S., Røthe, T. O., Perren, B. B. and Hormes, A. (2017), 'Holocene multi-proxy environmental reconstruction from lake Hakluytvatnet, Amsterdamøya Island, Svalbard (79.5° N)', *Quaternary Science Reviews* .

Glasser, N. F. and Hambrey, M. J. (2001), 'Styles of sedimentation beneath Svalbard valley glaciers under changing dynamic and thermal regimes', *Journal of the Geological Society* **158**(4), 697–707.

GLIMS and NSIDC (2018), 'Global Land Ice Measurements from Space glacier database', Compiled and made available by the international GLIMS community and the National Snow and Ice Data Center, Boulder CO, U.S.A.

Gripp, K. (1929), 'Glaciologische und geologische Ergebnisse der Hamburgischen Spitzbergen-Expedition 1927: mit 32 Tafeln und 39 Figuren im Text', *Abhandlungen aus dem Gebiete der Naturwissenschaften* **22**(3/4), 145–249.

Grove, J. M. (2004), *Little ice ages: ancient and modern*, Vol. 1, Taylor and Francis.

Hagen, J. O. and Liestøl, O. (1990), 'Long-term glacier mass-balance investigations in Svalbard, 1950-88', *Annals of Glaciology* **14**(1), 102–106.

Hagen, J. O., Liestøl, O., Roland, E. and Jørgensen, T. (1993), 'Glacier atlas of Svalbard and Jan Mayen'.

Hagen, J. O., Melvold, K., Pinglot, F. and Dowdeswell, J. A. (2003), 'On the net mass balance of the glaciers and ice caps in Svalbard, Norwegian Arctic', *Arctic, Antarctic, and Alpine Research* **35**(2), 264–270.

Hamilton, G. S. and Dowdeswell, J. A. (1996), 'Controls on glacier surging in Svalbard', *Journal of Glaciology* **42**(140), 157–168.

Hanssen-Bauer, I., Solås, M. K. and Steffensen, E. (1990), *Climate of Spitsbergen*, DNMI.

Harbor, J. M. (1995), 'Development of glacial-valley cross sections under conditions of spatially variable resistance to erosion', *Geomorphology* **14**(2), 99–107.

Harland, W. B., Anderson, L. M., Manasrah, D., Butterfield, N. J., Challinor, A., Doubleday, P. A., Dowdeswell, E. K., Dowdeswell, J. A., Geddes, I., Kelly, S. R. et al. (1997), *The geology of Svalbard*, Geological Society.

Harper, J. T., Humphrey, N. and Pfeffer, W. T. (1998), 'Crevasse patterns and the strain-rate tensor: a high-resolution comparison', *Journal of Glaciology* **44**(146), 68–76.

Hjelle, A. (1993), *Geology of Svalbard*, number 7 *in* 'Polarhåndbok', Norsk Polarinstitutt.

Hodgson, D. A., Graham, A. G., Griffiths, H. J., Roberts, S. J., Cofaigh, C. Ó., Bentley, M. J. and Evans, D. J. (2014), 'Glacial history of sub-Antarctic South Georgia based on the submarine geomorphology of its fjords', *Quaternary Science Reviews* **89**, 129–147.

Hoek, W., Woelders, L., Akkerman, K., van Hoof, T., Moller Just, R. and Wagner-Cremer, F. (2016), Climate and environmental changes during the last 2000 years on Barentsøya and Edgeøya (E-Svalbard)., *in* 'EGU General Assembly Conference Abstracts', Vol. 18, p. 18392.

Hogan, K. A., Dowdeswell, J. A., Noormets, R., Evans, J. and Cofaigh, C. Ó. (2010a), 'Evidence for full-glacial flow and retreat of the Late Weichselian Ice Sheet from the waters around Kong Karls Land, eastern Svalbard', *Quaternary Science Reviews* **29**(25), 3563–3582.

Hogan, K., Dowdeswell, J., Larter, R., Cofaigh, C. Ó. and Bartholomew, I. (2016), 'Subglacial meltwater channels in Marguerite Trough, western Antarctic Peninsula', *Geological Society, London, Memoirs* **46**(1), 215–216.

Hogan, K., Dowdeswell, J., Noormets, R., Evans, J., Cofaigh, C. Ó. and Jakobsson, M. (2010b), 'Submarine landforms and ice-sheet flow in the Kvitøya Trough, northwestern Barents Sea', *Quaternary Science Reviews* **29**(25), 3545–3562.

Hormes, A., Akçar, N. and Kubik, P. W. (2011), 'Cosmogenic radionuclide dating indicates ice-sheet configuration during MIS 2 on Nordaustlandet, Svalbard', *Boreas* **40**(4), 636–649.

Hormes, A., Gjermundsen, E. F. and Rasmussen, T. L. (2013), 'From mountain top to the deep sea - Deglaciation in 4D of the northwestern Barents Sea ice sheet', *Quaternary Science Reviews* **75**, 78–99.

Hughes, A. L., Gyllencreutz, R., Lohne, Ø. S., Mangerud, J. and Svendsen, J. I. (2016), 'The last Eurasian ice sheets - a chronological database and time-slice reconstruction, DATED-1', *Boreas* **45**(1), 1–45.

Humlum, O., Christiansen, H. H. and Juliussen, H. (2007), 'Avalanche-derived rock glaciers in Svalbard', *Permafrost and Periglacial Processes* **18**(1), 75–88.

Humlum, O., Elberling, B., Hormes, A., Fjordheim, K., Hansen, O. H. and Heinemeier, J. (2005), 'Late-Holocene glacier growth in Svalbard, documented by subglacial relict vegetation and living soil microbes', *The Holocene* **15**(3), 396–407.

Humlum, O., Instanes, A. and Sollid, J. L. (2003), 'Permafrost in Svalbard: a review of research history, climatic background and engineering challenges', *Polar research* **22**(2), 191–215.

Ingólfsson, Ó. (2011), 'Fingerprints of Quaternary glaciations on Svalbard', *Geological Society, London, Special Publications* **354**(1), 15–31.

Ingólfsson, Ó., Benediktsson, Í. Ö., Schomacker, A., Kjær, K. H., Brynjólfsson, S., Jonsson, S. A., Korsgaard, N. J. and Johnson, M. D. (2016), 'Glacial geological studies of surge-type glaciers in Iceland - Research status and future challenges', *Earth-Science Reviews* **152**, 37–69.

Ingólfsson, Ó. and Landvik, J. Y. (2013), 'The Svalbard-Barents Sea ice-sheet - Historical, current and future perspectives', *Quaternary Science Reviews* **64**, 33–60.

Jakobsson, M., Andreassen, K., Bjarnadóttir, L. R., Dove, D., Dowdeswell, J. A., England, J. H., Funder, S., Hogan, K., Ingólfsson, Ó., Jennings, A. et al. (2014), 'Arctic Ocean glacial history', *Quaternary Science Reviews* **92**, 40–67.

Jakobsson, M., Gyllencreutz, R., Mayer, L., Dowdeswell, J., Canals, M., Todd, B., Dowdeswell, E., Hogan, K. and Larter, R. (2016), 'Mapping submarine glacial landforms using acoustic methods', *Geological Society, London, Memoirs* **46**(1), 17–40.

Jessen, S. P., Rasmussen, T. L., Nielsen, T. and Solheim, A. (2010), 'A new Late Weichselian and Holocene marine chronology for the western Svalbard slope 30,000–0 cal years BP', *Quaternary Science Reviews* **29**(9-10), 1301–1312.

Jiskoot, H., Murray, T. and Boyle, P. (2000), 'Controls on the distribution of surge-type glaciers in Svalbard', *Journal of Glaciology* **46**(154), 412–422.

Kamb, B., Raymond, C., Harrison, W., Engelhardt, H., Echelmeyer, K., Humphrey, N., Brugman, M. and Pfeffer, T. (1985), 'Glacier surge mechanism: 1982–1983 surge of Variegated Glacier, Alaska', *Science* **227**(4686), 469–479.

King, E. C., Hindmarsh, R. C. and Stokes, C. (2009), 'Formation of mega-scale glacial lineations observed beneath a West Antarctic ice stream', *Nature Geoscience* **2**(8), 585.

Kristensen, L., Benn, D. I., Hormes, A. and Ottesen, D. (2009), 'Mud aprons in front of Svalbard surge moraines: Evidence of subglacial deforming layers or proglacial glaciotectonics?', *Geomorphology* **111**(3), 206–221.

Landvik, J., Hansen, A., Kelly, M., Salvigsen, O., Slettemark, Ø. and Stubdrup, O. (1992a), 'The last deglaciation and glacimarine/marine sedimentation on Barentsøya and Edgeøya, eastern Svalbard', *Lundqua Report* **35**, 61–83.

Landvik, J. Y., Alexanderson, H., Henriksen, M. and Ingólfsson, Ó. (2014), 'Landscape imprints of changing glacial regimes during ice-sheet build-up and decay: a conceptual model from Svalbard', *Quaternary Science Reviews* **92**, 258–268.

Landvik, J. Y., Bondevik, S., Elverhøi, A., Fjeldskaar, W., Mangerud, J., Salvigsen, O., Siegert, M. J., Svendsen, J.-I. and Vorren, T. O. (1998), 'The last glacial maximum of Svalbard and the Barents Sea area: ice sheet extent and configuration', *Quaternary Science Reviews* **17**(1), 43–75.

Landvik, J. Y., Hjort, C., Mangerud, J., Moller, P. and Salvigsen, O. (1995), 'The Quaternary record of eastern Svalbard - an overview', *Polar Research* **14**(2), 95–104.

Landvik, J. Y., Hjort, C. and Salvigsen, O. (1992b), 'The PONAM expedition to eastern Svalbard 1991 - progress and achievements', *LUNDQUA Report* **35**.

Landvik, J. Y., Ingolfsson, O., Mienrt, J., Lehmann, S. J., Solheim, A. and Elverhøi, Andersand Ottesen, D. (2005), 'Rethinking Late Weichselian ice-sheet dynamics in coastal NW Svalbard', *Boreas* **34**(1), 7–24.

Lefauconnier, B. and Hagen, J. O. (1991), *Surging and calving glaciers in eastern Svalbard*, number 116 *in* 'Meddelelser', Norsk Polarinstitutt.

Liestøl, O. (1969), 'Glacier surges in west Spitsbergen', *Canadian Journal of Earth Sciences* **6**(4), 895–897.

Liestøl, O. (1993), 'Glaciers of Europe - Glaciers of Svalbard, Norway', *Satellite image atlas of glaciers of the world. US Geological Survey Profesional Paper* **1386**, E127E151.

Lock, B., Pickton, C., Smith, D., Batten, D. and Harland, W. (1978), 'The geology of Edgeøya and Barentsøya, Svalbard'.

Lønne, I. (2014), 'The influence of climate during and after a glacial surge - A comparison of the last two surges of Fridtjovbreen, Svalbard', *Geomorphology* **207**, 190–202.

Lønne, I. and Lyså, A. (2005), 'Deglaciation dynamics following the Little Ice Age on Svalbard: Implications for shaping of landscapes at high latitudes', *Geomorphology* **72**(1-4), 300–319.

Lovell, H. and Boston, C. M. (2017), 'Glacitectonic composite ridge systems and surge-type glaciers: an updated correlation based on Svalbard, Norway', *Arktos* **3**(1), 2.

Lovell, H., Fleming, E. J., Benn, D. I., Hubbard, B., Lukas, S., Rea, B. R., Noormets, R. and Flink, A. E. (2015), 'Debris entrainment and landform genesis during tidewater glacier surges', *Journal of Geophysical Research: Earth Surface* **120**(8), 1574–1595.

Mangerud, J., Bolstad, M., Elgersma, A., Helliksen, D., Landvik, J. Y., Lønne, I., Lycke, A. K., Salvigsen, O., Sandahl, T. and Svendsen, J. I. (1992a), 'The last glacial maximum on Spitsbergen, Svalbard', *Quaternary Research* **38**(1), 1–31.

Mangerud, J., Bondevik, S., Ronnert, L. and Salvigsen, O. (1992b), 'Shore displacement and marine limits on Edgeøya and Barentsøya, eastern Svalbard', *Lundqua Report* **35**, 51–60.

Mangerud, J. and Svendsen, J. I. (2017), 'The Holocene Thermal Maximum around Svalbard, Arctic North Atlantic; molluscs show early and exceptional warmth', *The Holocene* .

Martín-Moreno, R., Allende Álvarez, F. and Hagen, J. O. (2017), "Little Ice Age' glacier extent and subsequent retreat in Svalbard archipelago', *The Holocene* .

8 References

Meier, M. F. and Post, A. (1969), 'What are glacier surges?', *Canadian Journal of Earth Sciences* **6**(4), 807–817.

Möller, P., Hjort, C. and Ingólfsson, Ó. (1992), *Weichselian and Holocene glacial and marine history of East Svalbard: preliminary report on the PONAM fieldwork in 1991: proceedings of the PONAM workshop in Asker, Norway 27-29.4 1992*, Lund University, Department of Quarternary Geology.

Murray, T., James, T. D., Macheret, Y., Lavrentiev, I., Glazovsky, A. and Sykes, H. (2012), 'Geometric changes in a tidewater glacier in Svalbard during its surge cycle', *Arctic, Antarctic, and Alpine Research* **44**(3), 359–367.

Murray, T., Strozzi, T., Luckman, A., Jiskoot, H. and Christakos, P. (2003), 'Is there a single surge mechanism? Contrasts in dynamics between glacier surges in Svalbard and other regions', *Journal of Geophysical Research: Solid Earth* **108**(B5).

Noormets, R., Kirchner, N. and Flink, A. (2016), 'Submarine medial moraines in Hambergbukta, southeastern Spitsbergen', *Geological Society, London, Memoirs* **46**(1), 61–62.

Nordli, Ø., Przybylak, R., Ogilvie, A. E. and Isaksen, K. (2014), 'Long-term temperature trends and variability on Spitsbergen: the extended Svalbard Airport temperature series, 1898–2012', *Polar Research* **33**(1), 21349.

NPI (2003), *The place names of Svalbard*, Norsk Polarinstitutt.

NPI (2014), 'Kartdata Svalbard 1 : 100 000 (S100 Kartdata) / Map Data', Norwegian Polar Institute.

NPI (2016), 'GeoSvalbard SG250 Raster: Offline geological map of Svalbard'.

NPI (2018), 'TopoSvalbard'.

Nuth, C., Kohler, J., König, M., Von Deschwanden, A., Hagen, J., Kääb, A., Moholdt, G. and Pettersson, R. (2013), 'Decadal changes from a multi-temporal glacier inventory of Svalbard', *The Cryosphere* **7**(5), 1603.

Nuth, C., Moholdt, G., Kohler, J., Hagen, J. O. and Kääb, A. (2010), 'Svalbard glacier elevation changes and contribution to sea level rise', *Journal of Geophysical Research: Earth Surface* **115**(F1).

Oerlemans, J. (2005), 'Extracting a climate signal from 169 glacier records', *Science* **308**(5722), 675–677.

Ottesen, D. and Dowdeswell, J. (2006), 'Assemblages of submarine landforms produced by tidewater glaciers in Svalbard', *Journal of Geophysical Research: Earth Surface* **111**(F1).

Ottesen, D. and Dowdeswell, J. A. (2009), 'An inter–ice-stream glaciated margin: Submarine landforms and a geomorphic model based on marine-geophysical data from Svalbard', *Geological Society of America Bulletin* **121**(11-12), 1647–1665.

Ottesen, D., Dowdeswell, J. A., Landvik, J. Y. and Mienert, J. (2007), 'Dynamics of the Late Weichselian ice sheet on Svalbard inferred from high-resolution sea-floor morphology', *Boreas* **36**(3), 286–306.

Ottesen, D., Dowdeswell, J., Bellec, V. and Bjarnadóttir, L. (2017), 'The geomorphic imprint of glacier surges into open-marine waters: Examples from eastern Svalbard', *Marine Geology* .

Ottesen, D., Dowdeswell, J., Benn, D., Kristensen, L., Christiansen, H., Christensen, O., Hansen, L., Lebesbye, E., Forwick, M. and Vorren, T. (2008), 'Submarine landforms characteristic of glacier surges in two Spitsbergen fjords', *Quaternary Science Reviews* **27**(15), 1583–1599.

Pelt, W., Kohler, J., Liston, G., Hagen, J. O., Luks, B., Reijmer, C. and Pohjola, V. A. (2016), 'Multidecadal climate and seasonal snow conditions in Svalbard', *Journal of Geophysical Research: Earth Surface* **121**(11), 2100–2117.

Plassen, L., Vorren, T. O. and Forwick, M. (2004), 'Integrated acoustic and coring investigation of glacigenic deposits in Spitsbergen fjords', *Polar Research* **23**(1), 89–110.

Powell, R. D. and Alley, R. B. (1997), 'Grounding-Line Systems: Processes, Glaciological Inferences and the Stratigraphic Record', *Geology and seismic stratigraphy of the Antarctic Margin, 2* pp. 169–187.

Rasmussen, T. L. and Thomsen, E. (2015), 'Palaeoceanographic development in Storfjorden, Svalbard, during the deglaciation and Holocene: evidence from benthic foraminiferal records', *Boreas* **44**(1), 24–44.

Raymond, C. F. (1987), 'How do glaciers surge? A review', *Journal of Geophysical Research: Solid Earth* **92**(B9), 9121–9134.

Rea, B. R. and Evans, D. J. (2011), 'An assessment of surge-induced crevassing and the formation of crevasse squeeze ridges', *Journal of Geophysical Research: Earth Surface* **116**(F4).

Robinson, P. and Dowdeswell, J. A. (2011), 'Submarine landforms and the behavior of a surging ice cap since the last glacial maximum: The open-marine setting of eastern Austfonna, Svalbard', *Marine Geology* **286**(1), 82–94.

Ronnert, L. and Landvik, J. Y. (1992), 'The Holocene glacial advances of Albrechtbreen, Edgeøya, Svalbard', *LUNDQUA Report* **35**.

Ronnert, L. and Landvik, J. Y. (1993), 'Holocene glacial advances and moraine formation at Albrechtbreen, Edgeøya, Svalbard', *Polar research* **12**(1), 57–63.

Rüther, D. C., Bjarnadóttir, L. R., Junttila, J., Husum, K., Rasmussen, T. L., Lucchi, R. G. and Andreassen, K. (2012), 'Pattern and timing of the northwestern Barents Sea Ice Sheet deglaciation and indications of episodic Holocene deposition', *Boreas* **41**(3), 494–512.

Rüther, D. C., Winsborrow, M., Andreassen, K. and Forwick, M. (2017), 'Grounding line proximal sediment characteristics at a marine-based, late-stage ice stream margin', *Journal of Quaternary Science* **32**(4), 463–474.

Salvigsen, O., Adrielsson, L., Hjort, C., Johansson, K., Kelly, M., Landvik, J. and Ronnert, L. (1992a), 'Ice movements in eastern Svalbard', *LUNDQUA Report* **35**, 9–16.

Salvigsen, O., Adrielsson, L., Hjort, C., Kelly, M., Landvik, J. Y. and Ronnert,

L. (1995), 'Dynamics of the last glaciation in eastern Svalbard as inferred from glacier-movement indicators', *Polar Research* **14**(2), 141–152.

Salvigsen, O., Elgersma, A., Hjort, C., Lagerlund, E., Liestøl, O. and Svensson, N.-O. (1990), 'Glacial history and shoreline displacement on Erdmannflya and Bohemanflya, Spitsbergen, Svalbard', *Polar Research* **8**(2), 261–273.

Salvigsen, O., Forman, S. L. and Miller, G. H. (1992b), 'Thermophilous molluscs on Svalbard during the Holocene and their paleoclimatic implications', *Polar Research* **11**(1), 1–10.

Schomacker, A., Benediktsson, Í. Ö. and Ingólfsson, Ó. (2014), 'The Eyjabakkajökull glacial landsystem, Iceland: geomorphic impact of multiple surges', *Geomorphology* **218**, 98–107.

Schomacker, A., Farnsworth, W., Ingolfsson, O., Allaart, L., Håkansson, L. and Retelle, M. (2017), Holocene glacier variations and sea level change in Wahlenbergfjorden, Nordaustlandet, Svalbard, *in* 'AGU Fall Meeting Abstracts'.

Schomacker, A. and Kjær, K. H. (2008), 'Quantification of dead-ice melting in ice-cored moraines at the high-Arctic glacier Holmströmbreen, Svalbard', *Boreas* **37**(2), 211–225.

Schytt, V. (1969), 'Some comments on glacier surges in eastern Svalbard', *Canadian Journal of Earth Sciences* **6**(4), 867–873.

Schytt, V., Hoppe, G., Blake Jr, W. and Grosswald, M. (1968), 'The extent of the Würm glaciation in the European Arctic', *Int. Assoc. Sci. Hydrol* **79**, 207–216.

Serreze, M. C. and Barry, R. G. (2014), *The Arctic climate system*, Cambridge University Press.

Sevestre, H. and Benn, D. I. (2015), 'Climatic and geometric controls on the global distribution of surge-type glaciers: implications for a unifying model of surging', *Journal of Glaciology* **61**(228), 646–662.

Sevestre, H., Benn, D. I., Hulton, N. R. and Bælum, K. (2015), 'Thermal structure of Svalbard glaciers and implications for thermal switch models of glacier surging', *Journal of Geophysical Research: Earth Surface* **120**(10), 2220–2236.

Sharp, M. (1985*a*), ''Crevasse-Fill' Ridges: A landform type characteristic of surging glaciers?', *Geografiska Annaler. Series A. Physical Geography* pp. 213–220.

Sharp, M. (1985*b*), 'Sedimentation and stratigraphy at Eyjabakkajökull—an Icelandic surging glacier', *Quaternary Research* **24**(3), 268–284.

Sharp, M. (1988*a*), 'Surging glaciers: behaviour and mechanisms', *Progress in Physical Geography* **12**(3), 349–370.

Sharp, M. (1988*b*), 'Surging glaciers: geomorphic effects', *Progress in Physical Geography* **12**(4), 533–559.

Shreve, R. L. (1985), 'Esker characteristics in terms of glacier physics, Katahdin esker system, Maine', *Geological Society of America Bulletin* **96**(5), 639–646.

Smith, M. J., Paron, P. and Griffiths, J. S. (2011), *Geomorphological mapping: methods and applications*, Vol. 15, Elsevier.

Snyder, J., Werner, A. and Miller, G. (2000), 'Holocene cirque glacier activity in western Spitsbergen, Svalbard: sediment records from proglacial Linnévatnet', *The Holocene* **10**(5), 555–563.

Solheim, A. (1986), 'Submarine evidence of glacier surges', *Polar Research* **4**(1), 91–95.

Solheim, A. (1991), *The depositional environment of surging sub-polar tidewater glaciers: a case study of the morphology, sedimentation and sediment properties in a surge affected marine basin outside Nordaustlandet, Northern Barents Sea*, number 194 *in* 'Skrifter', Norsk Polarinstitutt.

Solheim, A. and Pfirman, S. L. (1985), 'Sea-floor morphology outside a grounded, surging glacier; Bråsvellbreen, Svalbard', *Marine Geology* **65**(1-2), 127–143.

Solheim, A., Russwurm, L., Elverhøi, A. and Berg, M. N. (1990), 'Glacial geomorphic features in the northern Barents Sea: direct evidence for grounded ice and implications for the pattern of deglaciation and late glacial sedimentation', *Geological Society, London, Special Publications* **53**(1), 253–268.

Stäblein, G. (1970), 'Untersuchung der Auftauschicht über Dauerfrost in Spitzbergen', *Eiszeitalter und Gegenwart* **21**.

Steffensen, E. (1982), 'The climate at Norwegian Arctic stations', *Klima* **5**(1), 44.

Stokes, C. R. and Clark, C. D. (2002), 'Are long subglacial bedforms indicative of fast ice flow?', *Boreas* **31**(3), 239–249.

Summerhayes, V. S. (1928), 'Climatic Zones', *Journal of Ecology* **16**(2), 252–262.

Sund, M., Eiken, T., Hagen, J. O. and Kääb, A. (2009), 'Svalbard surge dynamics derived from geometric changes', *Annals of Glaciology* **50**(52), 50–60.

Sund, M., Eiken, T. and Rolstad Denby, C. (2011), 'Velocity structure, front position changes and calving of the tidewater glacier Kronebreen, Svalbard', *The Cryosphere Discussions* **5**(1), 41–73.

Sund, M., Lauknes, T. and Eiken, T. (2014), 'Surge dynamics in the Nathorstbreen glacier system, Svalbard', *The Cryosphere* **8**(2), 623–638.

Svendsen, J. I., Alexanderson, H., Astakhov, V. I., Demidov, I., Dowdeswell, J. A., Funder, S., Gataullin, V., Henriksen, M., Hjort, C., Houmark-Nielsen, M., Hubberten, H. W., Ingólfsson, Ó., Jakobsson, M., Kjær, K. H., Larsen, E., Lokrantz, H., Lunkka, J. P., Lyså, A., Mangerud, J., Matiouchkov, A., Murray, A., Möller, P., Niessen, F., Nikolskaya, O., Polyak, L., Saarnisto, M., Siegert, C., Siegert, M. J., Spielhagen, R. F. and Stein, R. (2004a), 'Late Quaternary ice sheet history of northern Eurasia', *Quaternary Science Reviews* **23**(11), 1229 – 1271. Quaternary Environments of the Eurasian North (QUEEN).

Svendsen, J. I., Gataullin, V., Mangerud, J. and Polyak, L. (2004b), 'The glacial history of the Barents and Kara Sea region', *Quaternary glaciations—extent and chronology* **1**, 369–378.

Svendsen, J. I. and Mangerud, J. (1997), 'Holocene glacial and climatic variations on Spitsbergen, Svalbard', *The Holocene* **7**(1), 45–57.

8 References

Tyrrell, G. W. (1921), 'Geographical observations in Spitsbergen, 1919 and 1920', *Scottish Geographical Magazine* **37**(4), 227–242.

Tyrrell, G. W. (1922), 'I. The glaciers of Spitsbergen', *Transactions of the Geological Society of Glasgow* **17**(1), 1–49.

van der Bilt, W. G., Bakke, J., Vasskog, K., D'Andrea, W. J., Bradley, R. S. and Ólafsdóttir, S. (2015), 'Reconstruction of glacier variability from lake sediments reveals dynamic Holocene climate in Svalbard', *Quaternary Science Reviews* **126**, 201–218.

van der Meer, J. J. (2004), *Spitsbergen Push Moraines: Including a Translation of K. Gripp: Glaciologische und Geologische Ergebnisse Der Hamburgischen Spitzbergen-Expedition 1927*, Vol. 4, Elsevier.

von Heuglin, T. (1872), *Reisen nach dem Nordpolarmeer in den Jahren 1870 und 1871*, Vol. 1, G. Westermann.

Vornberger, P. and Whillans, I. (1990), 'Crevasse deformation and examples from Ice Stream B, Antarctica', *Journal of Glaciology* **36**(122), 3–10.

Woelders, L., T., L. J., Hagemans, K., Keechy, A., van Hoof, T. B. and Hoek, W. Z. (2018), 'Recent climate warming drives ecological change in a remote high-Arctic lake', *Nature Scientific Reports* **8**(6858).